

New Sesterterpenes from Marine Sponges from the Tropical Waters of the Kingdom of Tonga

by
Taitusi Taufa



A thesis
submitted to Victoria University of Wellington
in fulfilment of the
requirements for the degree of
Master of Science
in Chemistry.

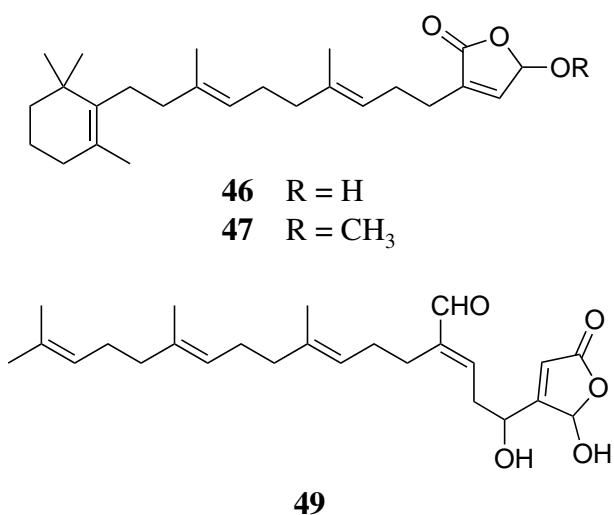
Victoria University of Wellington
2010

Abstract

Over the course of this study, various species of Tongan marine sponges were investigated using an NMR-based screening method and has resulted in the discovery of three new sesterterpenes and 11 known compounds.

Examination of the sponge *Fascaplysinopsis* sp. resulted in the isolation of two novel sesterterpenes, isoluffariellolide (**46**) and 1-*O*-methylisoluffariellolide (**47**). Compounds **46** and **47** share the same backbone pattern as the known luffariellolide (**45**) and 25-*O*-methyl-luffariellolide (**107**) respectively, and differ only in the substitution pattern of the butenolide rings. Isoluffariellolide (**46**) was found to be approximately six times less cytotoxic than 1-*O*-methylisoluffariellolide (**47**). Interestingly, these results suggested that the 1-*O*-methyl group in compound **47** plays an important role in the cytotoxicity of the compound.

Secothorectolide (**49**), a new ring-opened and geometric isomer of the known compound thorectolide (**48**), was obtained from a sponge of the order Dictyoceratida. This ring closure and opening relationship was also observed between manoalide (**109**) and secomanoalide (**110**), as well as luffariellins A (**141**) and B (**142**). Despite the different carbon skeleton, the functional groups in **141** and **142** are similar with those in **109** and **110**, respectively, and not surprisingly the biological properties are almost identical. The biological activities of compounds **48** and **49** were almost the same, which would give an insight into the structure-activity relationship (SAR) between these types of compounds.



Acknowledgments

It is a pleasure to thank the many people who made this thesis possible, but I would like to give the glory back to the Heavenly Father who Has given me the wisdom and strength to carry out this study to the end.

First and foremost I offer my sincerest gratitude to my supervisor, Assoc. Prof. Peter Northcote, whose encouragement, guidance and support from the initial to the final level enabled me to develop an understanding of the subject. Without his encouragement and constant guidance, I could not have finished this thesis. One simply could not wish for a better or friendlier supervisor. Thank you for accepting me to work in your lab and the series of dive trips back home.

In my daily work in the lab I have been blessed with friendly and cheerful workmates, Jonathan Singh and Jacqueline Barber. I am heartily thankful to Jono, who is always being there to help me with my lab work and to edit my thesis. Jono has been a friend and mentor. Jacqui thank you for always explaining things more clearly to my small Tongan brain.

I wish to thank Dr John Ryan for his amazing NMR skills and for retrieving my unsaved NMR data after being lost for more than a year. Thank you for introducing and helping me get on the road to L^AT_EX.

My sincere thanks go to the academic and general staff at the School of Chemical and Physical Sciences.

The School of Biological Sciences has kindly run a range of bioassays on my compounds, special thanks to Prof. John Miller and Dora Leahy from the Cell Biology Research group.

For special gratitude is due to my parents, Temaleti and Siopau, for always believing in me and all the prayers. To my aunties, Drs 'Anamaui Taufe'ulungaki and Sepi Taufe'ulungaki for always being there throughout my academic years. To aunty Vika for always making her house available for us during our diving collecting trips. To my sisters (Mepa, Malama, Seini) and brothers (Maikolo, Mosese Tava, Kanitiola) for everything.

I owe my loving thanks to my wife Salome Visitasio, and my daughter 'Iunisi Tupou. They have lost a lot due to my research abroad. Without their encouragement and understanding it would have been impossible for me to finish this work.

The financial support of the NZAiD is gratefully acknowledged.

Table of Contents

Abstract	ii
Acknowledgments	iii
Table of Contents	iv
List of Figures	viii
List of Schemes	xi
List of Tables	xii
Glossary	xiii
1 Introduction	1
1.1 The Role of Natural Products in Medicine	1
1.2 The Onset of the “Golden Era of Antibiotics”	2
1.3 Marine Natural Products	3
1.4 Marine Sponges	5
1.5 Tongan Marine Sponges and Chemistry	7
2 Isolation and Screening of Secondary Metabolites	14
2.1 Isolation Techniques	14
2.1.1 Cyclic Loading	14
2.2 Screening of Marine Organisms	16
2.2.1 Bioassay-Directed Screening	16
2.2.2 NMR-Based Screening	17
2.3 VUW Screening Methodology	17
2.3.1 HSQC Mask	18

2.4	Future Screening Methods	19
2.4.1	HMBC Screen	20
3	Sponges Investigated by Spectroscopic Screening	21
3.1	Sponges Screened from Tongatapu and ‘Eua	21
3.2	Sponges Screened from the Vava‘u Group	26
4	The Isolation of Known Compounds from Tongan Sponges	29
4.1	Order Verongida	29
4.1.1	Bromotyrosine Derivatives	29
4.1.2	PTN3_33F	30
4.1.3	PTN3_46E	35
4.2	Order Poecilosclerida	45
4.2.1	PTN4_10A	45
4.3	Biological Activity	51
5	Investigation of <i>Fascaplysinopsis</i> sp.	52
5.1	<i>Fascaplysinopsis</i> sp.	52
5.2	Chemical History of the Genus <i>Fascaplysinopsis</i>	53
5.3	Isolation	59
5.4	Isoluffariellolide	61
5.5	1- <i>O</i> -Methylisoluffariellolide	67
5.6	Biological Activity	74
5.7	Related Compounds	74
6	Investigation of Sponge from the Order Dictyoceratida	80
6.1	Order Dictyoceratida	80
6.2	Isolation	81
6.3	Secothorectolide	83

6.4	Biological Activity	88
6.5	Related Compounds	88
6.5.1	Biosynthetic relationship between all <i>Luffarella</i> metabolites . . .	90
7	Conclusion	92
8	Experimental	94
8.1	General Experimental	94
8.2	Investigation of Genus <i>Fascaplysinopsis</i>	95
8.2.1	Initial Fractionation of <i>Fascaplysinopsis</i> sp.	95
8.2.2	Isolation of Homofascaplysin A	96
8.2.3	Isolation of Luffariellolide, Isoluffariellolide, 1- <i>O</i> -Methylisoluffa- riellolide	96
8.3	Investigation of Dictyoceratid Sponge	98
8.3.1	Isolation of Secothorectolide and Thorectolide	98
8.4	Investigation of a Verongiïd Sponge	100
8.4.1	Isolation of Aplysamine-2 and Aerophobin-1	100
8.5	Investigation of Verongiïd Sponge	102
8.5.1	Isolation of Fistularin-3, Aeroplysinin-1 and LL-PAA216	102
8.6	Investigation of a Poecilosclerid Sponge	104
8.6.1	Isolation of of Makaluvamine G and Prianosin B	104
A	Existing Marine Chemistry Sponge Screening Protocol	107
B	Isoluffariellolide Spectra	113
C	1-<i>O</i>-Methylisoluffariellolide Spectra	118
D	Secothorectolide Spectra	123
E	Fistularin-3 Spectra	128

F	Aerophysinin-1 Spectra	133
G	LL-PAA216 Spectra	138
H	LL-PAA216 Spectra	143
	References	148

List of Figures

1.1	Map of the Kingdom of Tonga. Map courtesy of LINZ.	8
2.1	Schematic of the mass distribution in a typical marine sponge extract. . .	15
2.2	Schematic of the cyclic loading process.	16
2.3	(a) Computer generated mask of HSQC data (contains 160 sponges). (b) Common correlations in the HSQC masks.	19
2.4	(a) An uninteresting sponge screen. (b) An interesting screen.	19
3.1	Surface photo of the PTN3_13A sponge.	21
3.2	Surface photo of the PTN3_13C sponge.	22
3.3	Surface photo of the PTN3_14B sponge.	22
3.4	Surface photo of the PTN3_14E sponge.	23
3.5	Surface photo of the PTN3_14F sponge.	23
3.6	Surface photo of the PTN3_15C sponge.	24
3.7	Surface photo of the PTN3_16F sponge.	24
3.8	Surface photo of the PTN3_18C sponge.	25
3.9	Surface photo of the PTN3_25E sponge.	26
3.10	Surface photo of the PTN3_25F sponge.	27
3.11	Underwater photo of the <i>Leucetta</i> sp. (courtesy of Karen Stone).	27
3.12	Surface photo of the PTN4_05D.	28
4.1	Surface photograph of the sponge PTN3_33F.	30
4.2	HSQC NMR screen spectrum (600 MHz, CD ₃ OD) of the 75% Me ₂ CO/H ₂ O fraction of PTN3_33F.	33
4.3	COSY NMR screen spectrum (600 MHz, CD ₃ OD) of the 75% Me ₂ CO/H ₂ O fraction of PTN3_33F.	33
4.4	¹ H NMR screen spectrum (600 MHz, CD ₃ OD) of the 75% Me ₂ CO/H ₂ O fraction of PTN3_33F.	34

4.5	HMBC NMR screen spectrum (600 MHz, CD ₃ OD) of the 75% Me ₂ CO/H ₂ O fraction of PTN3_33F.	34
4.6	Underwater photograph of the sponge PTN3_46E. Courtesy of Karen Stone.	35
4.7	Proposed substructure of a compound isolated from PTN3_46E sponge.	39
4.8	Underwater photo of the PTN4_10A sponge (courtesy of Karen Stone).	46
4.9	HSQC NMR screen spectrum (600 MHz, CD ₃ OD) of the 75% Me ₂ CO/H ₂ O fraction of PTN4_10A.	49
4.10	COSY NMR screen spectrum (600 MHz, CD ₃ OD) of the 75% Me ₂ CO/H ₂ O fraction of PTN4_10A.	50
4.11	HMBC NMR screen spectrum (600 MHz, CD ₃ OD) of the 75% Me ₂ CO/H ₂ O fraction of PTN4_10A.	50
5.1	Surface photograph of the <i>Fascaplysinopsis</i> sp.	53
5.2	COSY and HMBC correlations establishing connectivity of C-16 to C-18 of isoluffariellolide.	61
5.3	HMBC correlations establishing connectivity of the trimethylcyclohexenyl ring system, substructure A, of isoluffariellolide.	62
5.4	COSY and HMBC correlations establishing connectivity of C-10 to C-13, substructure B, of isoluffariellolide.	63
5.5	COSY and HMBC correlations establishing connectivity of C-6 to C-9, substructure C, of isoluffariellolide.	63
5.6	COSY and HMBC correlations establishing connectivity of the α -substituted- γ -hydroxybutenolide ring, substructure D, of isoluffariellolide.	64
5.7	COSY and HMBC correlations establishing connectivity of C-18 to C-16 of 1- <i>O</i> -methylisoluffariellolide.	67
5.8	HMBC correlations establishing connectivity of the trimethylcyclohexenyl ring moiety, substructure A, of 1- <i>O</i> -methylisoluffariellolide.	68
5.9	COSY and HMBC correlations establishing connectivity of C-9 to C-6 of 1- <i>O</i> -methylisoluffariellolide.	69
5.10	COSY and HMBC correlations establishing connectivity of C-13 to C-6, substructure B, of 1- <i>O</i> -methylisoluffariellolide.	70
5.11	COSY and HMBC correlations establishing connectivity of the α -substituted- γ -methylbutenolide ring, substructure C, of 1- <i>O</i> -methylisoluffariellolide.	70
6.1	Surface photograph of the sponge PTN3_21C.	80

6.2	COSY and HMBC correlations establishing connectivity of the terminal isoprene unit, substructure A, of secothorectolide.	84
6.3	COSY and HMBC correlations establishing connectivity of the isoprene units, substructure B, of secothorectolide.	84
6.4	COSY and HMBC correlations establishing connectivity of the isopropene unit, substructure C, of secothorectolide.	85
6.5	COSY and HMBC correlations establishing connectivity of the isopropene unit, substructure D, of secothorectolide.	86


List of Schemes


4.1	Isolation of aplysamine-2 and aerophobin-1 from PTN3_33E, collected from Vava‘u, Tonga.	31
4.2	Isolation of fistularin-3, aeroplysinin-1 and LL-PAA216 from PTN3_46E, collected from Vava‘u, Tonga.	36
4.3	Isolation of makaluvamine G and prianosin B from PTN4_10A, collected from Vava‘u, Tonga.	47
5.1	Isolation of homofascaplysin A, isodehydroluffariellolide, luffariellolide, isoluffariellolide and 1- <i>O</i> -methylisoluffariellolide from <i>Fascaplysinopsis</i> sp. collected from ‘Eua, Tongatapu.	60
6.1	Isolation of thorectolide and secothorecetolide from PTN3_21C, collected from ‘Eua, Tongatapu.	82
6.2	Postulated biosynthetic relationship between all known <i>Luffariella</i> metabolites.	91

List of Tables

1.1	Taxonomic Classification to Order Level of Phylum Porifera.	7
4.1	Taxonomic Classification of the Order Verongida.	29
4.2	^{15}N (60 MHz), ^{13}C (150 MHz) and ^1H (600 MHz) NMR Data (CD_3OD) for Fistularin-3.	41
4.3	^{15}N (60 MHz), ^{13}C (150 MHz) and ^1H (600 MHz) NMR Data (CD_3OD) for Aeroplysinin-1.	42
4.4	^{15}N (60 MHz), ^{13}C (150 MHz) and ^1H (600 MHz) NMR Data (CD_3OD) for LL-PAA216.	43
4.5	^{15}N (60 MHz), ^{13}C (150 MHz) and ^1H (600 MHz) NMR Data (d_6 -DMSO) for LL-PAA216.	44
4.6	Taxonomic Classification of Selected Families of the Order Poecilosclerida	45
5.1	Taxonomic classification of genus <i>Fascaplysinopsis</i> from Class Demospongiae.	52
5.2	Comparison of the ^1H and ^{13}C NMR chemical shifts (CDCl_3) of the γ -hydroxybutenolide ring of isoluffariellolide, luffariellolide, and dictyodendrillin C.	65
5.3	^{13}C (150 MHz) and ^1H (600 MHz) NMR Data (CDCl_3) for Isoluffariellolide.	66
5.4	Comparison of the ^1H and ^{13}C NMR Chemical Shifts of the Butenolide Ring of Isoluffariellolide, 1- <i>O</i> -Methylisoluffariellolide, 25- <i>O</i> -Methyluffariellolide, and 1- <i>O</i> -Ethylhyrtiolide.	72
5.5	^{13}C (150 MHz) and ^1H (600 MHz) NMR data (CDCl_3) for 1- <i>O</i> -Methylisoluffariellolide.	73
6.1	Taxonomic classification of the order Dictyoceratida.	81
6.2	^{13}C (150 MHz) and ^1H (600 MHz) NMR Data (CDCl_3) for Secothorectolide.	87

Glossary

δ	Chemical shift (ppm)
ED₅₀	Dose that is effective in 50% of test subjects
IC₅₀	Concentration that is inhibitory in 50% of test subjects
CD₃OD	Deuterated methanol
CDCl₃	Deuterated chloroform
CH₂Cl₂	Dichloromethane
H₂O	Water
Me₂CO	Acetone
<i>J</i>	Scalar coupling constant
<i>m/z</i>	Mass to charge ratio
¹³C NMR	Carbon-13 Nuclear Magnetic Resonance
¹⁵N NMR	Nitrogen-15 Nuclear Magnetic Resonance
¹H NMR	Proton Nuclear Magnetic Resonance
2D NMR	Two Dimensional Nuclear Magnetic Resonance
Ac	(CH ₃ C(O)–)
br	Broad
C18	Octadecyl derivatised silica gel
COSY	Correlation spectroscopy (¹ H– ¹ H correlations depicted by )
d	Doublet
d₆-DMSO	Deuterated DMSO
dd	Doublet of doublet
DMSO	Dimethyl sulfoxide
EEZ	Exclusive Economic Zone
EtOAc	Ethyl acetate
HCOOH	Formic Acid

HMBC	Heteronuclear Multiple Bond Correlation (^1H to ^{13}C correlations depicted by )
HP20	PSDVB stationary support
HP20SS	PSDVB stationary support
HPLC	High Pressure Liquid Chromatography
HRESIMS	High Resolution Electro-Spray Ionisation Mass Spectrometry
HSQC	Heteronuclear Single Quantum Coherence
m	Multiplet
MeOH	Methanol
MS	Mass Spectrometry
NMR	Nuclear Magnetic Resonance
NOE	Nuclear Overhauser Effect
pet. ether	Petroleum ether (hexanes)
ppm	Parts per million
PSDVB	Poly(styrene-divinylbenzene)
s	Singlet
SCUBA	Self Contained Underwater Breathing Apparatus
t	Triplet
TLC	Thin Layer Chromatography
VUW	Victoria University of Wellington

Chapter 1

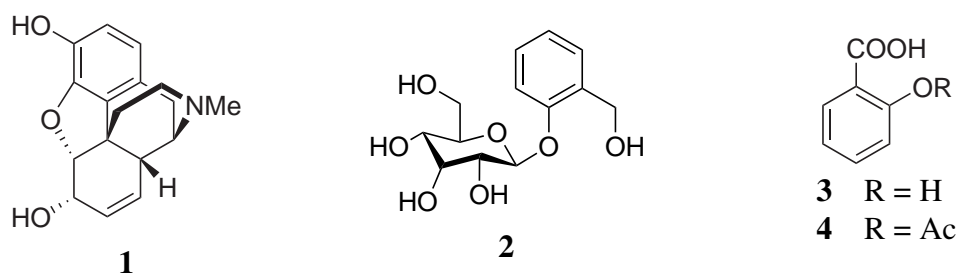
Introduction

1.1 The Role of Natural Products in Medicine

Historically, humankind has constantly relied on Nature to improve various aspects of our life. Nature has provided our basic needs for survival such as sources of food, shelter, textiles, cosmetics and medicines.¹ Terrestrial plants have been the basis for traditional medicines and herbal remedies for centuries and have been widely documented in many cultures. Records as early as 2600 BC from Mesopotamia on the use of plant materials in medicine were written on hundreds of clay tablets in cuneiform.¹ In ancient Egypt, medicines were used as early as 2900 BC, and the “Eber Papyrus” (written in about 1500 BC) is the best known medical text from this era, documenting over 700 (mostly plant-based) medicines.² The Chinese “Materia Medica”, has been repeatedly documented over centuries (~1100 BC) along with the “Shennong Herbal” (~100 BC) and the “Tang Herbal” (659 AD), documented the uses of thousands of plants as drugs or medicines.² The Indian Ayurveda (1000 BC) described in detail the uses of over 1000 different drugs or remedies.^{1,2} In the Western World, Greeks and Romans contributed to the development of the use of herbal medicines from around 300 BC, but it was the Arabs that were responsible for maintaining and expanding this knowledge.¹⁻³

The therapeutic effect of these traditional medicines is generally due to biologically active secondary metabolites present within the plant material. However, the study of secondary metabolites (also known as natural products) from terrestrial plants only began in the 1800s, where scientists isolated, purified, and defined these active substances. Subsequently, countless numbers of biologically active compounds have been isolated from terrestrial sources, many of which are used as modern-day drugs for treating various diseases and other medicinal purposes. For example, ancient texts from Mesopotamia indicated the use of poppy juice from the opium poppy (*Papaver somniferum*) for therapeutic means. But it was not until 1806 when the active compound, the narcotic

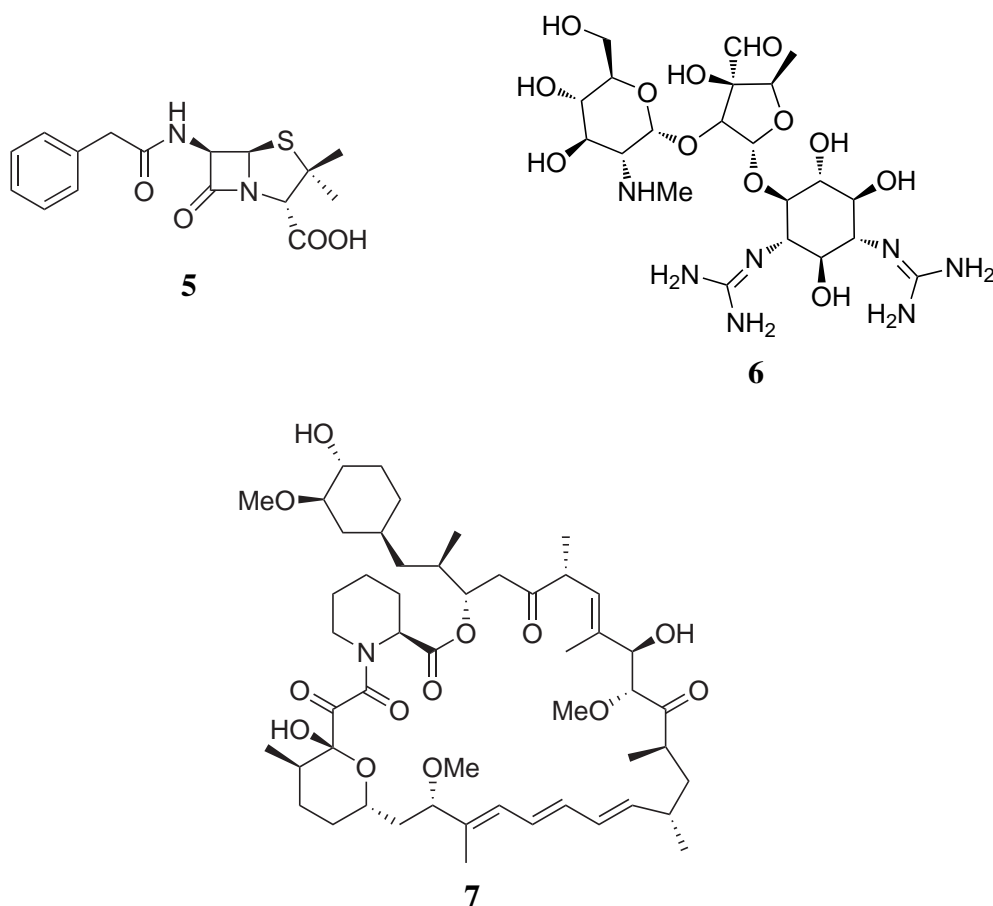
analgesic morphine (**1**), was isolated by Serturner.⁴ Morphine is considered as the first bioactive compound isolated from Nature and the first commercialised pure natural product used for medical purposes.⁴ Moreover, the “Eber Papyrus” mentioned the use of willow leaves as an antipyretic treatment. The Greeks and the Romans also discovered the antipyretic and analgesic properties of willow bark around 400 BC. In the mid 1800s, the bioactive compound salicin (**2**), was discovered, although it was its derivatives, salicylic acid (**3**) and aspirin (acetylsalicylic acid, **4**) that were commercialised in 1899.⁴ Aspirin (**4**) was the first semi-synthetic drug based on a natural product, and features as the most successful and widely used medication worldwide.^{3,4}



1.2 The Onset of the “Golden Era of Antibiotics”

The serendipitous discovery of penicillin G (**5**) from the fungus *Penicillium notatum* in 1929 heralded the modern era of antibiotics.^{1,2} This discovery signaled what many then believed to be the end of infectious disease. Followed by the success of large-scale production of penicillin during the World War II, pharmaceutical companies and scientists all over the world shifted their focus to the newly discovered world of microbes.⁵ From the 1940s to the 1970s, microbes were found to be prolific sources of structurally diverse, biologically active metabolites. This led to the discovery of new antibiotics ranging from antibacterial agents such as penicillins, aminoglycosides (e.g. streptomycin, **6**), antiparasitic drugs (e.g. ivermectins) to immunosuppressive agents such as rapamycin (also known as sirolimus, **7**).^{1,2,5} This large collection of bioactive metabolites served as the modern foundation for the treatment of infectious disease, and along with the introduction of better hygiene standards, led to a dramatic reduction in worldwide morbidity and mortality due to bacterial infections.⁶ About one-half of the drugs commonly used today were discovered during this era, referred to

as the “Golden Age of Antibiotics”.⁶ Unfortunately, this period has been short-lived, due to the resurgence of disease-causing pathogens and parasites that have developed resistance to these chemotherapies.⁷ Today, natural product chemists and pharmacologists are increasingly turning to new sources in the search for biologically active compounds, especially the marine realm.⁷

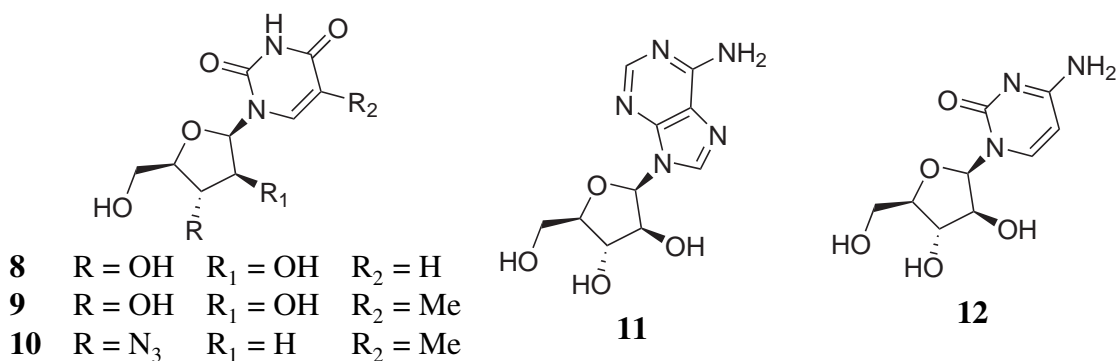


1.3 Marine Natural Products

The marine environment covers more than 70% of our planet's surface and life on Earth has its origin in the sea.⁸ This environment contains 34 of the 36 known phyla of life and offers a greater biodiversity than that of the terrestrial environment.⁹ Secondary metabolites isolated from the marine environment often have unusual and complex structures with unique functionalities and possess pronounced biological activity. This is due partially to the harsh and extreme environments in which the marine organisms may inhabit, such as high salinity, extreme pressure, low light intensity, variable temperature and low nutrient availability. Because environmental conditions in the

marine environment are so noticeably distinct, the chemistry produced by its inhabitants is also quite varied. As the terrestrial sources of pharmaceuticals and biochemicals have been considerably explored, less than 1% percent of marine species have been examined for novel chemistry.^{10–13} Thus, the oceans represent a rich and still largely untapped resource for biologically active compounds. In addition, completely unknown biochemical pathways in pathogens or disease may be discovered and targeted by such unique chemotypes, leading to the development of novel therapeutics.

Marine natural products were largely unexplored because of the difficulties involved in collecting samples. The development of technologies such as SCUBA in the 1950s, and more recently submersible vehicles, has allowed underwater exploration in both shallow- and deep-water more achievable. The first therapeutic agents from marine environment were reported in the 1950s by Bergmann *et al.* through their discovery and isolation of two novel biologically active nucleosides, spongouridine (**8**) and spongothymidine (**9**), from a Caribbean marine sponge *Cryptothia crypta*.^{14–16} Subsequent development of synthetic analogues has provided clinically relevant agents, including the anti-HIV drug azidothymidine (AZT, **10**), the antiviral agent vidarabine (Ara-A, **11**) and the arabinosyl cytosine (Ara-C, **12**). Compound **12** in particular is the first marine-derived anti-cancer agent, used for the treatment of acute myelocytic leukemia and non-Hodgkin's lymphoma.¹⁷ The discovery and development of compounds **8** and **9** created interest in the marine derived secondary metabolites and is considered to be the first significant discovery of biologically active compounds from the marine environment. Since then, through combined efforts, marine natural product chemists and pharmacologists have isolated an impressive number of promising compounds that are either already at advanced stages of clinical trials (mostly in the treatment of cancer), or have been selected as promising candidates for extended preclinical evaluation.¹⁸ The majority of these compounds are produced by invertebrates such as sponges, tunicates, soft corals, sea squirts, molluscs or bryozoans.



1.4 Marine Sponges

Marine sponges, or poriferans (from Latin *porus* “pore”, and *ferre* “to bear”), belong to phylum Porifera, and are considered to be the most primitive group of multicellular animals because they do not have true organs or tissues.¹⁹ For this reason, sponges were excluded from the animal kingdom until the late 1800s.¹⁹ Sponges are ubiquitous benthic creatures, found at all latitudes beneath the world’s oceans, from intertidal zones to the deep sea. Molecular genetics evidence placed the divergence of sponges to around 800 million years ago,²⁰ suggesting that sponges were widespread inhabitants of the reefs and their simplistic nature was a highly successful and persistent one.¹⁹ At this time, about 15,000 extant species have been described, and there are possibly twice as many undescribed species.²¹

Sponges are simple multicellular invertebrates that filter large quantities of seawater and acquire nutrients by phagocytosis of captured bacteria.²² They are sessile, soft-bodied, and are prone to predation and other environmental stress factors. Sponges have experienced an intense evolutionary pressure to evolve and produce biologically active and antagonistic metabolites. These compounds are rapidly diluted after being released into the water and hence have to be of outstanding potency to retain their efficacy.⁸ These secondary metabolites serve as a chemical defense mechanism which compensates for their lack of morphological defense structure, such as spines or a protective shell. This is no coincidence but it reflects the ecological importance of these constituents for the marine sponge. A great diversity of highly toxic compounds or distasteful metabolites is an effective strategy to fight off potential predators or to force back neighbours competing for space.¹⁸ These metabolites affect numerous biological targets which make these

organisms of great interest to marine natural products chemists and pharmacologists.

Most of the known species of sponges feed on bacteria and some host photosynthesising micro-organisms in an endosymbiotic relationship.²² Some sponges have been shown to harbour a large number of bacteria, in some cases up to 60% of the tissue volume.²³ The sponges provide the micro-organisms with a protected environment for growth and reproduction, and the sponges obtain oxygen and nutrients from the micro-organisms. Due to this relationship, there is an uncertainty as whether the biologically active metabolites isolated from sponges are in fact produced by the sponges or the micro-organisms. Recent studies have shown that a number of secondary metabolites can be attributed to the symbiotic micro-organisms.^{24,25}

Sponges display an incredible variety of colours and shapes. In general, sponge species are difficult to identify by casual comparison to some illustration or photograph. Sponges have indeterminate growth patterns, such as shape, size, colour and showed considerable plasticity in response to environmental factors and location. The lack of structural features make them hard to characterise, which leads to problems with their classification. However, most sponges have spicules; microscopic skeletal structures that provide support and sometimes deter predators. Comparison of the shapes and sizes of these spicules found in the sponge with data from the literature aid the identification of sponge species (since spicules are the only consistent structures in sponges). From these characterisations, the Porifera have been divided into three classes: Hexactinellida (siliceous/glass spicules), Calcarea (spicules of crystalline CaCO_3) and Demospongiae (siliceous spicules and/or collagen fibres).²¹ The largest class, Demospongiae contains about 90% of the sponge species within 15 orders and 25 families. The Calcarea is divided into 24 families within five orders, and the class Hexactinellida contains five orders and 17 families (Table 1.1).²¹ Recently, different techniques have also been used as tools in sponge taxonomic classification such as chemotaxonomic trends and molecular biology, leading to the re-examination of sponge taxonomy at the order level and below.²⁶

Table 1.1. Taxonomic Classification to Order Level of Phylum Porifera.²¹

Kingdom	Phylum	Class	Sub-class	Order
Metazoa	Porifera	Demospongiae	Ceractinomorpha	Agelasida
				Dendroceratida
				Dictyoceratida
				Halichondrida
				Halisarcida
				Haplosclerida
		Hexactinellida	Tetractinomorpha	Poecilosclerida
				Verongida
				Verticillitida
				Astrophorida
		Homoscleromorpha	Homoscleromorpha	Chondrosida
				Hadromerida
				“Lithistids”
		Hexasterophora	Hexasterophora	Spirophorida
				Homosclerophida
				Aulocalycoida
				Hexaactinosida
		Amphodiscophora	Amphodiscophora	Lychnicosida
				Lyssacosida
		Calcareia	Calcareia	Amphodiscosida
				Lithonida
				Leucosolenida
		Calcinea	Calcinea	Baerida
				Clathrinida
				Murrayonida

1.5 Tongan Marine Sponges and Chemistry

Secondary metabolites isolated from tropical marine sponges are noted for their novelty and high chemical diversity, exhibiting a broad range of biological activities and unusual structures. The intense tropical coral reefs and warm waters comprise some of the densest and most diverse habitats for enormous numbers of organisms. As a result, the tropical sponges tend to use less energy through homeostasis due to the warmer waters in which they live, therefore they are able to devote more energy to producing biologically active compounds as chemical defenses. Additionally, the higher grazing pressure from many different predators enhanced the production of biologically active compounds.

The Kingdom of Tonga is an archipelago in the Central Indo-Pacific Ocean consisting of 176 islands (36 of which are inhabited). Tonga is located at latitude 20° 0' 0'' S and longitude 175° 0' 0'' W (Figure 1.1) and is divided into four main groups; Tongatapu, Vava'u, Ha'apai and 'Eua. The largest island, Tongatapu, on which the capital of

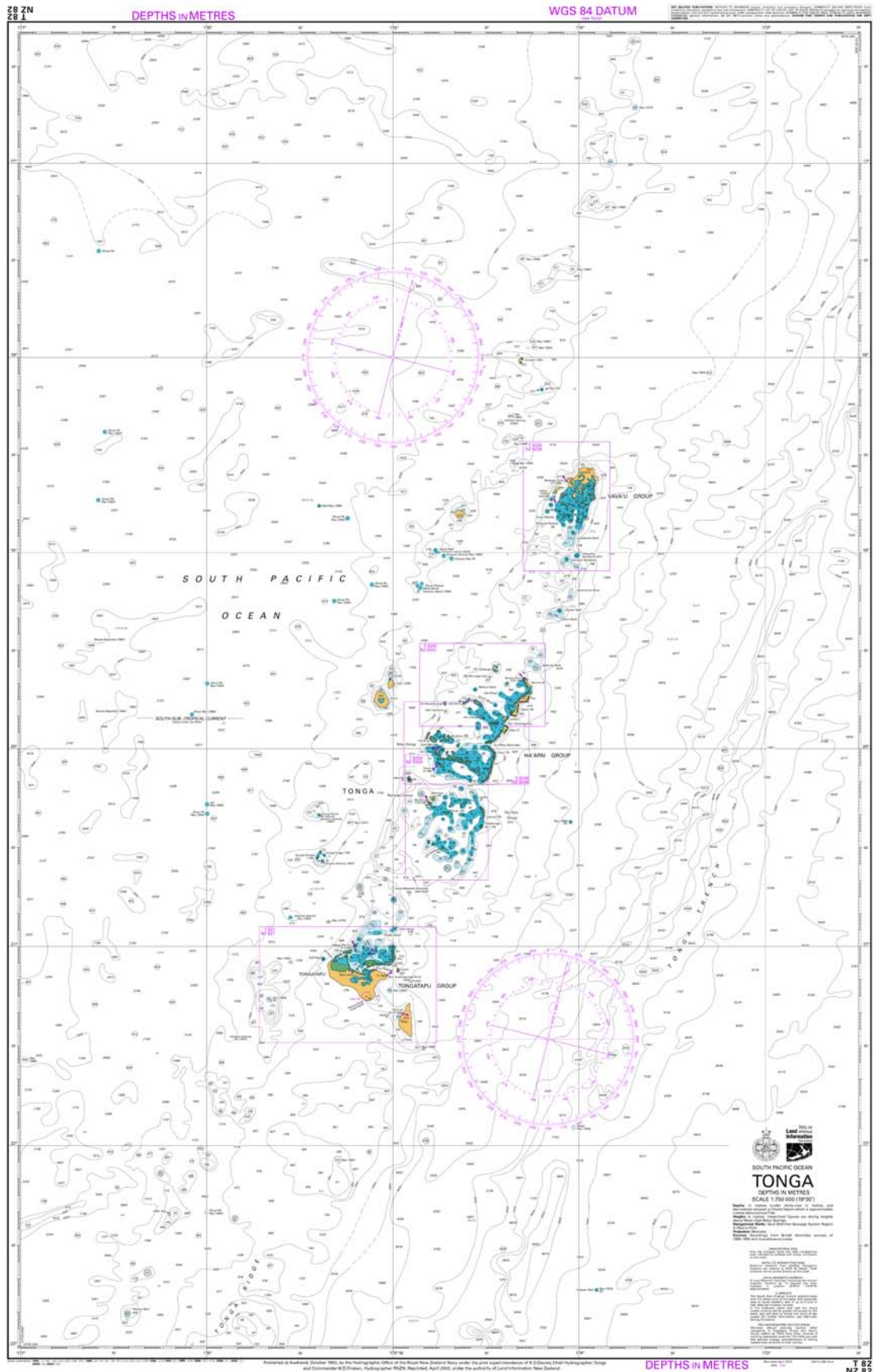


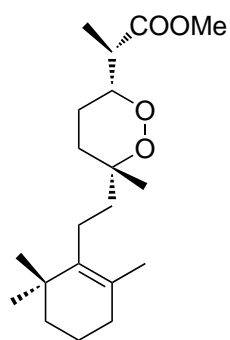
Figure 1.1. Map of the Kingdom of Tonga. Map courtesy of LINZ.

Nuku‘alofa is located covers 257 square kilometres. Geologically the Tongan islands are of two types: most have a limestone base formed from uplifted coral formations; others

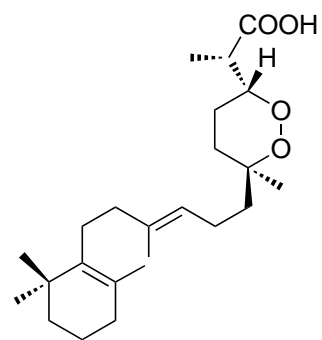
consist of limestone overlaying a volcanic base. Due in part to its geographical central location at the meeting of two oceans (Indian and Pacific Oceans), Tongan waters have a distinct marine realm and comprise one of the greatest diversity of marine life. Tonga has a total land area of 688 sq km with Exclusive Economic Zone (EEZ) of 700,000 sq km, 1000 times more its land area, thus Tonga is an excellent place to study marine natural products.

There are few reports of marine natural products isolated from Tongan marine organisms, even though its marine environment offers an amazing and fascinating biodiversity. The first marine natural products research group to investigate the Tongan sponges was led by Phillip Crews from the University of California at Santa Cruz. Their collections were made in the early 1980s from Vava'u and the Ha'apai groups, located in northern Tonga.

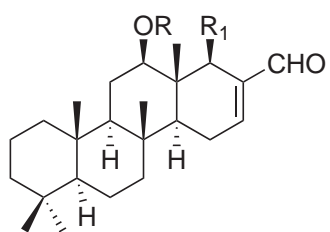
The first novel compound reported from the Tongan marine environment was nuapapu A methyl ester (**13**) (formerly known as methyl nuapauanoate) isolated together with the known norsesterterpene muquibilin (**14**).^{27,28} Compound **13** was obtained from a large soft drab sponge initially identified as *Prianos* sp., but revised to *Diacarnus* cf. *spinopoculum*, and is considered to be the first norditerpene isolated from a marine sponge.^{28,29} Nuapapu A (**13**) demonstrated selective cytotoxicity against eight tumour cell lines in the soft agar assay, with GI₅₀ values of less than 0.5 μ M.²⁸ Interestingly, the norditerpene peroxides clearly demonstrated superior profiles compared to the norsesterterpene peroxides.²⁸ A study of the anti-inflammatory active extracts from the sponge *Hyrtios erecta* revealed a novel scalarane norsesterterpenoid, hytrial (**15**).³⁰ Hytrial (**15**) was re-isolated with a further five novel scalarane-type sesterterpenes (**16–20**).³¹ Compound **15** has shown to decrease by 43% the weight of mouse ear oedema induced by PMA at a concentration of *ca.* 50 μ g per ear.³¹ Heteronemin acetate (**17**) was also cytotoxic against the human normal cell line (human oral fibroblasts) with an IC₅₀ value of 16.09 μ M.³² 12-Deacetyl-12-*epi*-scalaradial (**16**) and **17** showed antitubercular activity with MIC values of 63 μ M and 3 μ M respectively.³² It was suggested that the oxygenated pattern at C-24 and C-25 of the scalarane-type sesterterpenes might assert a strong influence on their resultant biological activities.³¹



13

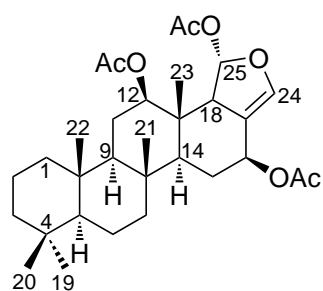


14



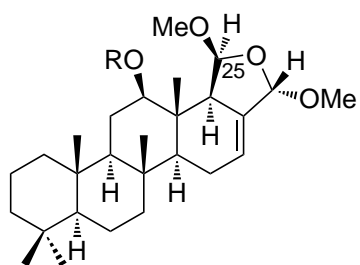
15 R = Ac R₁ = H

16 R = H R₁ = CHO



17

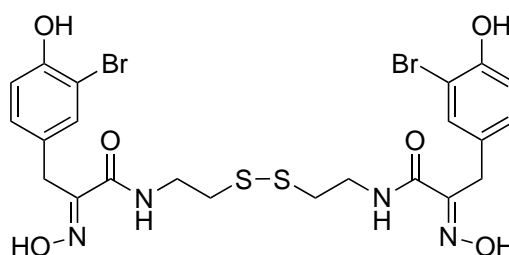
18 12-*epi*



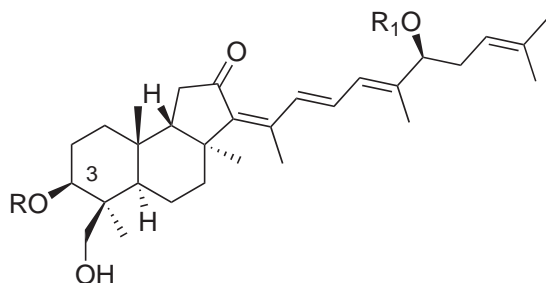
19 R = Ac

20 25-*epi*, R = H

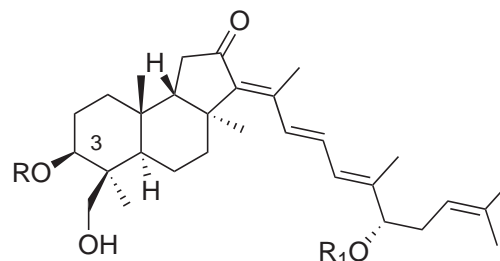
Psammaplin A (**21**) was reported in 1987 from the marine sponge *Psammaplysilla* sp., and is the first example of a disulfide derived from a marine sponge.³³ In 2007, 20 years after the first report, there were 45 articles published based on the chemical study of **21**.³⁴ Compound **21** inhibits the activities of several key enzymes in prokaryotic and eukaryotic systems, including those involved in epigenetic control of gene expression, DNA replication, angiogenesis, microbial detoxification, and tumor cell growth.^{35–44} Three novel isomalabaricane triterpenes (**22–24**) were obtained from the organic extract of the specimen of *Japsis* sp. collected near Tonga, along with known triterpene 3-*epi*-29-hydroxystelliferin E (**25**).⁴⁵ As isomalabaricane triterpenes are known to isomerise upon exposure to light, the isomeric mixtures of the four compounds were tested against melanoma (MALME-3M) and leukemia (MOLT-4) cell lines. Against MALME-3M cell line the mixtures of 29-hydroxystelliferin A (**23**)/29-hydroxystelliferin B (**26**) and stelliferin G (**24**)/13*E*-stelliferin G (**27**) were the most growth-inhibitory (IC₅₀ values of 0.11 and 0.23, $\mu\text{g/mL}$ respectively).⁴⁵ The other two mixtures, 29-hydroxystelliferin E (**22**)/13*E*-29-hydroxystelliferin E (**28**) and 3-*epi*-29-hydroxystelliferin E (**25**)/13*E*-3-*epi*-29-hydroxystelliferin E (**29**), were approximately 10-fold less potent with a similar trend observed with the MOLT-4 results.



21



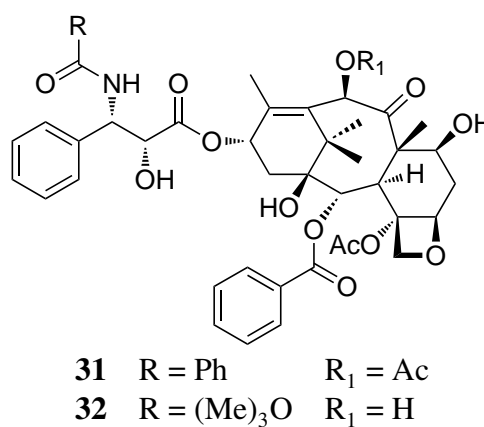
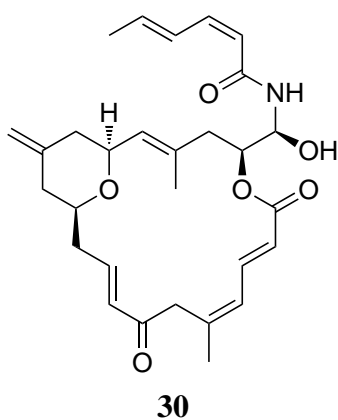
- | | | | |
|-----------|-----------------|---------------------|---------------------|
| 22 | R = Ac | R ₁ = Ac | |
| 23 | R = Ac | R ₁ = H | |
| 24 | 3- <i>epi</i> , | R = H | R ₁ = Ac |
| 25 | 3- <i>epi</i> , | R = Ac | R ₁ = Ac |

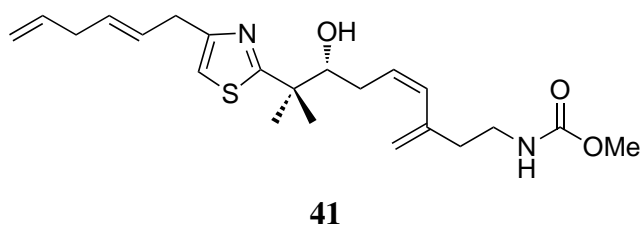
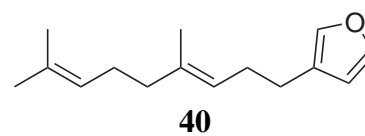
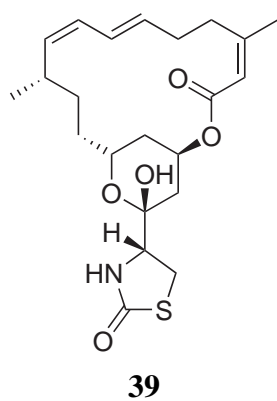
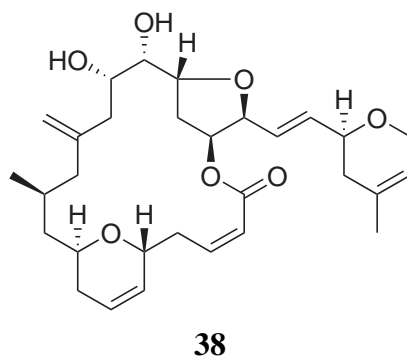
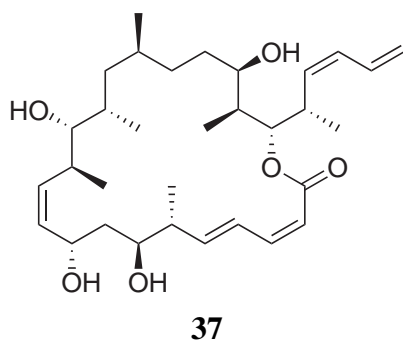
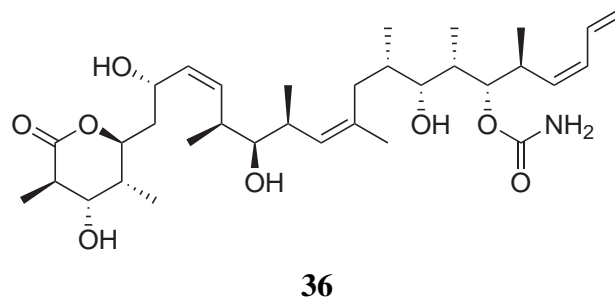
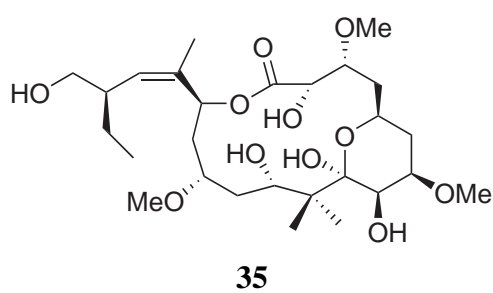
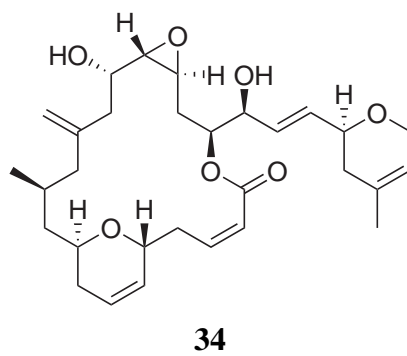
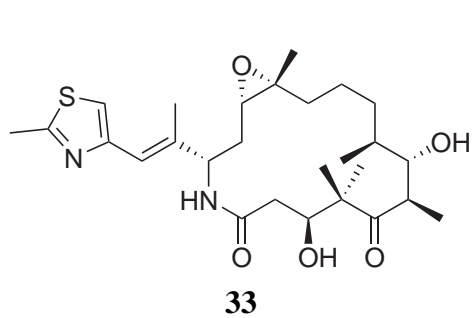


- | | | | |
|-----------|-----------------|---------------------|---------------------|
| 26 | R = Ac | R ₁ = H | |
| 27 | 3- <i>epi</i> , | R = Ac | R ₁ = Ac |
| 28 | R = Ac | R ₁ = Ac | |
| 29 | 3- <i>epi</i> , | R = H | R ₁ = Ac |

The paucity of investigation and analysis on Tongan marine fauna and the promising

results mentioned above suggested that more research should be carried out on Tongan marine organisms. To date, there are no reported marine natural products isolated from Tongan marine organisms other than sponges. For the last two years, the Marine Natural Products group at Victoria University of Wellington (VUW) has shifted their research and attention from New Zealand marine organisms to the tropical Pacific marine environment of Tonga. Recent results include the re-isolation of zampanolide (**30**), a potent 20-membered macrolide from the Tongan marine sponge *Cacospongia mycofijiensis*.⁴⁶ Although compound **30** was originally reported from the Japanese marine sponge *Fasciospongia rimosa*, and exhibited potent cytotoxicity against several cell lines (IC₅₀ 1–5 ng/mL), there was no information available on the mode of action.⁴⁷ The recent isolation of **30** allowed further investigation on its mode of action, which proved to be a novel and potent microtubule-stablising compound. This places zampanolide (**30**) in an important group of anti-cancer compounds that includes the clinically valuable paclitaxel (**31**), docetaxel (**32**), ixabepilone (azaepothilone B, **33**); and a number of other potent microtubule-stabilising agents, including laulimalide (**34**), peloruside A (**35**), discodermolide (**36**), and dictyostatin (**37**).^{48,49} Zampanolide (**30**) is cytotoxic in nanomolar concentrations by arresting cells in the G₂M phase of the cell cycle by polymerising microtubules.^{46,50} Further examination of *C. mycofijiensis* generated a number of known bioactive compounds, including laulimalide (**34**) and isolaulimalide (**38**) (both are microtubule-stabilising agents), latrunculin A (an actin-destabilising agent, **39**), dendrolasin (having pheromonal activity, **40**), and mycothiazole (**41**).⁵⁰





Chapter 2

Isolation and Screening of Secondary Metabolites

2.1 Isolation Techniques

The goal of the Marine Natural Products Group at VUW is to isolate novel chemical structures with interesting and useful biological activities, utilising novel techniques. These include a chromatographic method, cyclic loading, as well as NMR-based screening methods, which are discussed below.

2.1.1 Cyclic Loading

For biological activity of secondary metabolites to be effective, the structure must possess a mixture of both hydrophilic and hydrophobic properties that enables them to be easily transported across cell membranes and other biological barriers.⁵¹ The crude extracts of sponges contain a wide range of compounds with varying degrees of polarity, ranging from polar amino acids, salts and sugars to non-polar fats, lipids and steroids. This can be best described in terms of a “mass window” (Figure 2.1), where the intermediate region (lowest relative mass, mid-polarity) contains few primary metabolites, making the mass window an ideal target for the first stage of fractionation of a crude extract.

The Marine Natural Products group at VUW has developed a technique known as “cyclic loading”.⁵² This reversed-phase chromatographic technique utilises poly(styrene-divinylbenzene) (PSDVB), as the stationary phase. The resin is an inexpensive, chemically inert, crosslinked polymeric resin, that is highly porous, lacks polar sites, and is stable over a large pH range.⁵³ These characteristics contribute to the repeated use of PSDVB without any significant decrease in performance. The first stage of cyclic loading involves passing the extract(s) through the column. This allows most of the non-polar compounds in the extracts to adhere to the PSDVB beads. The eluent is then diluted

with H₂O and passed back through the column. Under the normal circumstances, addition of H₂O to a crude extract would result in the precipitation of the non-polar compounds, which is avoided during cyclic loading, as the most non-polar fats and triglycerides have adsorbed to the column during the first pass. As the eluent is gradually made more polar by each dilution with H₂O, the more polar compounds in the extract are adsorbed to the column. The cyclic process is repeated until all the compounds of interest are adhered to the PSDVB beads in the column.

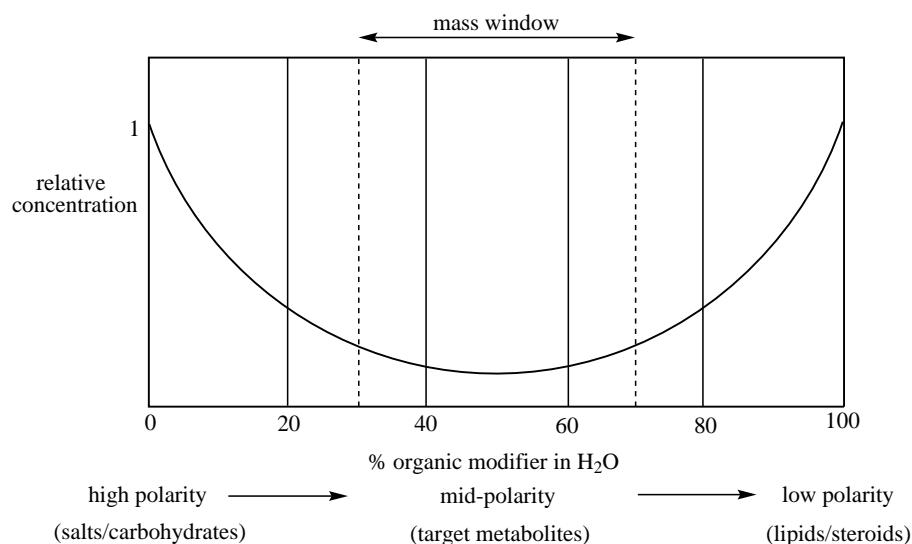


Figure 2.1. Schematic of the mass distribution in a typical marine sponge extract.

Once the crude sponge extracts are retained in the column, it is washed with distilled H₂O to remove any remaining salts. The loaded column then can be sequentially eluted with a gradient of increasing organic modifier (Me₂CO or MeOH)/H₂O to obtain a number of fractions of decreasing polarity. During the elution process, the earlier fractions usually contain mostly highly polar materials such as amino acids and sugars. The non-polar materials such as lipids and steroids usually come off in the later fractions. The mid-polarity materials that contain most of the interesting secondary metabolites are eluted in the middle fractions (with few exceptions). The fractions obtained from cyclic loading contain varying amounts of H₂O, which is a major problem if the fraction must be concentrated under vacuum or reduced pressure. This problem is overcome by using a modified cyclic loading method called “back loading”. The fractions containing water are further diluted with H₂O and cyclic loaded back through the column. The column is then eluted with pure organic solvent (Me₂CO or MeOH), creating a fraction with almost no water that can be concentrated under reduced pressure more easily.

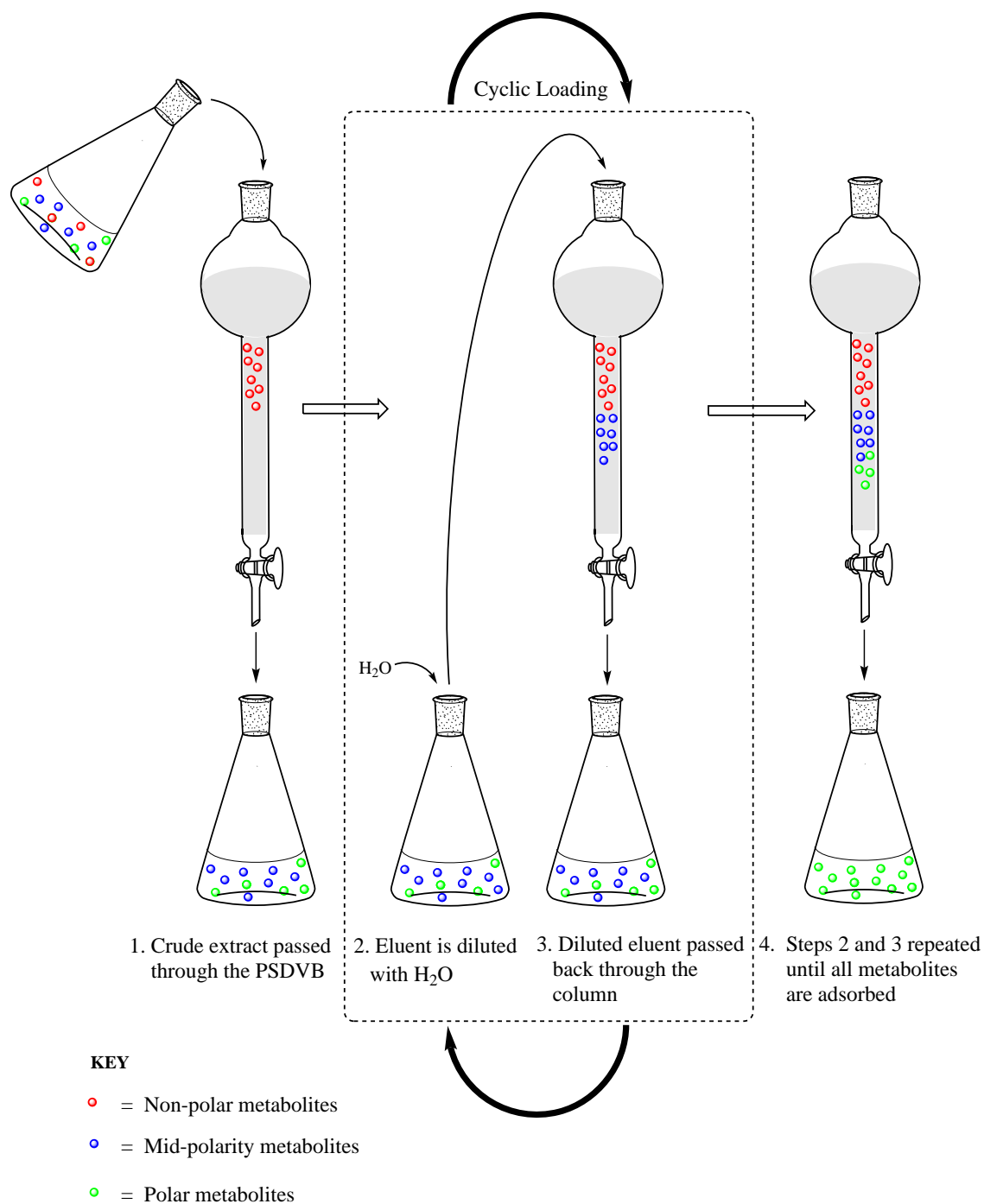


Figure 2.2. Schematic of the cyclic loading process.

2.2 Screening of Marine Organisms

2.2.1 Bioassay-Directed Screening

Bioassay (biological assay) directed isolation is the most common technique used for identifying novel and biologically active secondary metabolites from crude extracts. The main goal of a bioassay is to find and identify a biologically active compound. Extracts

with any biological activity are iteratively fractionated and subjected to the same assay until the pure compound(s) is isolated. The major advantage of this method is the isolation of a pharmaceutically active secondary metabolite and maybe novel activity against the chosen target. However, the large number of fractions to be assayed is time consuming and often costly. Additionally, the activity of lower concentration metabolites can be masked by a higher concentration metabolite since an organism can produce numerous biologically active compounds.

2.2.2 NMR-Based Screening

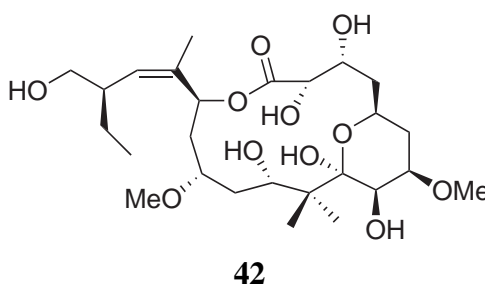
In the case of NMR-based screening, the main goal is to find and isolate novel secondary metabolites and then investigate their biological activity after isolation. Secondary metabolites have a biological function and therefore they may have medical and pharmaceutical application. This spectroscopy-directed isolation technique employs NMR spectroscopy as a guide for the isolation and identifies the interesting compounds. The advantages of this technique is that it is applicable to the isolation of most secondary metabolites. It has a good response factor and potential for vast structural information content. However, a solubility issue is a major problem due to larger range of polarities present in the crude extracts. This problem is overcome by using cyclic loading as the primary partition stage after extraction.

2.3 VUW Screening Methodology

The VUW Marine Natural Products Group has developed a NMR-based screening protocol for screening marine sponges and guiding the isolation procedure. Generally, for screening a typical New Zealand sponge, about 100 g of sponge is extracted twice with MeOH. For a Tongan sponge, approximately 25 g is required due to the fact that tropical sponges are richer in chemical contents (smaller amount of sponges are collected as well). The extracts are then cyclic loaded onto a PSDVB column and then the column is desalted with distilled H₂O. The loaded column is then sequentially eluted with 30%,

75% Me₂CO/H₂O and 100% Me₂CO. The biologically active secondary metabolites tend to elute in the intermediate region, the 75% Me₂CO/H₂O fraction.

The idea behind the NMR-based screening protocol is to analyse the 75% Me₂CO/H₂O fraction by differentiating between common and unusual resonances present in the NMR spectra of semi-purified extracts. This simple screening technique resulted in the isolation of biologically active compounds such as peloruside A (**35**) and B (**42**), among others.^{52,53} However, the presence of primary metabolites conceals a large portion of the ¹H NMR spectrum, limiting the amount of structural information available. As a result, 2D NMR experiments (COSY, HSQC, and HMBC) have been used as a screening tool, since 2D NMR spectroscopy offers more detailed structural information, and a great advantage in the detection of novel secondary metabolites.



2.3.1 HSQC Mask

Initially, the COSY experiment was used as a screening tool, but it was deemed too complicated to be readily converted to a database form, so HSQC spectra with their relatively simple ¹H–¹³C correlation data were chosen.⁵⁴ In addition, the HSQC experiment provided more functional information in the carbon dimension. To construct the electronic mask, the HSQC data of the 75% Me₂CO/H₂O screen fractions are added together to generate a digital mask. For any given screen, the HSQC spectrum is compared to the mask where common signals (**green peaks**) are distinguished from those that are interesting. Correlations that are frequently observed are from compounds that are common amongst the screened sponges and are therefore likely to be primary or known metabolite(s). Thus, uncommon correlations (**red peaks**) may indicate the presence of novel secondary metabolite(s). The intensity of a particular correlation also indicates the

relative amount of the compound present in the sponge. This current screen has been used in the isolation of new secondary metabolites from sponges and also adapted for red algae screening.^{54–57} Unfortunately, this screening method is based only on New Zealand marine organisms and has not been applied to Tongan specimens, which is a major problem during the course of this study, which led to isolation of compounds already known from the literature.

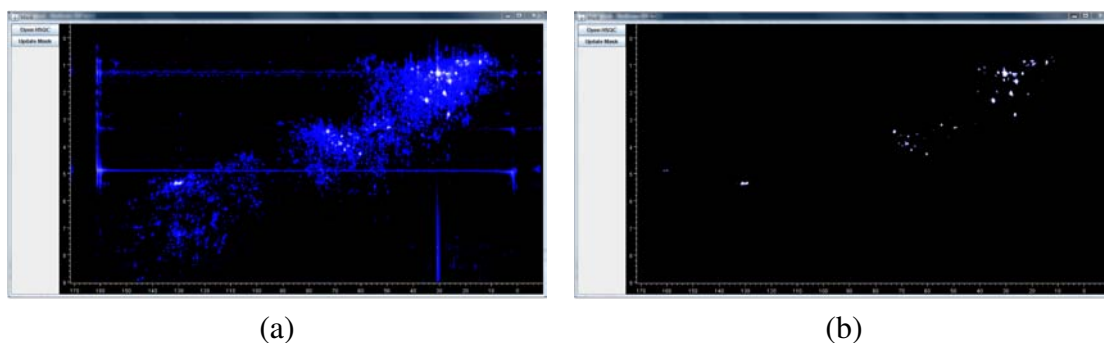


Figure 2.3. (a) Computer generated mask of HSQC data (contains 160 sponges). (b) Common correlations in the HSQC masks.

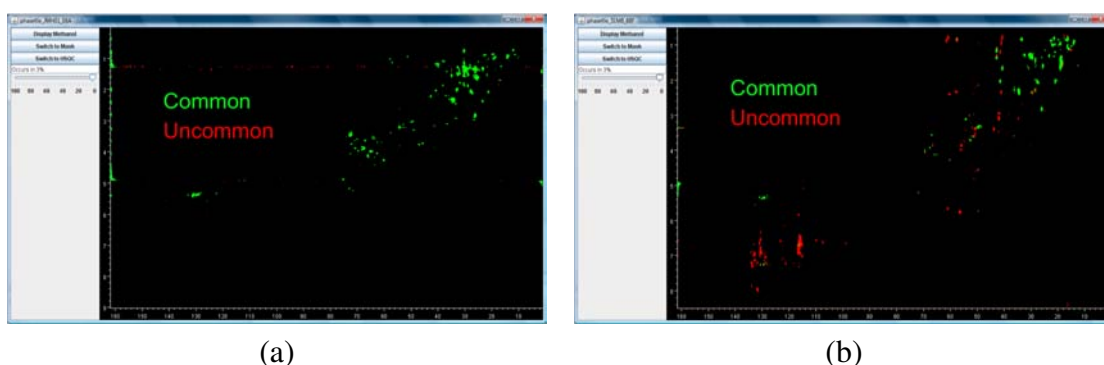


Figure 2.4. (a) An uninteresting sponge screen. (b) An interesting screen.

2.4 Future Screening Methods

The HSQC screen has been successful in reducing the volume of extraneous information which is presented to the analyst by masking out correlations in HSQC spectra which are of little or no interest due to their repeated occurrence in extracts. At the same time, this computer-based NMR screen has its limitations. Firstly, the non-protonated functional groups are not taken into account; for example carbonyl carbons (except aldehydes), non-protonated olefinic carbons, nitriles, imines, and sp^3 quaternary carbons. Secondly, the selection of the $^1J_{CH}$ value dictates which correlations appear most intense. Since

$^1J_{\text{CH}}$ ranges from about 110 to 320 Hz, the current HSQC screen has a optimum $^1J_{\text{CH}}$ value of 140 Hz, which allows $^1J_{\text{CH}}$ values between 110-170 Hz to appear with the highest intensity. Therefore, functional groups with $^1J_{\text{CH}}$ values outside this range appear proportionally weaker or missing unless the optimum value is changed.

2.4.1 HMBC Screen

An additional screen based on the HMBC experiment is currently being developed in a similar manner to the HSQC screen. As the HSQC experiment correlates ^{13}C nuclei with directly attached ^1H only, the HMBC experiment offers multiple-bond correlations between ^1H and ^{13}C nuclei (^1H – ^{15}N HMBC is also utilised) thus providing more information, especially in the carbon dimension. The experiment can be performed concurrently with the HSQC screen experiment (mentioned before) and thus interesting one-bond correlations in the HSQC screen can be extended to multiple-bond correlations from the HMBC screen. An HMBC screen would potentially be an extremely powerful technique at an early stage of purification and this would help decide if a sponge extract is worthy of further investigation without fully committing to the purification process.

Chapter 3

Sponges Investigated by Spectroscopic Screening

During the course of this study, two collection trips were made to Tonga. The first collection trip was to Tongatapu and 'Eua in late 2008 and the second was to the Vava'u Group in late 2009 (Figure 1.1). A total of 17 marine sponges were screened using the VUW method. Several sponges were selected for investigation based on their promising results in the 2D NMR spectra screening method, which led to isolation of novel and known compounds which are detailed in the following chapters.

3.1 Sponges Screened from Tongatapu and 'Eua

PTN3_13A

PTN3_13A is a very soft, unidentified orange coloured sponge (940 g) collected by snorkel from the Popua shoreline, near the capital Nuku'alofa, Tongatapu, Tonga. The sponge (22 g) was screened and the screen spectra contained resonances attributed to aromatics and evidence of peptides observed in HMBC spectrum. A second, large-scale bulk extraction of the sponge (329 g) was performed. Subsequent analysis of this extract showed no evidence of the interesting resonances and solubility issues with the NMR solvents were encountered. No further analysis was performed.



Figure 3.1. Surface photo of the PTN3_13A sponge.

PTN3_13C

PTN3_13C is an unidentified sponge (833 g) collected from the front coast of Popua near the capital Nuku‘alofa, Tongatapu, Tonga. 23 g of the sponge was screened. The screen spectra of the 75% Me₂CO/H₂O fraction contained non-interesting resonances. Further purification and analysis was automatically discontinued.



Figure 3.2. Surface photo of the PTN3_13C sponge.

PTN3_14B

PTN3_14B is an unidentified yellow coloured, finger sponge (130 g) from ‘Ohonua Harbour, ‘Eua, Tonga. The screen spectra of the 75% Me₂CO/H₂O fraction contained a number of resonances largely attributed to aromatics. No further analysis was performed.



Figure 3.3. Surface photo of the PTN3_14B sponge.

PTN3_14E

PTN3_14E is an unidentified sponge (104 g) collected from 'Ohonua Harbour, 'Eua, Tonga. With 22 g of the sponge being screened, the screen spectra contained resonances attributed to aromatics, oxymethylene and oxymethine regions. Due to encountering solubility issues with the NMR solvents, no further analysis was performed.



Figure 3.4. Surface photo of the PTN3_14E sponge.

PTN3_14F

PTN3_14F is an unidentified sponge (274 g) collected from 'Ohonua Harbour, 'Eua, Tonga. 24 g of the sponge was screened and the screen spectra contained resonances largely attributed to terpenoids with great similarity to that of PTN3_19A and PTN3_22B. Therefore, further purification and analysis was discontinued.



Figure 3.5. Surface photo of the PTN3_14F sponge.

PTN3_15C

PTN3_15C is a leathery grey unidentified sponge (525 g) collected from the coastline of Houma, 'Eua, Tonga. A 23 g of the sponge was screened. The screen spectra of the 75% Me₂CO/H₂O fraction contained resonances attributed to aromatics, olefinic and oxymethine regions. Further purification and analysis was discontinued.



Figure 3.6. Surface photo of the PTN3_15C sponge.

PTN3_16F

PTN3_16F is an unidentified yellowed coloured, rubble-like sponge (150 g) from the coastline of Houma, 'Eua, Tonga. 23 g of the sponge was screened and the screen spectra of the 75% Me₂CO/H₂O fraction contained resonances largely attributed to oxymethine, oxymethylene, and oxymethyl regions with few in the aromatic region. Further purification and analysis was discontinued.



Figure 3.7. Surface photo of the PTN3_16F sponge.

PTN3_18C

PTN3_18C is an unidentified grey dictyoceratid sponge (21 g) collected from the coast of Houma, 'Eua, Tonga. The screen spectra of the 75% Me₂CO/H₂O contained resonances attributed to aromatics, oxymethyls and oxymethines. No further analysis was performed.



Figure 3.8. Surface photo of the PTN3_18C sponge.

PTN3_19A and PTN3_22B

PTN3_19A and PTN3_22B were an unidentified sponges (250 g), reddish-coloured of the genus *Fascaplysinopsis* were collected from an underwater cave in southwestern 'Eua, Tonga, with only 25 g of the sponges screened. The screen spectra of the 75% Me₂CO/H₂O fraction contained resonances largely attributed to aromatics and terpenoids. A second, large-scale bulk extraction of the sponge (200 g) was performed. Purification and analysis of the bulk extracts led to isolation of the three known compounds homofascaplysin A (**43**), isodehydroluffariellolide (**44**) and luffariellolide (**45**), along with two novel sesterterpenes, isoluffariellolide (**46**) and 1-*O*-methylisoluffariellolide (**47**). Isolation and the structure elucidation of the two novel sesterterpenes (**46–47**) will be discussed in Chapter 5.

PTN3_21C

PTN3_21C is an unidentified sponge (350 g) from the order Dictyoceratida collected from an underwater cave in southwestern 'Eua, Tonga. Only 26 g of the sponge was originally screened. The screen spectra of the 75% Me₂CO/H₂O fraction contained resonances largely attributed to terpenoids and sign of aldehydes. Further purification

led to the isolation of the known sesterterpene thorectolide (**48**) and a novel sesterterpene, secothorectolide (**49**). The isolation and structural elucidation of secothorectolide (**49**) is dealt with in Chapter 6.

PTN3_25E

PTN3_25E is an unidentified orange coloured sponge (400 g) collected from Fāfā Island, located off the coast of Nuku‘alofa, Tongatapu, Tonga. The sponge (22 g) was screened and the screen spectra contained resonances attributed to aromatics and evidence of peptides observed in the HMBC spectrum. It was concluded that it is the same sponge as PTN3_13A. No further analysis was performed.



Figure 3.9. Surface photo of the PTN3_25E sponge.

PTN3_25F

PTN3_25F is an unidentified sponge (700 g) collected from Fāfā Island, located off the coast of Nuku‘alofa, Tongatapu, Tonga. Only 23 g of the sponge was taken for screening. The screen spectra of the 75% Me₂CO/H₂O fraction contained resonances attributed to aromatics and oxymethylene regions. Further purification and analysis was discontinued.

3.2 Sponges Screened from the Vava‘u Group

PTN3_33F

PTN3_33F is an unidentified sponge (1989 g) belong to the order Verongida was collected from Ano Beach, Vava‘u, Tonga by snorkel. 27 g was screened and the screen spectra of



Figure 3.10. Surface photo of the PTN3_25F sponge.

the 75% Me₂CO/H₂O fraction contained resonances attributed to aromatics, oxymethine and oxymethyl regions. Further purification of this fraction led to the isolation of two known bromotyrosine alkaloid compounds aplysamine-2 (**50**) and aerophobin-1 (**51**). The isolation of compounds (**50–51**) will be discussed in Chapter 4.

PTN3_45H

PTN3_45H is a bright yellow calcareous sponge (825 g) of the genus *Leucetta* collected from an underwater cave from Tu‘ungasika Island, Vava‘u, Tonga. 21 g was taken for screening. The screen spectra of the 75% Me₂CO/H₂O fraction contained interesting resonances largely attributed to aromatics. Subsequent purification and analysis of the 75% Me₂CO/H₂O was discontinued and set aside due to the small sample and lack of time for large-scale extracts.

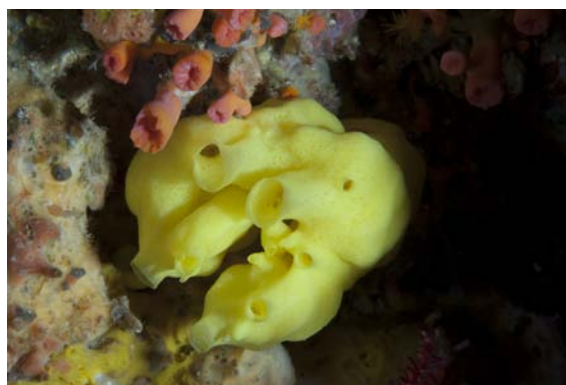


Figure 3.11. Underwater photo of the *Leucetta* sp. (courtesy of Karen Stone).

PTN3_46E

PTN3_46E is an unidentified sponge (365 g) of the order Verongida, collected from Tu‘ungasika Island, Vava‘u, Tonga. The sponge (27 g) was extracted and the screen spectra of the 75% Me₂CO/H₂O contained resonances attributed to aromatics, oxymethine, oxymethylene, and oxymethyl regions. Further purification of this fraction led to isolation of three known bromotyrosine compounds fistularin-3 (**52**), aeroplysinin-1 (**53**) and LL-PAA216 (**54**), which will be discussed in Chapter 4.

PTN4_05D

PTN4_05D is an unidentified sponge (701 g) collected near Hunga, Vava‘u, Tonga. The sponge (27 g) was selected for screening due to its similarity to genus *Fascaplysinopsis* (PTN3_19A collected from ‘Eua). However, the screen spectra of the 75% Me₂CO/H₂O fraction contained resonances attributed to terpenoids and nothing in the aromatic regions (similar to PTN3_14F). Further purification and analysis was discontinued.



Figure 3.12. Surface photo of the PTN4_05D.

PTN4_10A

PTN4_10A is an unidentified black sponge (1449 g) collected from Fakafotulā, Vava‘u, Tonga. 21 g was screened and the screen spectra of the 75% Me₂CO/H₂O fraction contained resonances largely attributed to heteroaromatics. Further purification of this fraction led to the isolation of known compounds makaluvamine G (**55**) and prianosin B (**56**). The isolation of compounds **55** and **56** will be discussed in Chapter 4.

Chapter 4

The Isolation of Known Compounds from Tongan Sponges

4.1 Order Verongida

The lack of mineral spicules in the order Verongida makes their taxonomic identification more difficult. Verongid sponges range in form, from tall tubular vases to thin spreading crusts. Stalk formation is also a common feature. Verongids show a common marked oxidative colour change at death or exposure to air, changing from yellow/yellow-green to dark brown, or more frequently deep purple/black. Pigmentation in some sponges is attributable to cyanobacteria. The order consists of four families: Aplysinidae, Aplysinellidae, Ianthellidae and Pseudoceratinidae, as shown in Table 4.1.²¹ Verongids are extremely distinct biochemically, they contain a vast array of bromotyrosine-derived compounds, which occur in all genera that have been studied.²¹ In this study, two sponges (Figures 4.1 and 4.6) were examined and were tentatively identified as Verongid sponges based on their chemical constituents.

Table 4.1. Taxonomic Classification of the Order Verongida.²¹

Class	Order	Family
Demospongiae		
	Verongida	
		Aplysinidae
		Aplysinellidae
		Ianthellidae
		Pseudoceratinidae

4.1.1 Bromotyrosine Derivatives

As mentioned before, marine sponges of the order Verongida have been noted to be a rich source of bromotyrosine-derived secondary metabolites with interesting biological

activities. The unusually large number of biosynthetically related compounds has been linked to the potentially large number of chemical variations that are possible within the aromatic ring and/or side chains of the tyrosine moiety. The aromatic ring can be either maintained, reduced, oxidised or mono- or dibrominated.^{58–60} The bromotyrosine moiety can also undergo rearrangement to a spirooxepinisoxaline system, presumably via a common oxide intermediate as in the case of the psammaphysins.^{61–63} Alternatively, the bromotyrosine can be rearranged to form the spirocyclooxazoline moiety, such as in fistularins and aerotionin-1.^{64,65} The bromotyrosine units can also link up to form linear chains through amide bonds as in the case of fistularin-3,⁶⁴ or through ether bonds as in the formation of macrocyclic bastadins.^{66–68} Currently, there are over 300 metabolites isolated from Verongid sponges,⁶⁹ and therefore the isolation of new metabolites from these sponges is a real challenge.^{70,71}

4.1.2 PTN3_33F

PTN3_33F was collected by snorkel from Ano Beach, Vava'u, Tonga. The sponge was massive, with a yellow-green pigmented surface and yellow interior (Figure 4.1). The sponge oxidised rapidly to dark black at death. The sponge was extracted twice in MeOH and the extracts were cyclic loaded onto reversed-phase PSDVB beads. The resin was batch eluted with increasing amounts of Me₂CO in H₂O (Scheme 4.1). NMR examination of the screen fractions showed that the interesting signals were confined to the 75% Me₂CO/H₂O fraction, containing two major structural related compounds.

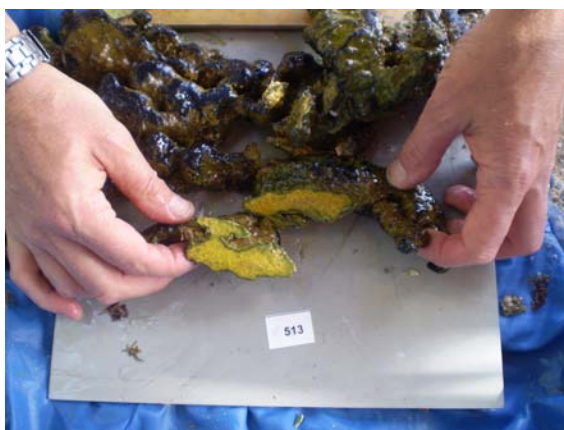
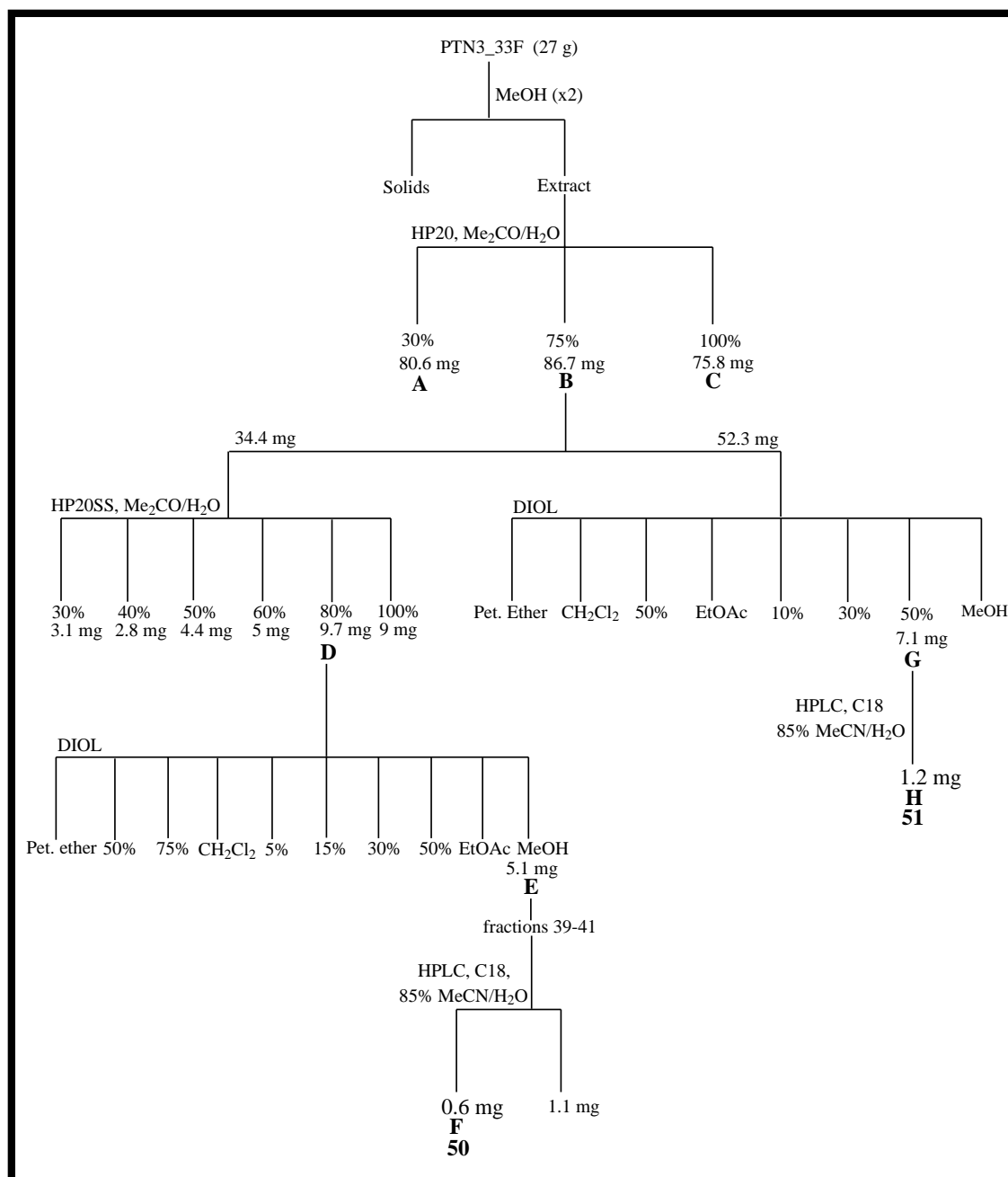


Figure 4.1. Surface photograph of the sponge PTN3_33F.

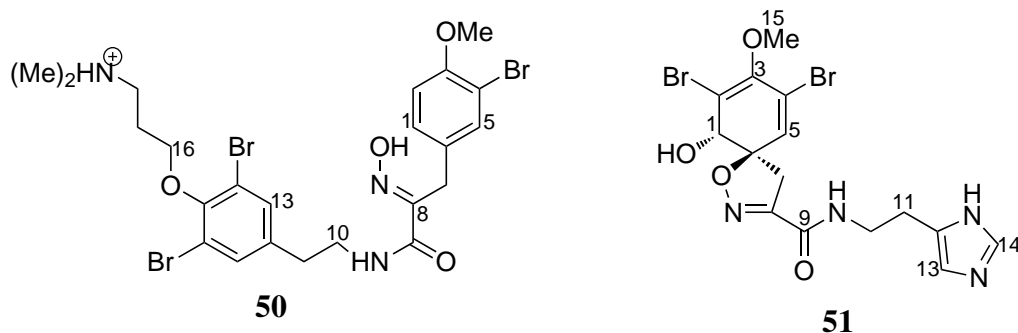


Scheme 4.1. Isolation of alypsamine-2 (**50**) and aerophobin-1 (**51**) from PTN3_33E, collected from Vava'u, Tonga.

The HSQC screen spectrum (Figure 4.2) revealed interesting correlations from several aromatic methines (δ_{H} 6.90–7.43; δ_{C} 113.1–134.7) and a number of deshielded methylene (δ_{H} 3.43–4.08; δ_{C} 28.7–71.6) resonances, attributed to one major compound. Analysis of the COSY correlations from these aromatic resonances allowed construction of one spin system (Figure 4.3). This was supported by the characteristic coupling pattern in the ^1H NMR spectrum (Figure 4.4), which is consistent with a 1,2,4-trisubstituted benzene ring (H-5: δ_{H} 7.44, d, 2.2 Hz; H-2: δ_{H} 6.90, d, 8.5 Hz; H-1: δ_{H} 7.18, dd, 2.2, 8.5 Hz). The ^1H NMR spectrum, showed a signal of an isolated aryl proton (H-13:

δ_{H} 7.43, 2H, br s), consistent with a symmetrically tetrasubstituted aromatic ring. Several of the aromatic proton resonances showed further COSY correlations into the aliphatic region of the spectrum. Purification of the 75% Me₂CO/H₂O fraction using NMR-guided fractionation, led to the isolation of the compound. Comparison of the NMR data with published data revealed the known compound aplysamine-2 (**50**). Compound **50** was originally reported in 1989 from an Australian marine sponge *Aplysina* sp.⁷²

Analysis of the HMBC (Figure 4.5) and HSQC screen spectra revealed interesting correlations from several olefinic methines (δ_{H} 6.41–8.30; δ_{C} 117.7–135.4) and an oxygenated methyl (CH₃-15: δ_{H} 3.71; δ_{C} 60.4) and methine (CH-1: δ_{H} 4.08; δ_{C} 75.5), attributed to the other major compound. COSY correlations from these olefinic methine resonances revealed two individual spin systems. Inspection of the ¹H, ¹³C, COSY and HMBC NMR spectra suggested that the following proton signals belonged to the same spin system (H-5: δ_{H} 6.41, H-1: δ_{H} 4.08, H-15: δ_{H} 3.71) and an AB system (H₂-7: δ_{H} 3.76 and δ_{H} 3.08) characteristic of a spirocyclooxazoline ring system previously encountered in other Verongida compounds.⁶⁵ The other spin system contained two aromatic methines appearing as broad singlets at δ_{H} 7.15 (H-13) and 8.30 (H-14); which showed weak COSY correlation to each other. In the HSQC spectrum, δ_{H} 7.15 and 8.30 have large ¹J_{CH} (198 Hz and 214 Hz respectively), which were consistent with coupling constants of an imidazole ring. Further analysis of the NMR data and sub-structure searches of the literature revealed the known compound aerophobin-1 (**51**). Compound **51** was first isolated from marine sponge *Verongia aerophoda*.⁷³



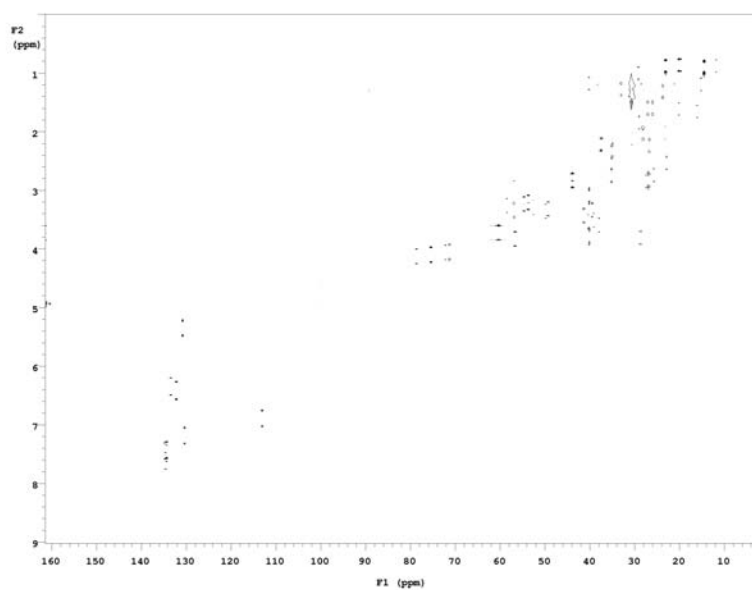


Figure 4.2. HSQC NMR screen spectrum (600 MHz, CD_3OD) of the 75% $\text{Me}_2\text{CO}/\text{H}_2\text{O}$ fraction of PTN3_33F.

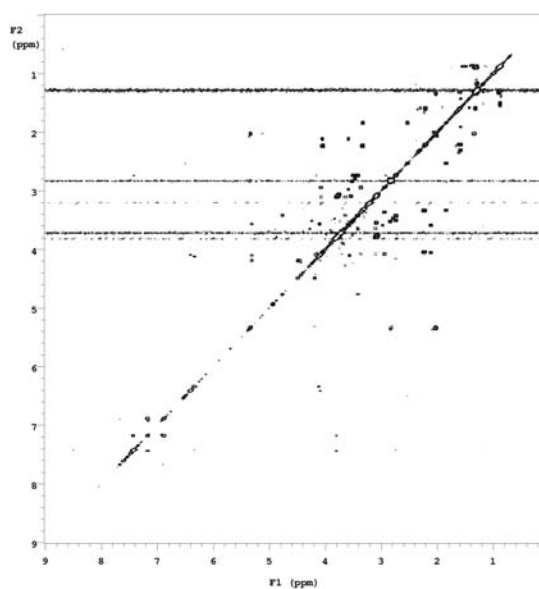


Figure 4.3. COSY NMR screen spectrum (600 MHz, CD_3OD) of the 75% $\text{Me}_2\text{CO}/\text{H}_2\text{O}$ fraction of PTN3_33F.

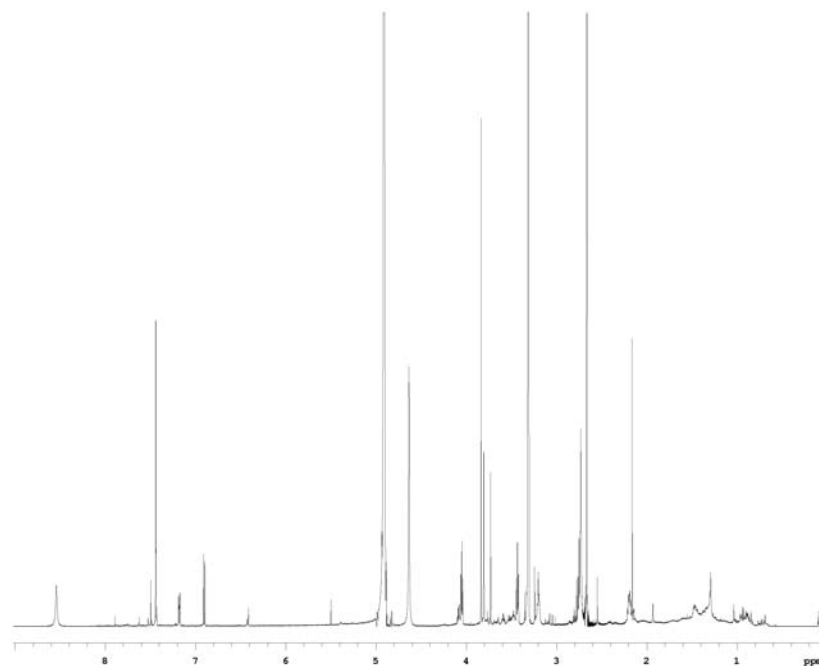


Figure 4.4. ¹H NMR screen spectrum (600 MHz, CD₃OD) of the 75% Me₂CO/H₂O fraction of PTN3_33F.

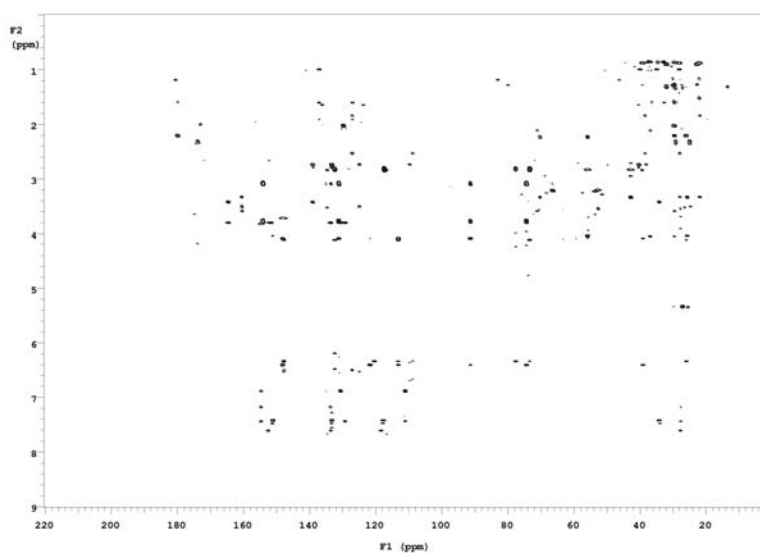


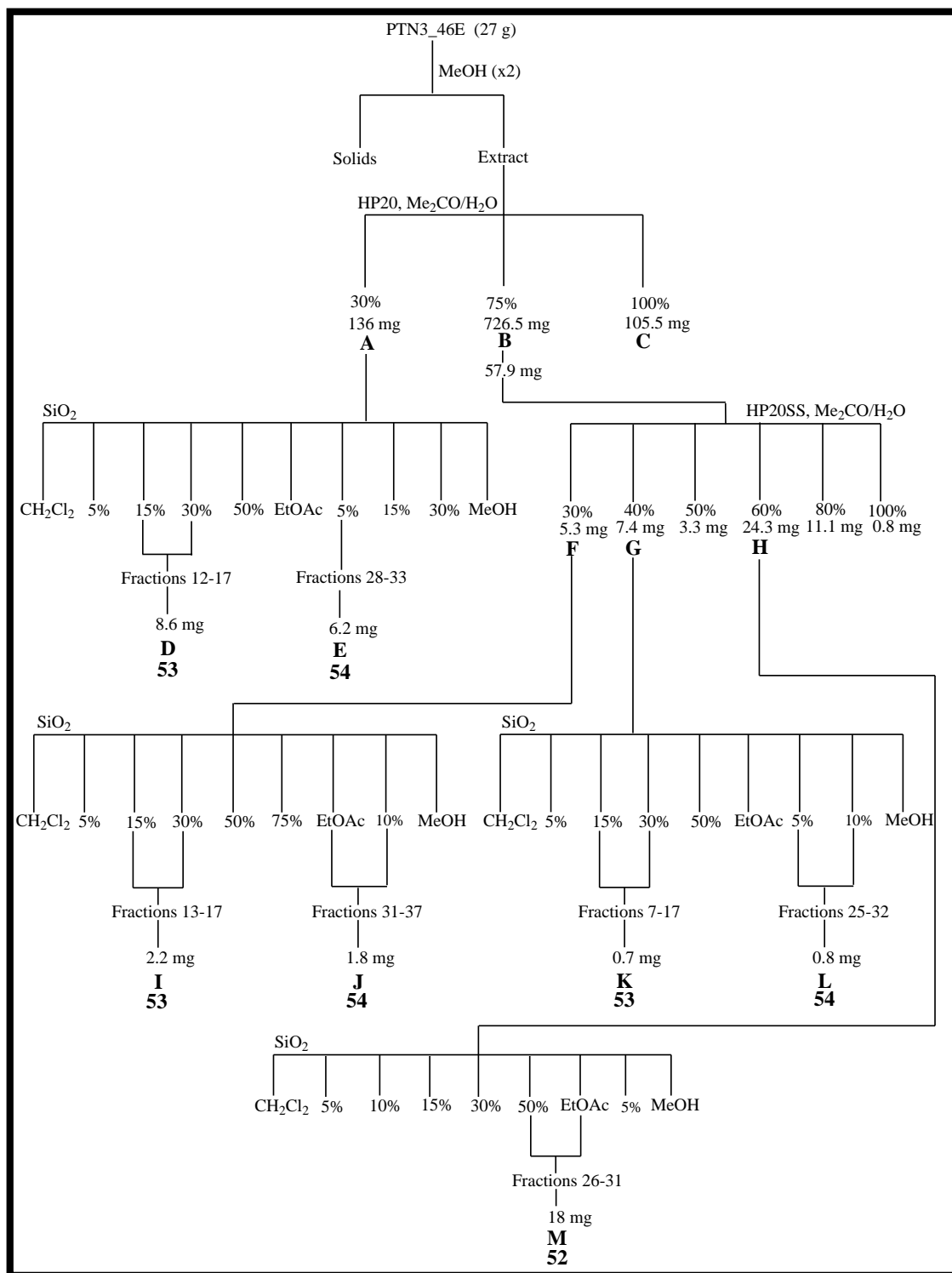
Figure 4.5. HMBC NMR screen spectrum (600 MHz, CD₃OD) of the 75% Me₂CO/H₂O fraction of PTN3_33F.

4.1.3 PTN3_46E

PTN3_46E was a small creamy-pink sponge with thin spreading crusts, collected from Tu‘ungasika Island, Vava‘u, Tonga in late November 2009 (Figure 4.6). Interestingly, upon exposure to air or at death, no change in pigmentation was observed. The sponge was extracted twice in MeOH and the extracts were cyclic loaded on to a column of reversed-phase PSDVB resin. The resin was batch eluted with increasing amounts of Me₂CO in H₂O and the fractions analysed by NMR. The 75% Me₂CO/H₂O fraction appeared to contain one main compound and a mixture of structurally similar compounds. Further chromatographic steps employing bench-top reversed- and normal-phase chromatography (depicted in Scheme 4.2) led to the isolation of the three known bromotyrosine compounds.



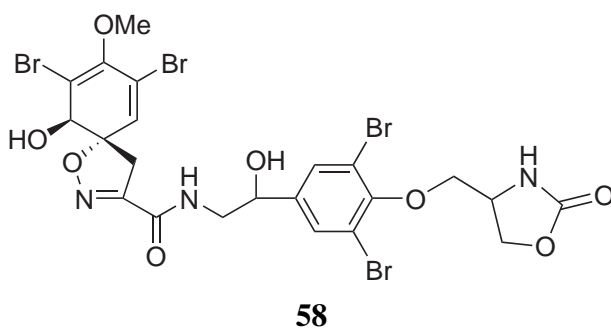
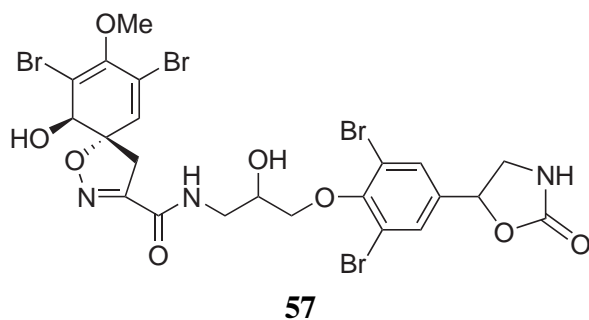
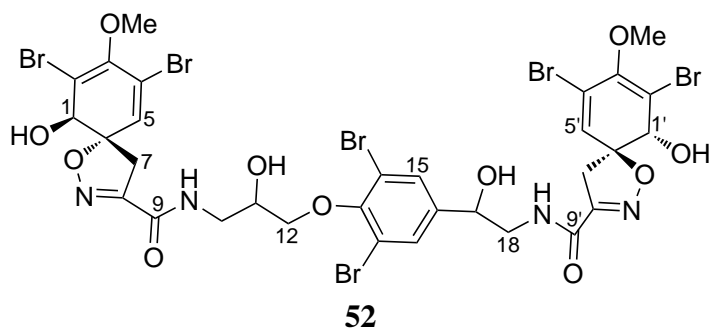
Figure 4.6. Underwater photograph of the sponge PTN3_46E. Courtesy of Karen Stone.



Scheme 4.2. Isolation of fistularin-3 (**52**), aerophysinin-1 (**53**) and LL-PAA216 (**54**) from PTN3_46E, collected from Vava'u, Tonga.

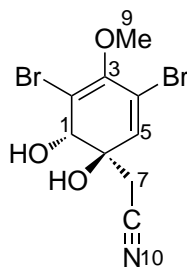
Initial analysis of the NMR spectra of the major compound showed characteristics of a spirocyclooxazoline ring system (H-5: δ_{H} 6.42, H-1: δ_{H} 4.11, H-19 δ_{H} 3.73, and an AB system (H-7: δ_{H} 3.78 and δ_{H} 3.10) as encountered in aerophobin-1 (**51**). The compound also has a symmetrically tetrasubstituted aromatic ring (H-15: δ_{H} 7.62, 2H, bs) similar to that of aplysamine-2 (**50**), thus identifying the major segments of the molecule.

The HSQC spectrum revealed the presence of two highly polarised oxymethines (C-11 δ_{H} 4.11; δ_{C} 70.0; C-17 δ_{H} 4.77; δ_{C} 71.6) (consistent by their large $^1J_{\text{CH}}$ of 145 and 146 Hz). Further analysis of the NMR spectra (see Table 4.2 and Appendix E for NMR data and spectra respectively) revealed fistularin-3 (**52**). In 1979, fistularin-3 (**52**) was reported along with fistularin-1 (**57**) and fistularin-2 (**58**) from the marine sponge *Aplysina fistularis*.⁶⁴



Analysis of the NMR spectra for the second bromotyrosine compound, initially suggested the presence of another spirohexadienyl moiety. However, the chemical shifts of C-7 (δ_{H} 2.81, 2.85; δ_{C} 25.5) and C-8 (δ_{C} 116.6) in this compound were different from those (H-7: δ_{H} 3.10, 3.78; C-7: δ_{C} 40.1; C-8: δ_{C} 155.1) of **52**. In addition, the chemical shift of the oxygenated spiro-carbon (C-6: δ_{C} 74.3) was considerably different from the spirocarbon of the isoxazoline structure in compound **52** (C-6: δ_{C} 92.5). A correlation was observed from the methylene proton H₂-7 to N-10 in the ^1H - ^{15}N HMBC spectrum. The ^{15}N chemical shift appears at -134.6, which is consistent with that of a nitrile,

revealing **53** (see Table 4.3 and Appendix F for NMR data and spectra respectively). This was confirmed by the positive-ion mode HRESIMS analysis of the compound, which gave the molecular formula of $C_9H_9NO_3Br_2$ (359.8847 $[M + Na]^+$, Δ 0.0 ppm) with pseudomolecular ion clusters ($[M + Na]^+$: $[M + 2 + Na]^+$: $[M + 4 + Na]^+$, requiring five double-bond equivalents. Aeroplysinin-1 (**53**) was obtained from the sponge *Verongia aerophoba* and is the first example of a naturally occurring 1,2-dihydroarene-1,2-diol.⁷⁴



53

Structural elucidation of the last bromotyrosine compound revealed a substructure similar to that of fistularin-3 (**52**), but without the two spiroisoxazoline rings on either side (shown in Figure 4.7). Therefore this was thought to be a novel derivative of **52**. HRESIMS of the compound showed a characteristic pseudomolecular ion cluster ($[M + Na]^+$: $[M + 2 + Na]^+$: $[M + 4 + Na]^+$: $[M + 6 + Na]^+$: $[M + 8 + Na]^+$) indicating a molecular formula of $C_{26}H_{24}N_4O_{10}Br_4$ (890.8124 $[M + Na]^+$, Δ 0.0 ppm), requiring fifteen double-bond equivalents. Since there were only 13 carbons resonance observed in the ^{13}C NMR spectrum, the molecule was suspected to be a dimer with a symmetrical structure. Attempted acetylation of the compound did not indicate the presence of any hydroxyl groups. Therefore, the sample was re-submitted for mass analysis using both positive- and negative-ion modes. Negative-ion mode HRESIMS analysis of the compound gave rise to pseudomolecular ion clusters ($[M - H]^-$: $[M + 2 - H]^-$: $[M + 4 - H]^-$, indicated a molecular formula of $C_{13}H_{12}N_2O_5Br_2$ (432.9035 $[M - H]^-$, 0.0 ppm). The positive-ion mode HRESIMS analysis of the compound gave the same molecular formula of $C_{13}H_{12}N_2O_5Br_2$ (456.9011 $[M + Na]^+$, Δ 0.0 ppm) with pseudomolecular ion clusters ($[M + Na]^+$: $[M + 2 + Na]^+$: $[M + 4 + Na]^+$, requiring eight double-bond equivalents. Further analysis of the NMR spectra using the latter molecular formula with no hydroxyl groups present, and comparison with published literature, revealed LL-PAA216 (**54**) (see Table 4.4 and Appendix G for NMR data and spectra respectively). LL-PAA216 (**54**) was

the first bromo-compound containing 2-oxazolidone, obtained from *Verongia lacunosa*, collected off the coast of Puerto Rico in 1974.⁷⁵ The problem encountered with the mass spectrometry in this study was also encountered in zamamistatin.

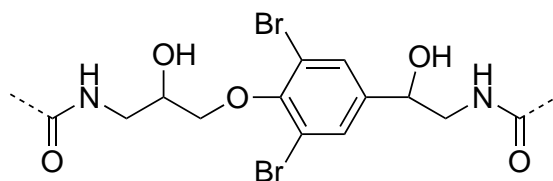
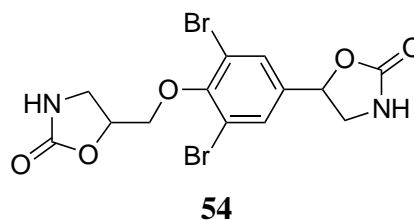
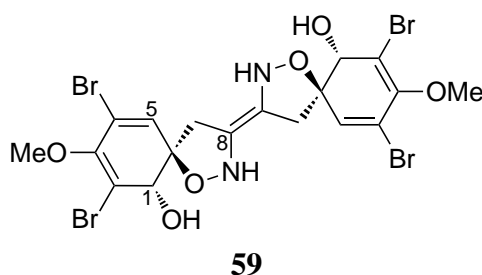
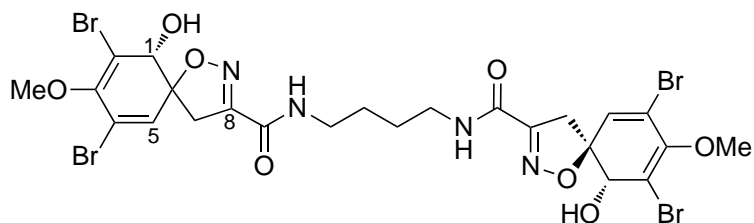


Figure 4.7. Proposed substructure of a compound isolated from PTN3_46E sponge.

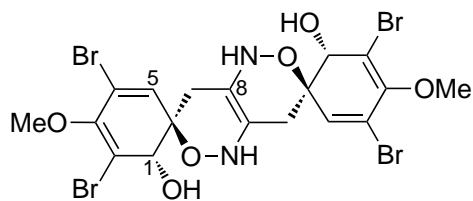


Zamamistatin, a novel bromotyrosine derivative, was obtained from the Okinawan sponge *Pseudoceratina purpurea* in 2001 by Takada *et al.*⁷⁶ In its ESIMS spectrum, zamamistatin showed 1:4:6:4:1 quintet ion peaks at m/z 697, 699, 701, 703, and 705, indicative of the presence of four bromine atoms with a molecular formula of $C_{18}H_{18}Br_4N_2O_6$. Detailed analysis of the NMR spectra suggested a symmetrical structure for zamamistatin as in **59**. However, the chemical shift of the oxygenated spiro-carbon of zamamistatin (C-6: δ_C 74.3) was considerably different from the spirocarbon of the isoxazoline structure in aerothionin (**60**) (C-6: δ_C 91.5). Thus, an endo-type dimer of the azaoxa-spiro[6.6] unit possessing a dihydro-1,2-oxazine ring, as shown in **61**, was proposed as another plausible structure in 2006 by Hayakawa *et al.*⁷⁷ In 2008, Kita *et al.* revised the structure of zamamistatin to that of the known compound aeroplysinin-1 (**53**), but not an exo- or endo-type dimer **59** or **61** which were described previously.⁷⁸





60

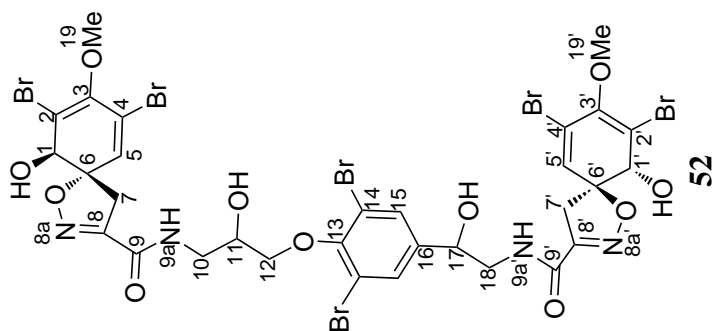


61

The NMR data for fistularin-3 (**52**), aeroplysinin-1 (**53**) and LL-PAA216 (**54**) in the literature are quite old and the ^{15}N chemical shifts have not yet been published. Here we report the NMR data for the three compounds (**52–54**) including the ^{15}N chemical shifts and the $^1J_{\text{CH}}$ values (Tables 4.2, 4.3, 4.4 and 4.5).

Table 4.2. ^{15}N (60 MHz), ^{13}C (150 MHz) and ^1H (600 MHz) NMR Data (CD_3OD) for Fistularin-3 (**52**).

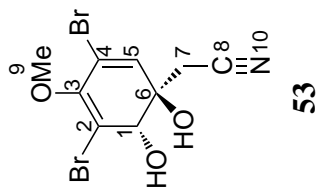
Position	^{13}C or ^{15}N		^1H		COSY	HMBC (^1H to ^{13}C)
	δ (ppm)	mult	J_{CH} (Hz)	δ (ppm)	mult	J (Hz)
1	75.40	CH	152	4.11	dd	0.7,3.3
1'	75.44	CH	152	4.11	dd	0.7,3.3
2	122.77	C				
2'	122.80	C				
3	149.2	C				
3'	149.2	C				
4	114.15	C				
4'	114.16	C				
5	132.19	CH	176	6.42	dd	0.9,6.5
5'	132.22	CH	176	6.42	dd	0.9,6.5
6	92.48	C				
6'	92.51	C				
7a	40.06	CH_2	140	3.10	m	
7b	40.06	CH_2	140	3.78	m	
7a'	40.10	CH_2	140	3.10	m	
7b'	40.10	CH_2	140	3.78	m	
8	155.1	C				
8a	*	N				
8'	155.3	C				
8a'	*	N				
9	161.7	C				
9'	161.8	C				
9a	-272.6	NH	*			
9a'	-271.8	NH	*			
10a	43.7	CH_2	140	3.49	m	
10b	43.7	CH_2	140	3.73	m	
11	70.0	CH	145	4.21	m	
12	75.8	CH_2	145	4.00	m	
12	75.8	CH_2	145	4.00	m	
13	153.2	C				
14	118.9	C				
15	131.8	CH	167	7.62	m	
16	143.2	C				
17	71.6	CH	146	4.77	m	
18a	47.7	CH_2	141	3.40	m	
18b	44.7	CH_2	141	3.51	m	
19	60.40	CH_3	148	3.73	s	
19'	60.41	CH_3	148	3.73	s	



†Weak correlations.
*Unable to be determined.

Table 4.3. ^{15}N (60 MHz), ^{13}C (150 MHz) and ^1H (600 MHz) NMR Data (CD_3OD) for Aeropylsinin-1 (**53**).

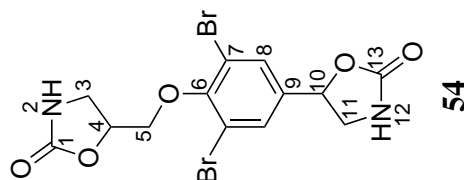
Position	^{13}C or ^{15}N		^1H		COSY	HMBC (^1H to ^{13}C)
	δ (ppm)	mult	$^1J_{\text{CH}}$ (Hz)	δ (ppm)	mult	J (Hz)
1	78.8	CH	150	4.11	d	1.0
2	121.5	C				
3	148.9	C				
4	114.2	C				
5	133.5	CH	172	6.34	d	1.2
6	74.5	C				
7a	27.0	CH_2	137	2.80	d	16.8
7b	27.0	CH_2	137	2.84	d	16.8
8	118.4	C				
9	60.2	CH_3	146	3.73	s	
10	-134.6	N				



† Weak correlations.

Table 4.4. ^{15}N (60 MHz), ^{13}C (150 MHz) and ^1H (600 MHz) NMR Data (CD_3OD) for LL-PAA216 (**54**).

Position	^{13}C or ^{15}N		^1H		COSY	HMBC (^1H to ^{13}C)
	δ (ppm)	mult	$^1J_{\text{CH}}$ (Hz)	δ (ppm)	mult	J (Hz)
1	162.1	C				
2	*	NH	*			
3	43.0	CH_2	147	3.81	m	3,4
4	76.4	CH	158	5.05	m	3,5
5a	73.8	CH_2	148	4.24	m	4
5b	73.8	CH_2	148	4.24	m	4
6	153.7	C				
7	119.5	C				
8	131.5	CH	168	7.66	d	10 [†]
9	140.2	C				
10	77.1	CH	158	5.63	m	8 [†] 11a,11b
11a	49.0	CH_2	148	3.43	dd	7.0,9.3
11b	49.0	CH_2	148	3.98	t	9.0
12	*	NH	*			
13	161.5	C				

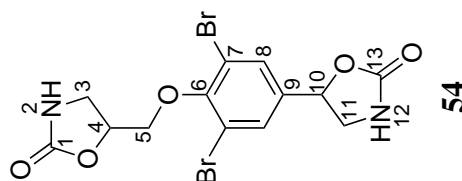


[†]Weak correlations.

*Unable to be determined.

Table 4.5. ^{15}N (60 MHz), ^{13}C (150 MHz) and ^1H (600 MHz) NMR Data (d_6 -DMSO) for LL-PAA216 (**54**).

Position	^{13}C or ^{15}N		^1H		COSY	HMBC (^1H to ^{13}C)
	δ (ppm)	mult	$^1J_{\text{XH}}$ (Hz)	δ (ppm)	mult	J (Hz)
1	158.7	C				
2	-304.6	NH	97	7.63	s	
3a	41.3	CH_2	146	3.52	m	
3b	41.3	CH_2	146	3.64	t	9.0
4	73.7	CH	158	4.95	m	
5a	73.2	CH_2	148	4.13	m	
5b	73.2	CH_2	148	4.13	m	
6	151.8	C				
7	117.8	C				
8	130.6	CH	168	7.71	d	0.5
9	139.1	C				
10	74.5	CH	158	5.59	m	
11a	47.1	CH_2	148	3.36	m	
11b	47.1	CH_2	148	3.84	t	9.0
12	-303.9	NH	97	7.77	s	
13	158.3	C				



[†]Weak correlations.

4.2 Order Poecilosclerida

The order Poecilosclerida is the most diverse order of Porifera, both in terms of numbers of species and morphology. The order belongs to the sub-class Ceractinomorpha, which is characterised by a skeleton composed of both spicule and spongin fibres. The order consists of 25 families, 129 genera and several thousands of described species worldwide, distributed from intertidal to abyssal depths.²¹ The *Latrunculia*, *Strongylodesma*, and *Tsitsikamma* of the family Latrunculiidae (Table 4.6) have a characteristic base pigmentation of deep brownish black that is often and variously tinged with forest green and deep blue. These specimens exude a dark brownish or greenish black pigment; the ethanol preservative is always oily-looking and deeply pigmented. Preserved specimens always retain their dark pigmentation.²¹

Table 4.6. Taxonomic Classification of Selected Families of the Order Poecilosclerida.²¹

Class	Order	Suborder	Family	Genus
Demospongiae	Poecilosclerida	Microcionina	Acarnidae	<i>Zyzzya</i>
		Myxillina		
		Mycalina		
		Latrunculina	Latrunculiidae	<i>Latrunculia</i> <i>Sceptrella</i> <i>Strongylodesma</i> <i>Tsitsikamma</i>

4.2.1 PTN4_10A

The sponge, PTN4_10A, examined in this study (Figure 4.8) was a massive, soft sponge with deep black colour, both exterior and interior. The methanol extracts of the sponge has a very dark greenish pigment. The sponge was extracted twice in MeOH and the extracts were cyclic loaded on to a column of reversed-phase PSDVB resin. The resin was batch eluted with increasing amounts of Me₂CO in H₂O and the fractions analysed by NMR spectroscopy. The NMR spectra of the 75% Me₂CO/H₂O fraction appeared to contain

interesting signals, attributed to two major compounds. Further chromatographic steps employing bench-top normal-phase chromatography followed by reversed-phase HPLC (depicted in Scheme 4.3) led to the isolation of two structurally related known compounds.

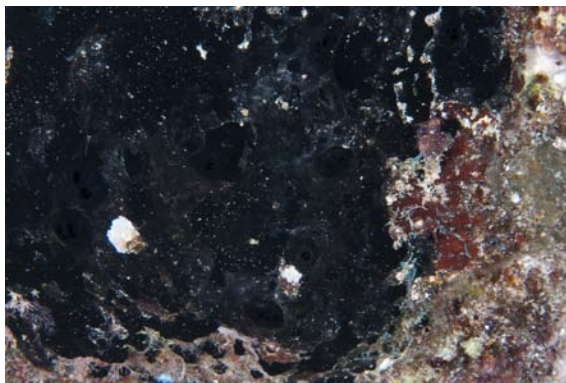
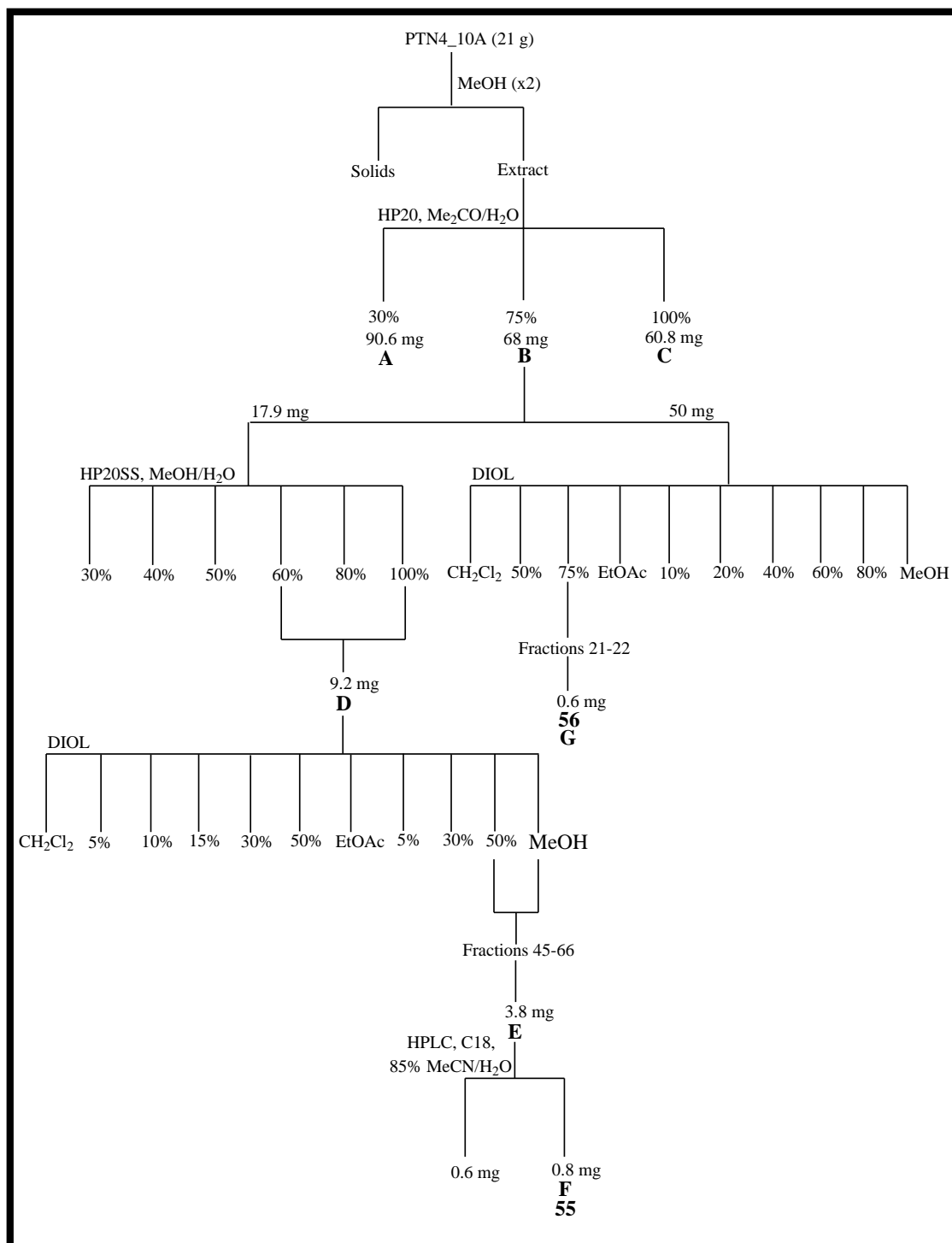


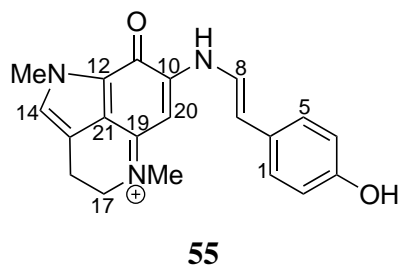
Figure 4.8. Underwater photo of the PTN4_10A sponge (courtesy of Karen Stone).



Scheme 4.3. Isolation of makaluvamine G (**55**) and prianosin B (**56**) from PTN4.10A, collected from Vava'u, Tonga.

One of the major compounds was isolated as a green-black solid. Inspection of the HSQC screen spectrum indicated the presence of a large variety of deshielded aromatic methines (δ_{H} 5.91–7.37; δ_{C} 85.6–130.5) and accompanied by two *N*-methyls (δ_{H} 3.86, 3.99; δ_{C} 35.0, 35.2) and two methylene resonances (δ_{H} 2.96–3.86; δ_{C} 18.1–42.7). Substantial numbers of couplings from these ¹H resonances were noted in the COSY spectrum. Further analysis of the HMBC spectrum and comparison with published

literature indicated that is a discorhabdin-like compound, revealing makaluvamine G (**55**). Compound **55**, is a cytotoxic pigment originally reported in 1993 by Scheuer *et al.* from an Indonesian sponge *Histodemella* sp.⁷⁹ The first examples of the series, makaluvamines A-F, were reported as cytotoxic pigments of a Fijian sponge *Zyzzya* cf. *marsailis*⁸⁰ (an incorrect spelling of *massalis*). The marine sponges *Histodemella* sp. and *Z. cf. marsailis* were later re-identified as *Z. fuliginosa*.⁸¹



The other compound was isolated as red crystals. As for compound **55**, several olefinic methines (δ_{H} 7.55–8.31; δ_{C} 126.3–158.2) were observed in the HSQC spectrum. Several of these olefinic methines showed correlations in the COSY spectrum. In addition, the HSQC spectrum revealed two methylenes (CH₂-7: δ_{H} 2.79, 2.97; δ_{C} 40.8 and CH₂-4: δ_{H} 2.79, 3.08; δ_{C} 46.5), which indicated the presence of chiral centres in the molecule. Also of interest were two methines with large $^1J_{\text{CH}}$ values (CH-5: δ_{H} 4.72; δ_{C} 57.5, $^1J_{\text{CH}}$ 149 Hz and CH-8: δ_{H} 5.47; δ_{C} 62.6, $^1J_{\text{CH}}$ 163 Hz). In its HRESIMS spectrum, this compound showed a molecular formula of C₁₈H₁₂N₃OSBr, which taken together with the detailed analysis of the NMR spectra, revealed this compound as prianosin B (**56**). Compound **56**, a sulfur-containing alkaloid with potent antineoplastic activity, was first obtained from an Okinawan marine sponge *Prianos melanos* together with prianosins C and D.⁸² The structures of prianosins C and D were later revised by Kobayashi *et al.* in 1991 to known compounds 2-hydroxydiscorhabdin D (**62**) and discorhabin D (**63**), respectively.⁸³

In the past, chemotaxonomic trends within marine sponges producing pyrroloquinoline metabolites have suggested that discorhabdins/prianosins and makaluvamines are definitive chemotaxonomic markers for *Latrunculia* and *Zyzzya* species, respectively.^{84,85} Further isolation of discorhabdin/prianosin and makaluvamine metabolites from other species within the order Poecilosclerida suggest that this broad chemotaxonomic generalisation may have to be treated with some circumspection. For the same reason, *P. melanos* has

been re-identified as a species of *Strongylodesma*.²¹

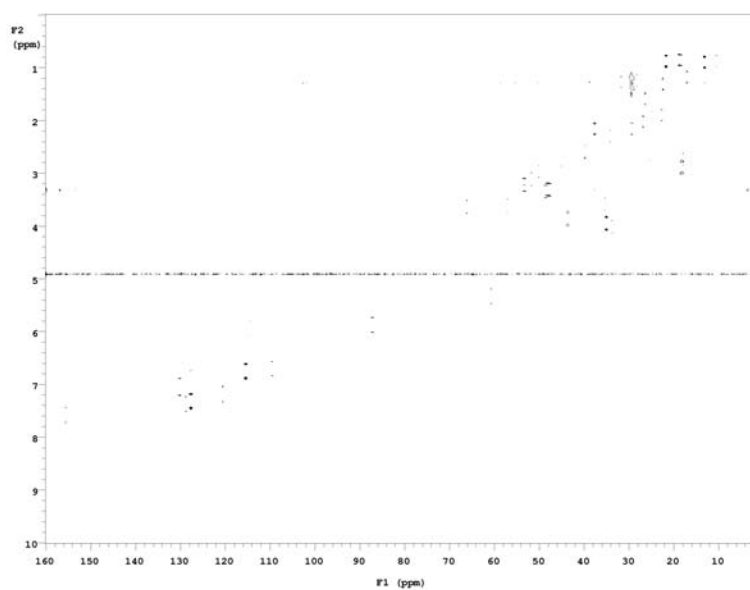
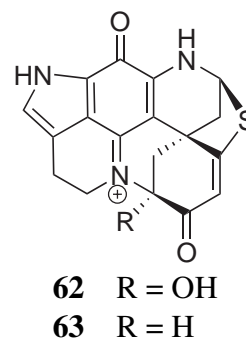
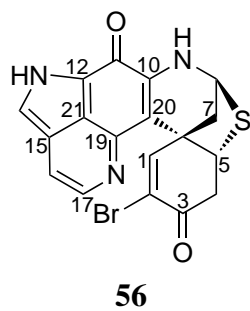


Figure 4.9. HSQC NMR screen spectrum (600 MHz, CD₃OD) of the 75% Me₂CO/H₂O fraction of PTN4_10A.

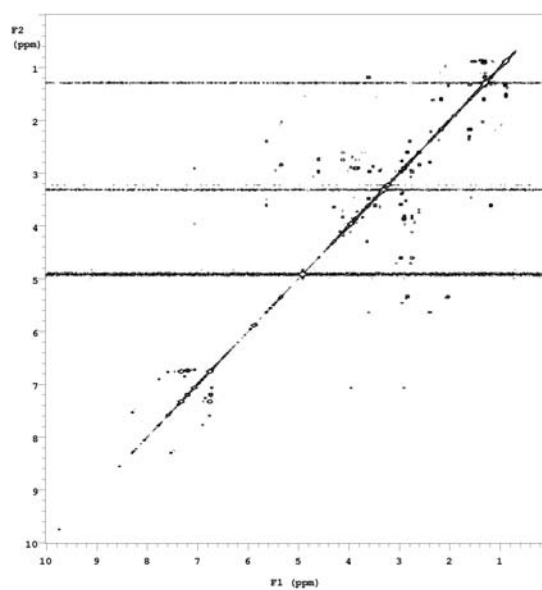


Figure 4.10. COSY NMR screen spectrum (600 MHz, CD₃OD) of the 75% Me₂CO/H₂O fraction of PTN4_10A.

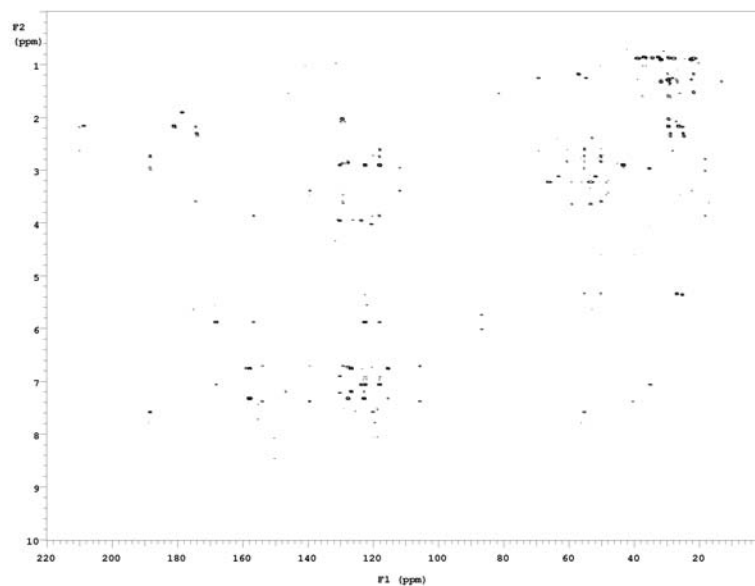


Figure 4.11. HMBC NMR screen spectrum (600 MHz, CD₃OD) of the 75% Me₂CO/H₂O fraction of PTN4_10A.

4.3 Biological Activity

Fistularin-3 (**52**), aeroplysinin-1 (**53**) and prianosin B (**56**) were evaluated for cytotoxicity against the human promyelocytic leukaemia cell line HL-60 at the School of Biological Sciences, VUW. Compounds **52**, **53** and **56** were found to be moderately cytotoxic with IC₅₀ values in the micromolar range (5.09 μ M, 1.14 μ M, 2.17 μ M respectively).⁸⁶ LL-PAA216 (**54**) has been submitted for biological testing to the School of Biological Sciences at VUW, however the results are still pending.

Chapter 5

Investigation of *Fascaplysinopsis* sp.

5.1 *Fascaplysinopsis* sp.

The genus *Fascaplysinopsis* belongs to the family Thorectidae, a member of the order Dictyoceratida (Table 5.1). Dictyoceratids do not possess siliceous spicules, which makes their taxonomic identification more difficult. Thorectids are differentiated from other members of the Dictyoceratida by their strongly laminated skeletal fibres, diplodal choanocyte chambers, and lack of fine skeletal filaments. They range from low and encrusting to massive in growth form and are distributed throughout tropical and temperate oceans. Genera within Thorectidae are differentiated by the absence or presence of a cortical armour.²¹ The genus *Fascaplysinopsis* has strong and thick primary fibres, collagenous throughout the mesophyl of the sponge. They are found throughout the Indo-Pacific. The *Fascaplysinopsis* sp. collected from Tongan waters in this study was a massive globular sponge with a shiny red-brown appearance (Figure 5.1).

Table 5.1. Taxonomic classification of genus *Fascaplysinopsis* from Class Demospongiae.²¹

Class	Order	Family	Genus
Demospongiae			
	Dictyoceratida		
		Dysideidae	
		Irciniidae	
		Spongiidae	
		Thorectidae	
			<i>Aplysinopsis</i>
			<i>Cacospongia</i>
			<i>Fasciospongia</i>
			<i>Fascaplysinopsis</i>
			<i>Hytrios</i>
			<i>Luffariella</i>
			<i>Thorectandra</i>



Figure 5.1. Surface photograph of the *Fascaplysinopsis* sp.

5.2 Chemical History of the Genus *Fascaplysinopsis*

Nitrogen-containing metabolites are not commonly observed from Dictyoceratid sponges, as this order is known to be a rich source of di- or sesterterpenes, while family Thorectidae are sources for both sesterterpenes and amino acid derivatives.^{26,87,88} The first *Fascaplysinopsis* compounds reported were aplysinopsins (**64** and **65**), monomeric tryptophan derivatives isolated from a marine sponge of the genus *Aplysinopsis* (now considered a synonym of *F. reticulata*), which were unaccompanied by terpenoids.^{21,89} Fascaplysin (**66**), a pentacyclic pyridinium salt from the Fijian sponge *Fascaplysinopsis* sp., was isolated alongside the known compound luffariellolide (**45**).⁹⁰ The structure of compound **66** was determined by spectral and X-ray analysis. Compound **66** inhibits the growth of several microbes including *Staphylococcus aureus*, *Escherichia coli*, *Candida albicans*, *Saccharomyces cerevisiae*, and showed cytotoxicity towards murine leukemia L1210 cells with an IC₅₀ of 0.2 $\mu\text{g/mL}$.⁹⁰

Subsequently, several structurally related unusual alkaloid-sesterterpene salts have been reported from the Fijian sponge *F. reticulata*, including fascaplysin A (**67**), fascaplysin B (**68**), reticulatine A (**69**), reticulatine B (**70**) and homofascaplysin A (**71**), together with sesterterpenoid anions dehydroluffariellolide diacid (**72**) and isodehydroluffariellolide diacid (**73**).^{91,92} These compounds were accompanied by neutral alkaloids homofascaplysin B (**74**), homofascaplysin C (**75**), secofascaplysin A (**76**) and sesterterpene isodehydroluffariellolide (**44**).^{91,92} In 2003, analysis of the same sponge species collected from Indonesia, obtained three compounds 3-bromofascaplysin (**77**), 14-bromoreticulatine

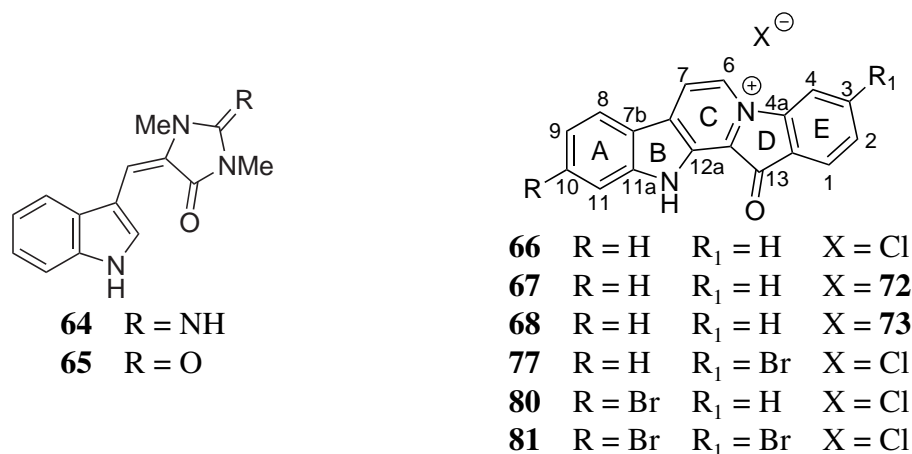
(**78**), and 14-bromoreticulatate (**79**).⁹³ Eight fascaplysin derivatives (**80–87**) were subsequently isolated from the marine sponge *F. reticulata* collected off different locations in Fiji and Indonesia.⁹⁴

These fascaplysin derivatives were grouped into three main classes due to inconsistent nomenclature in the current literature for tetracyclic and pentacyclic natural products. The first class contains most structural variants closely related to **66**, based on the changes in the extent of conjugation present in the fused pentacyclic chromophore.⁹⁴ These includes homofascaplysin B (**74**), homofascaplysin C (**75**), 3-bromofascaplysin (**77**), 10-bromofascaplysin (**80**), 3-10-dibromofascaplysin (**81**) and homofascaplysate A (**82**). The other two classes were based on a single bond disconnection severing ring D of the parent compound **66**, as exemplified by the reticulatines (**78**, **79**, **83–85**) and the secofascaplysin (**76**, **86**, **87**). Compound **80** exhibited human solid tumor selectivity unlike compounds **66** and **84** showed significant selectivity for human leukemia.⁹⁴ Other studies revealed that compound **67** showed comparable activity in several tumor lines to **66** but the presence of the sesterterpene anion causes activity in some cell lines where **66** is inactive.⁹⁴ Interestingly, the presence of a bromine in **77** produces an overall increase in activity as compared to **66** and **67** but also causes inactivity in cell lines that are sensitive to **66** and **67**.⁹⁴

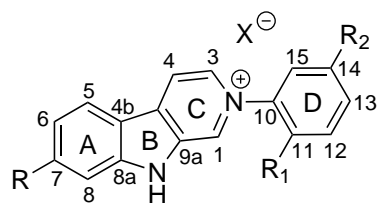
A specimen of *Fascaplysinopsis* sp. from Palau contained the anti-inflammatory sesterterpene palauolol (**88**), which was accompanied by known compounds palauolide (**89**) and fascaplysin (**66**).⁹⁵ Palauolol (**88**) was chemically recognised as being a secondary alcohol that upon dehydration yields its known congener palauolide (**89**). Compound **89** was first obtained as an antimicrobial sesterterpene from a three sponge association collected in Palau which was later identified as *Fascaplysinopsis* sp.^{95,96} Two closely related lipodepsipeptides, taumycins A and B (**90** and **91**) have been isolated from an undescribed *Fascaplysinopsis* species from Madagascar.⁹⁷ Taumycins A and B (**90** and **91**) have the same 12-membered oxodepsipeptide ring system. Compound **90** shows cytotoxic activity against the human UT-7 leukemic cell line. In 2008, Bishara *et al.* reported three nitrogenous macrolides salarin A and B (**92** and **93**) and tulearin A (**94**) from the Madagascan sponge *Fascaplysinopsis* sp.⁹⁸ A year later, the relative

configuration of **92** was determined by X-ray diffraction.⁹⁹ In 2010, the structure of salarin B (**93**) was later revised to have a tetrahydrofuran ring system instead of the 16,17-diol.¹⁰⁰ Tulearin A (**94**) carries a naturally rare carbamate ester, and its relative and absolute configurations were determined by X-ray diffraction and modified Mosher's methods respectively.¹⁰¹ Both **92** and **94** exhibit cytotoxicity toward leukemia cell lines.⁹⁸

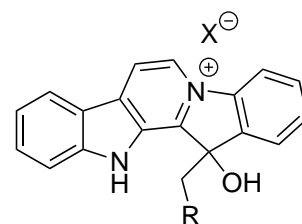
Shortly thereafter, Bishara *et al.* reported salarin C (**95**) from the same Madagascan sponge.¹⁰² Compound **95** is closely related to **92** and **93** and upon air oxidation, **95** was found to transform to **92**. Compound **95** was found to inhibit cell proliferation of human leukemic and murine cell lines. Tulearins B and C (**96** and **97**) were reported in 2009 followed by tausalarin C (**98**), a novel bismacrolide.^{99,101} It is suggested that tausalarin C (**98**) is assembled from salarin A and pretaumycin A. Salarins D-J (**99–105**) were reported from the same Madagascan sponge by Bishara *et al.* in 2010, and are closely related to salarins A–C.¹⁰⁰ Salarins D (**99**), E (**100**), H (**103**) and J (**105**) showed significant cytotoxic activity against human leukemia cells, while salarins F (**101**) and I (**104**) were inactive. There are striking structural similarities of these metabolites to known metabolites of microbial and fungal origin*, suggesting that marine microorganisms may be the true sources of these metabolites.^{105–107}



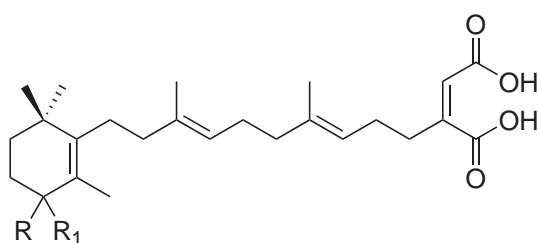
*e.g. Madangolide and laingolide A, metabolites from the cyanobacteria *Lyngbya bouillonii*.^{103,104}



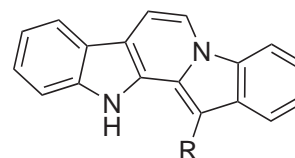
- 69** R = H R₁ = COOMe R₂ = H X = **73**
70 R = H R₁ = COOMe R₂ = H X = **72**
78 R = H R₁ = COOMe R₂ = Br X = HCO₂⁻
79 R = H R₁ = COO⁻ R₂ = Br
83 R = Br R₁ = COOMe R₂ = Br X = Cl
84 R = H R₁ = OH R₂ = H X = Cl
85 R = H R₁ = OH R₂ = Br X = Cl



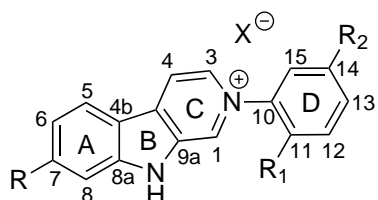
- 71** R = COCH₃ X = **72**
82 R = COOH X = Cl



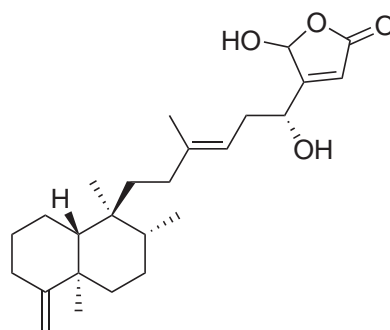
- 72** R = R₁ = H
73 R = R₁ = O



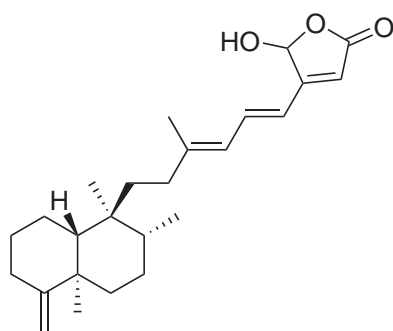
- 74** R = COCOOMe
75 R = CHO



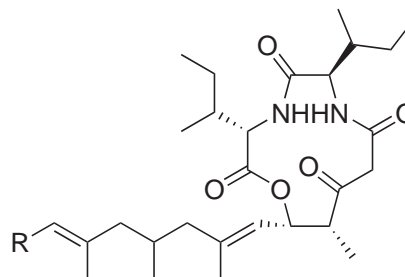
- 76** R = COCOCH₃ R₁ = H
86 R = COCOCH₃ R₁ = Br
87 R = COCHO R₁ = Br

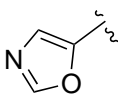


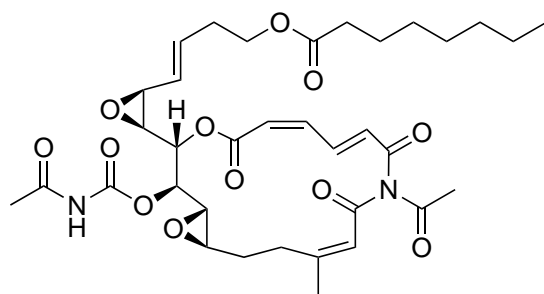
88



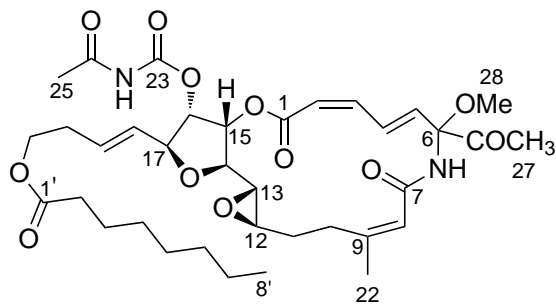
89



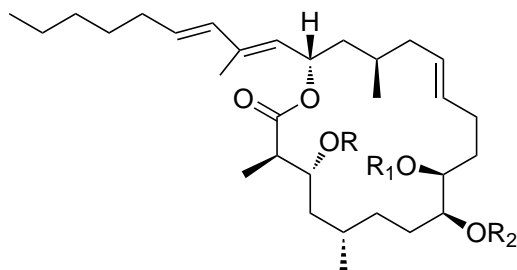
- 90** R = 
91 R = COOH



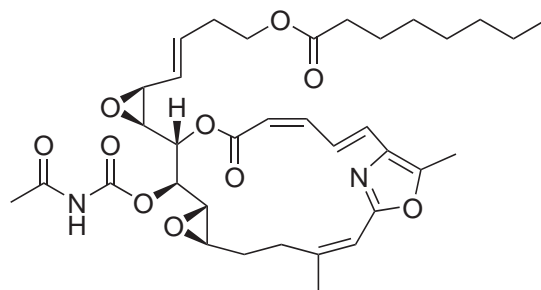
92



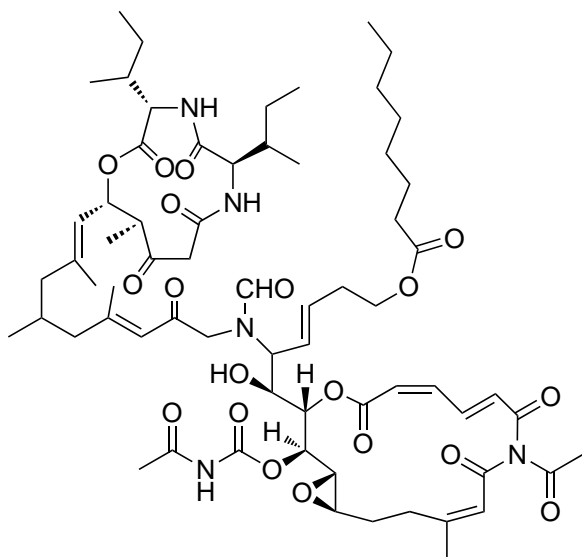
93



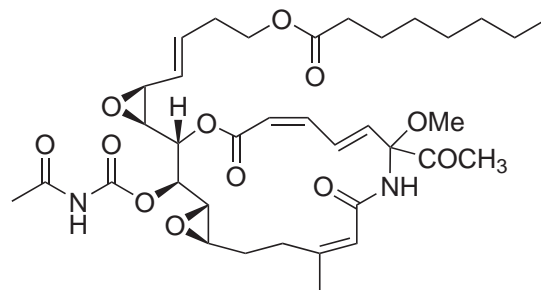
94 R = H R₁ = H R₂ = CONH₂
96 R = CONH₂ R₁ = H R₂ = CONH₂
97 R = H R₁ = H R₂ = H



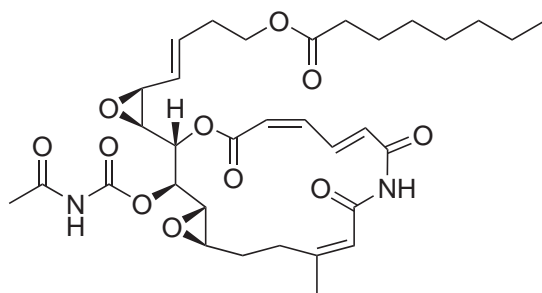
95



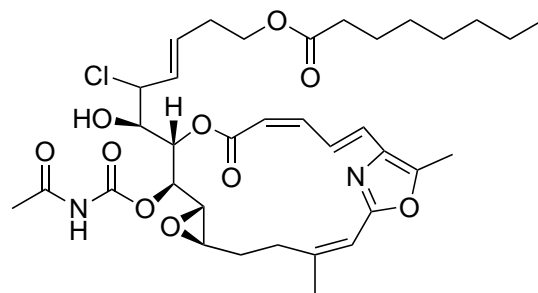
98



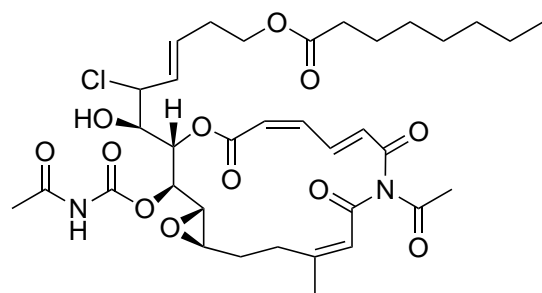
99



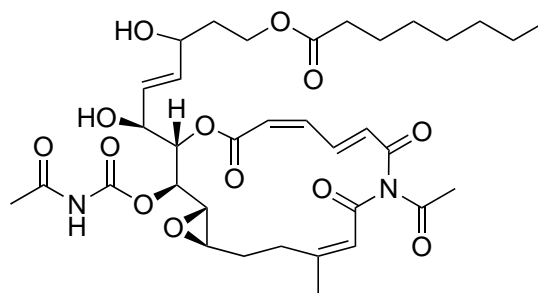
100



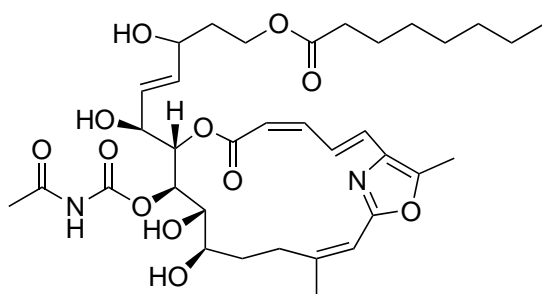
101



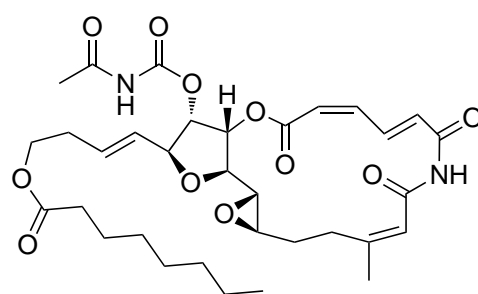
102



103



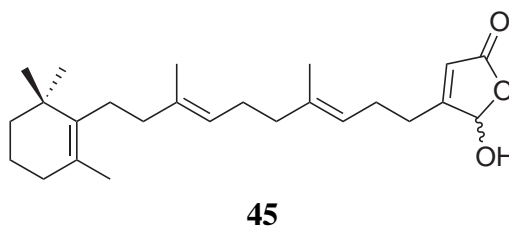
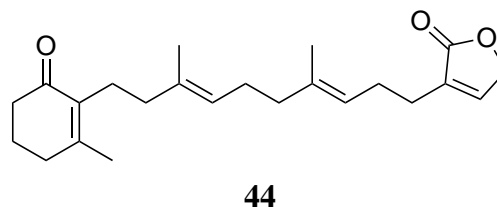
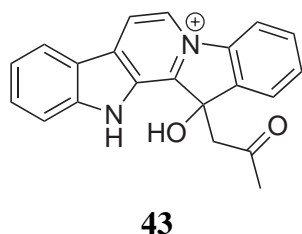
104

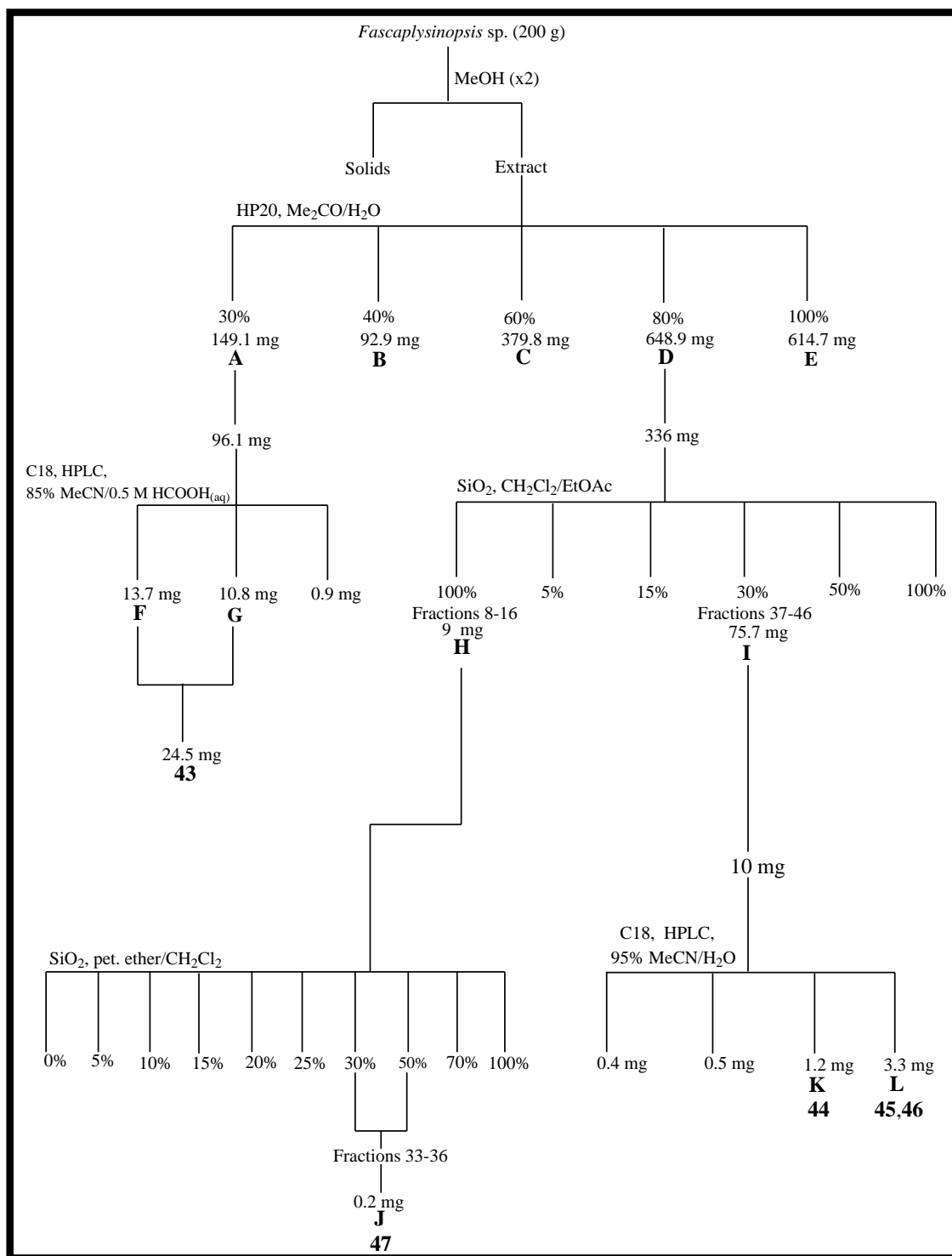


105

5.3 Isolation

A sponge identified as *Fascaplysinopsis* sp. was collected from an underwater cave off the southwestern coast of 'Eua, Tonga. The sponge was extracted twice in MeOH and the methanolic extracts were cyclic loaded onto a column of reversed-phase PSDVB beads. The resin was batch eluted with increasing amounts of Me₂CO/H₂O. NMR examination of the eluted fractions showed that the interesting signals were confined in the 30% and 80% Me₂CO/H₂O fractions. Further chromatographic steps employing bench-top normal-phase chromatography followed by reversed-phase HPLC (depicted in Scheme 5.1) led to the isolation of three known compounds, homofascaplysin A (**43**), isodehydroisoluffariellolide (**44**), and luffariellolide (**45**), along with two novel compounds, isoluffariellolide (**46**) and 1-*O*-methylisoluffariellolide (**47**). Homofascaplysin A (**43**) and isodehydroluffariellolide (**44**) were originally isolated in 1991 from the Fijian sponge *Fascaplysinopsis reticulata*,⁹¹ while luffariellolide (**45**) was first obtained from the Palauan sponge *Luffariella* sp.¹⁰⁸ Compound **43** was isolated in this study without the sesterterpenoid anion.





Scheme 5.1. Isolation of homofascaplysin A (**43**), isodehydroluffariellolide (**44**), luffariellolide (**45**), isoluffariellolide (**46**) and 1-*O*-methylisoluffariellolide (**47**) from *Fascaplysinopsis* sp. collected from 'Eua, Tongatapu.

5.4 Isoluffariellolide

Isoluffariellolide (**46**) was isolated as stable, light yellowish oil. Accurate mass measurement of the molecular formula $C_{25}H_{38}O_3$ was determined for **46** by HRESIMS with the $[M + Na]^+$ pseudomolecular ion at m/z 409.3471 (Δ 0.1 ppm), requiring seven double bond equivalents. Despite repeated chromatography, compound **46** was always accompanied by a small amount of compound **45** ($\sim 18\%$) as illustrated in the 1H NMR spectrum (see Appendix B). 1H NMR resonances were observed for H-1 and H-3 attributed to **45** (δ_H 6.00 and 5.85 ppm respectively) and H-1 and H-2 attributed to **46** (δ_H 6.84 and 6.10 ppm respectively).

The ^{13}C NMR spectrum of **46** contained 24 distinct resonances while the 1H NMR spectrum accounted for 37 of the 38 protons. An HSQC experiment confirmed the attachment of 37 of these protons to carbon, indicating the presence of one exchangeable proton. All 25 carbon resonances were identified through interpretation of the 1H and HSQC NMR spectra; five methyls (δ_C 16.2; 16.3; 20.0, 28.8, 28.8), nine methylenes (δ_C 19.7; 25.3; 25.7; 26.7; 28.1; 32.9; 39.8; 40.0; 40.4), three olefinic methines (δ_C 122.5; 123.5; 143.6), one oxymethine (δ_C 96.9), and seven quaternary carbons (δ_C 35.1; 127.1; 136.4; 137.2; 137.3; 138.1; 171.8) (Table 5.3).

COSY correlations between methylene H_2 -18 (δ_H 1.90; δ_C 32.9) and methylene H_2 -17 (δ_H 1.55; δ_C 19.7), and between H_2 -17 and methylene H_2 -16 (δ_H 1.40; δ_C 40.0) established the methylene chain C-16 to C-18. HMBC correlations from H_2 -18 to C-16 and C-17, in conjunction with HMBC correlations from H_2 -16 to C-17 and C-18 confirmed these connections (Figure 5.2).

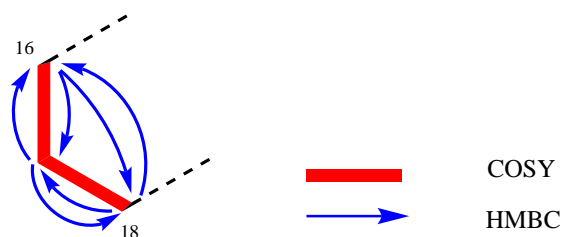


Figure 5.2. COSY and HMBC correlations establishing connectivity of C-16 to C-18 of isoluffariellolide (**46**).

Analysis of the HMBC spectrum revealed that H₂-18 showed three other correlations to C-14 (δ_C 137.2), C-19 (δ_C 127.1), and CH₃-20 (δ_H 1.60; δ_C 20.0). The singlet ¹H signal of CH₃-20 indicates attachment to a double bond at a quaternary carbon. This was confirmed by HMBC correlations from H₃-20 to C-14, C-18, and C-19. An HMBC correlation from H₂-17 to C-19 firmly established the connectivity between C-18 and C-19, as well as the attachment of CH₃-20 to C-19. A six-proton methyl singlet at CH₃-21/CH₃-22 (δ_H 0.99; δ_C 28.8) was assigned as a *gem*-dimethyl pair, connected to the alkyl quaternary carbon C-15 which in turn is adjacent to C-14 and C-16 on either side. An HMBC correlation observed from H-16 to C-14 and C-15, confirmed this connection. The HMBC correlations from H₃-21/22 to C-14, C-15, and C-16 suggested that substructure A (depicted in Figure 5.3), is a trimethylcyclohexenyl ring, which is also encountered in luffariellolide, the mokupalides and the luffariolides.^{108–110}

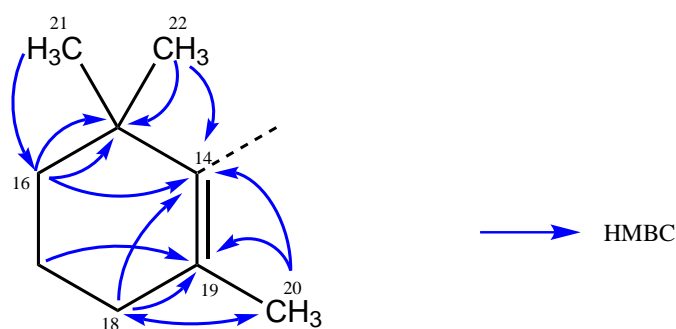


Figure 5.3. HMBC correlations establishing connectivity of the trimethylcyclohexenyl ring system, substructure A, of isoluffariellolide (**46**).

Methylene protons H₂-13 (δ_H 2.04; δ_C 28.1) showed HMBC correlations to C-14 and C-19, indicating the connection between C-13 and C-14. Vicinal couplings between H₂-13 and methylene protons H₂-12 (δ_H 1.99; δ_C 40.4) extended the fragment further and provided the connection between C-12 and C-13. HMBC correlations observed from H₂-13 to C-12 and H₂-12 to C-13 confirmed this connection. Analysis of the HMBC spectrum showed two correlation from H₂-12 to a quaternary olefinic carbon C-11 (δ_C 136.4) and to a olefinic methine CH-10 (δ_H 5.10; δ_C 123.5) suggesting a trisubstituted double bond. The methyl singlet CH₃-23 (δ_H 1.63; δ_C 16.2) must be connected to C-11, which is supported by a HMBC correlation from H₃-23 to C-11. HMBC correlations from H₃-23 to C-12 and C-10 confirmed this connection, which was further supported by a long-range COSY correlation between H-10 to H₃-23, establishing substructure B (Figure 5.4).

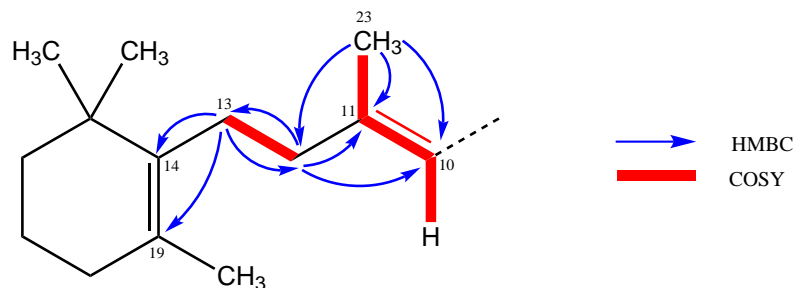


Figure 5.4. COSY and HMBC correlations establishing connectivity of C-10 to C-13, substructure B, of isoluffariellolide (**46**).

A similar substructure was revealed in the COSY spectrum from a correlation between the two methylenes CH₂-9 (δ_{H} 2.08; δ_{C} 26.7) and CH₂-8 (δ_{H} 2.00; δ_{C} 39.8) as the two methylenes show vicinal coupling to each other. This connection was confirmed by HMBC correlations from H₂-9 to C-8 and H₂-8 to C-9. The assignment of C-10 and C-9 as adjacent carbons was supported by HMBC correlations from H₂-9 to C-10 and C-11, and H-10 to C-9, strong correlations from H₂-8 to an olefinic carbon C-7 (δ_{C} 137.3) and to an olefinic methine CH-6 (δ_{H} 5.10; δ_{C} 122.5). Again a trisubstituted double bond was established using HMBC correlations from CH₃-24 (δ_{H} 1.61; δ_{C} 16.3) to CH-6, C-7 and C-8, establishing substructure C (Figure 5.5).

Due to spectral overlap, NOE enhancements were of limited utility in determining the geometry of the double bonds. Fortunately, methyl groups (CH₃-23 and CH₃-24) on the trisubstituted double bonds show characteristic NMR shifts: δ_{H} <1.6 and δ_{C} <20 for the *E*, and δ_{H} >1.6 and δ_{C} >20 for *Z* geometry.¹¹¹ Thus, the methyl groups revealed the double bonds $\Delta_{6,7}$ and $\Delta_{10,11}$ to both have *E* geometry.

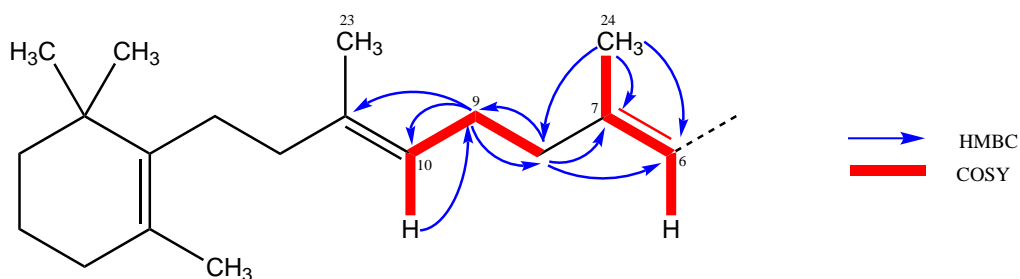


Figure 5.5. COSY and HMBC correlations establishing connectivity of C-6 to C-9, substructure C, of isoluffariellolide (**46**).

COSY correlations between two methylenes CH₂-5 (δ_{H} 2.26; δ_{C} 25.7) and CH₂-4 (δ_{H} 2.35; δ_{C} 25.3), and HMBC correlations from H₂-5 to C-4 and H₂-4 to C-5, indicated

the linkage between C-5 and C-4. An HMBC correlation from H₂-5 to C-6 and C-7 was evident, confirming the connectivity of C-5 and C-6. Analysis of the HMBC spectrum showed extra correlations from H₂-4 to three carbons: a carbonyl C-25 (δ_{C} 171.7), an olefinic carbon C-3 (δ_{C} 138.1), and an olefinic methine carbon CH-2 (δ_{H} 6.84; δ_{C} 143.6), suggesting that C-4 is adjacent to C-3. The deshielded shift of carbon C-25 suggested the presence of an α,β -unsaturated lactone unit. The HMBC correlations from H-2 to C-25, C-3 and CH-1 (δ_{H} 6.10; δ_{C} 96.9), in conjunction with the HMBC correlation from H-1 to C-25 and C-3 formed a γ -hydroxybutenolide ring, which accounted for the last remaining three double bond equivalents. The α,β -unsaturated carbonyl shields the α -carbon and deshields the β -carbon. This places CH-2 at the β -position, and the alkyl attachment at C-3. An excellent confirmation of this assumption arose from the homoallylic relationship between H-1 and H₂-4, illustrated by an ¹H-¹H COSY long range correlation. This established substructure D (depicted in Figure 5.6), as an α -substituted- γ -hydroxybutenolide ring.

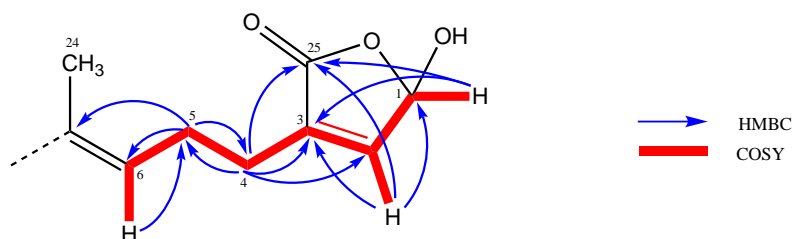


Figure 5.6. COSY and HMBC correlations establishing connectivity of the α -substituted- γ -hydroxybutenolide ring, substructure D, of isoluffariellolide (**46**).

The NMR data for the γ -hydroxybutenolide ring for isoluffariellolide (**46**) was compared to that of luffariellolide (**45**)¹⁰⁸ and dictyodendrillin C (**106**)¹¹² to ensure the correct structural isomer of **46** was assigned (Table 5.2). In **46** and **106**, an α -substituted- α,β -butenolide ring is proposed, while **45** contains a β -substituted- α,β -butenolide ring. The substitution position affects the proton chemical shifts of the olefinic methine proton and the oxymethine proton. In **46**, the olefinic methine proton appears at δ_{H} 6.84 ppm compared to δ_{H} 5.85 ppm in **45**. The oxymethine proton in **46** appears at 6.10 ppm compared to 6.01 ppm in **45**. Thus, the substitution on the α -position of the γ -hydroxybutenolide ring, as opposed to the β -position, causes the downfield shift of the H-2 and H-1 resonances in the ¹H NMR spectrum. This also has a great effect on the chemical shifts of the olefinic methine carbon and the quaternary olefinic carbon. The

olefinic methine carbon in **46** appears at δ_C 138.1 ppm and resonates at δ_C 117.0 ppm in **45**, whilst in **45**, the quaternary olefinic carbon appears at δ_C 169.9 ppm compared to δ_C 138.1 ppm in **46**. Both carbons showed dramatically changed chemical shifts. Thus, the substitution point on the γ -hydroxybutenolide ring system greatly affected the ^1H and ^{13}C chemical shift for the α - and β -position. The ^1H and ^{13}C NMR data for **46** were consistent with that for **106**, supporting the substitution at the α -position. Therefore the structure of isoluffariellolide is given as **46** with NMR data presented in Table 5.3.

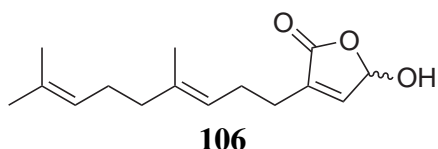
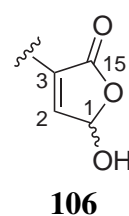
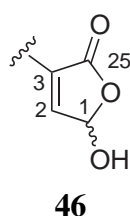
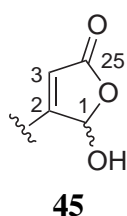


Table 5.2. Comparison of the ^1H and ^{13}C NMR chemical shifts (CDCl_3) of the γ -hydroxybutenolide ring of luffariellolide (**45**), isoluffariellolide (**46**), and dictyodendrillin C (**106**).

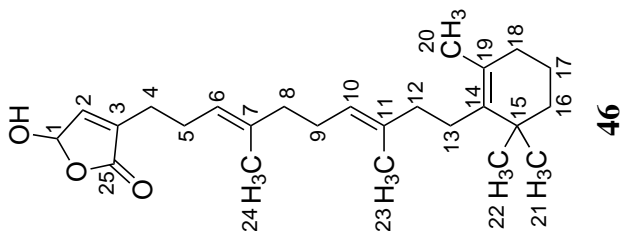


Position	^1H			^{13}C		
	45	46	106	45	46	106
1	6.01	6.10	6.07	99.5	96.9	96.7
2		6.84	6.83	169.9	143.6	143.6
3	5.85			117.0	138.1	137.7
25 (15^\dagger)				171.9	171.7	171.1 †

† Assigned as carbon 25 (C-15).

Table 5.3. ^{13}C (150 MHz) and ^1H (600 MHz) NMR Data (CDCl_3) for Isoluffariellolide (**46**).

Position	^{13}C		^1H		COSY	HMBC (^1H to ^{13}C)
	δ (ppm)	mult	$^1J_{\text{CH}}$ (Hz)	δ (ppm)	mult	J (Hz)
1	96.9	CH	176	6.10	s	2.4
2	143.6	CH	176	6.84	d	1.2
3	138.1	C				1.4
4	25.3	CH_2	122	2.35	m	1,2,5
5	25.7	CH_2	122	2.26	m	4,6,24
6	122.5	CH	153	5.10 [†]	m	5,24
7	137.3	C				1,2,5,6,25
8	39.8	CH_2	121	2.00 [†]	m	7,9
9	26.7	CH_2	125	2.08 [*]	m	8,10
10	123.5	CH	153	5.10 [†]	m	9,12,23
11	136.4	C				
12	40.4	CH_2	122	1.99 [†]	m	10,11,13,23
13	28.1	CH_2	121	2.04 [*]	m	12,14,15,19
14	137.2	C				
15	35.1	C				
16	40.0	CH_2	123	1.40	m	17
17	19.7	CH_2	126	1.55	m	14,15,17,18,21,22
18	32.9	CH_2	124	1.90	t	15,16,18,19
19	127.1	C				16,18
20	20.0	CH_3	125	1.60	s	17
21	28.8	CH_3	126	0.99	s	14,15,16,17
22	28.8	CH_3	126	0.99	s	14,15,16,17
23	16.2 ^{**}	CH_3	125	1.63	s	10,11,12
24	16.3 ^{**}	CH_3	125	1.61	s	6,7,8
25	171.7	C				



[†]Assignment interchangeable.

[‡]Assignment interchangeable.

^{*}Assignment interchangeable.

^{**}Assignment interchangeable.

5.5 1-*O*-Methylisoluffariellolide

1-*O*-Methylisoluffariellolide (**47**) was isolated as a light yellowish oily residue. Positive-ion mode HRESIMS analysis of **47** showed a characteristic pseudomolecular ion peak at m/z 423.2867 ($[M + Na]^+$, Δ 0.0 ppm), indicative of a molecular formula of $C_{26}H_{40}O_3$, requiring seven double-bond equivalents. The molecular formula for compound **47** differs from luffariellolide (**45**) and isoluffariellolide (**46**) by a CH_2 unit, supporting the gain of one oxymethyl group as indicated by the appearance of a deshielded methyl resonance (δ_H 3.55, δ_C 57.0) in the NMR spectra of **47**.

The ^{13}C NMR spectrum contained 26 distinct carbon resonances while the 1H NMR spectrum accounted for all 40 protons, which a multiplicity-edited HSQC experiment confirmed were all attached to carbon. A detailed analysis of the ^{13}C , HSQC and HMBC NMR spectra of 1-*O*-methylisoluffariellolide (**47**) (Table 5.4) assigned all 26 carbons in the molecule; five methyls (δ_C 16.2; 16.3; 20.0, 28.8, 28.8), nine methylenes (δ_C 19.7; 25.5; 25.6; 26.7; 28.1; 32.9; 39.8; 40.0; 40.4), three olefinic methines (δ_C 122.5; 123.5; 142.2), one oxymethyl (δ_C 57.0), one oxymethine (δ_C 102.6), and seven quaternary carbons (δ_C 35.1, 127.1; 136.3; 137.2; 137.3; 138.5; 171.6).

The structure of **47** was elucidated in a similar fashion to isoluffariellolide (**46**), beginning at the methylene chain in the trimethylcyclohexenyl ring. A series of sequential COSY correlations were observed starting from methylene proton resonances of CH_2 -18 (δ_H 1.90; δ_C 32.9) to a second methylene proton H_2 -17 (C-17: δ_C 19.7; δ_H 1.55), and between H_2 -17 to third methylene proton H_2 -16 (δ_H 1.40; δ_C 40.0) established the methylene chain C-16 to C-18. This was confirmed through two and three bond HMBC correlations between CH_2 -16, CH_2 -17, and CH_2 -18 (Figure 5.7).

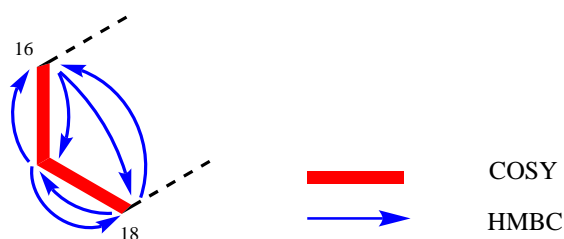


Figure 5.7. COSY and HMBC correlations establishing connectivity of C-18 to C-16 of 1-*O*-methylisoluffariellolide (**47**).

Further analysis of the HMBC spectrum showed another three correlations from H₂-16 to quaternary *sp*³ carbon C-15 (δ_C 35.1), olefinic quaternary carbon C-14 (δ_C 137.3), and *gem*-dimethyl carbons CH₃-21/22 (δ_H 0.99; δ_C 28.8). The *gem*-dimethyl singlet showed strong HMBC correlations to C-14, C-15, C-16, suggested that they are connected to the alkyl quaternary carbon (C-15), which in turn is adjacent to C-16 and C-14 on the other sides. The methylene protons H₂-18 also exhibited HMBC correlations to C-14 and C-19 (δ_C 127.1), suggesting C-19 placement on the other side, establishing the presence of a fully substituted double bond. An HMBC correlation from methyl singlet proton CH₃-20 (δ_H 1.60; δ_C 20.0) to C-19 confirmed this connection and established substructure A (depicted in Figure 5.8), as a trimethylcyclohexenyl ring which is also observed in isoluffariellolide (**46**).

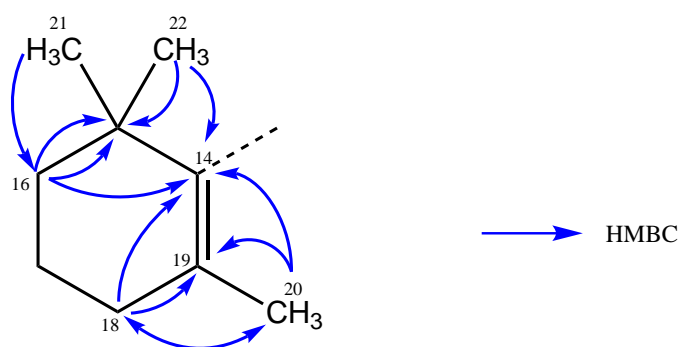


Figure 5.8. HMBC correlations establishing connectivity of the trimethylcyclohexenyl ring moiety, substructure A, of 1-*O*-methylisoluffariellolide (**47**).

HMBC correlations observed from H₂-13 (δ_H 2.04; δ_C 28.1) to C-14 and C-19, indicating the connection between C-13 and C-14. Observation of a COSY correlation between methylene proton H₂-13 and methylene protons of CH₂-12 (δ_H 1.98; δ_C 40.4) extended the partial structure, shown in Figure 5.10. An HMBC correlation from H₂-13 to C-12 and from H₂-12 to C-13, confirmed this assignment between C-13 to C-12. Further HMBC correlations from H₂-12 to olefinic carbon C-11 (δ_C 136.3) and olefinic methine CH-10 (δ_H 5.10; δ_C 123.5), suggested the presence of another trisubstituted double bond (C-11 to C-10). The methyl singlet carbon CH₃-23 (δ_H 1.63; δ_C 16.2) placement on the double bond was established through HMBC correlations from methyl proton H₃-23 to C-11 and C-10. An HMBC correlation from olefinic methine proton H-10 to C-23 established the connection between C-11 and C-10, and the adjacent of C-23 to the non-protonated olefinic carbon C-11. Analysis of the COSY spectrum showed long range

coupling from olefinic methine proton H-10 to methyl proton H₃-23 that confirmed this connection (Figure 5.9).

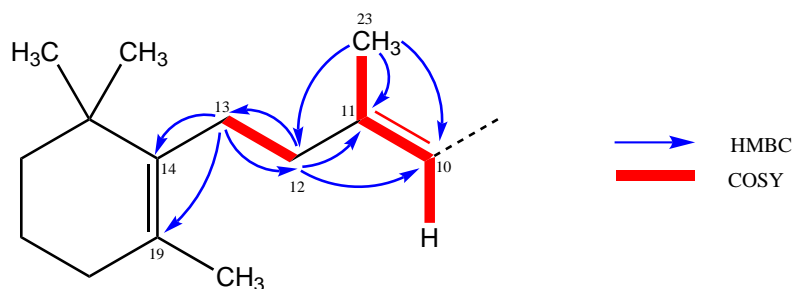


Figure 5.9. COSY and HMBC correlations establishing connectivity of C-9 to C-6 of 1-*O*-methylisulfariellolide (**47**).

Two further methylenes (C-9: δ_{H} 2.06; δ_{C} 26.7, C-8: δ_{H} 2.00; δ_{C} 39.8) were placed next to the double bond (C-11 to C-10) based on COSY correlations observed from H-10 to H₂-9 and from H₂-9 to H₂-8. Together with an HMBC correlation from olefinic methine proton H-10 to C-9, this confirmed the placement of adjacent C-10 and C-9. An HMBC correlation from H₂-9 to C-8 and H₂-8 to C-9 confirmed the connection between C-9 and C-8. The methylene proton H₂-8 showed extra HMBC correlations to two carbons; non-protonated olefinic carbon C-7 (δ_{C} 137.2) and olefinic methine carbon CH-6 (δ_{H} 5.09; δ_{C} 122.5). Unsurprisingly, the structure was unveiling itself as another isopropene unit with HMBC and COSY correlations establishing the presence of another trisubstituted double bond. The methyl singlet proton H₃-24 (δ_{H} 1.60; δ_{C} 16.3) showed HMBC correlations to C-6 and C-7 which confirmed this assignment. This established substructure B, as depicted in Figure 5.10.

Due to spectral overlap, NOE enhancements were of limited utility in determining the geometry of the double bonds. The methyl groups (CH₃-23 and CH₃-24) on the isolated trisubstituted double bonds show characteristic NMR shifts: δ_{H} <1.6 and δ_{C} <20 for the *E*, and δ_{H} >1.6 and δ_{C} >20 for *Z* geometry.¹¹¹ Based on this, and the similarity of chemical shifts with related compounds (same in **46**), the double bonds $\Delta_{6,7}$ and $\Delta_{10,11}$ were assigned as *E*.

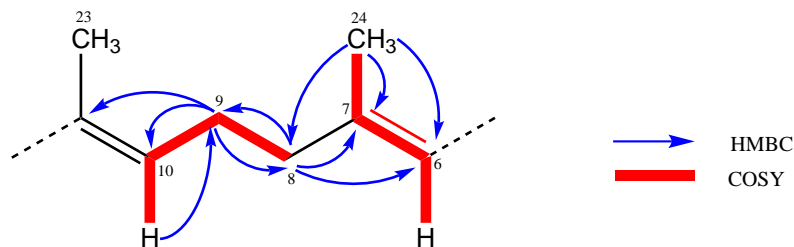


Figure 5.10. COSY and HMBC correlations establishing connectivity of C-13 to C-6, substructure B, of 1-*O*-methylisulfariellolide (**47**).

The substructures A and B accounted for four double bond equivalents suggesting the compound contained a ring system and two double bonds. COSY correlations observed between two methylenes CH₂-5 (δ_{H} 2.25; δ_{C} 25.6) and CH₂-4 (δ_{H} 2.33; δ_{C} 25.5), and HMBC correlation from H₂-5 to C-4 and H₂-4 to C-5 indicated the placement between C-5 and C-4. HMBC correlations from H-5 to C-7 and C-6 was evident, confirming the connectivity of C-5 and C-6. The methylene proton H₂-5 and H₂-4 showed HMBC correlations to an olefinic carbon C-3 (δ_{C} 138.5), establishing the connectivity between C-3 and C-4.

Further analysis of the HMBC spectrum showed correlations from H₂-4 to an ester carbonyl carbon C-25 (δ_{C} 171.6) and olefinic methine carbon CH-2 (δ_{H} 6.76; δ_{C} 142.2). HMBC correlations from olefinic methine proton H-2 to C-25, C-3, CH-1 (δ_{H} 5.72; δ_{C} 102.6), CH₂-4, and from oxymethine proton H-1 to C-25 and C-3, suggested the presence of an α,β -butenolide ring. A series of COSY correlations between H-2, H-1 and H₂-4 placed C-4 at the α -position of the butenolide. The butenolide ring system accounted for the last remaining three double bond equivalents. HMBC correlations from oxymethyl proton H₃-26 to C-1, placed an oxymethyl at the γ -position of the butenolide ring instead of a hydroxyl group as observed in **46** (Figure 5.11).

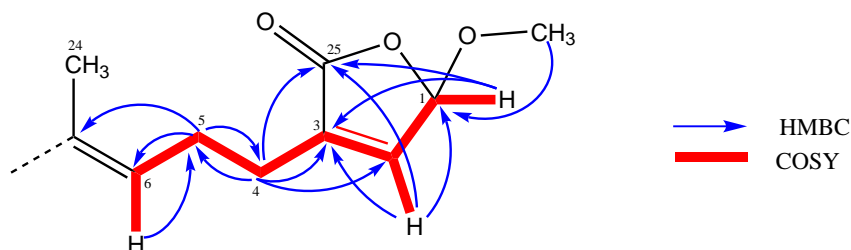


Figure 5.11. COSY and HMBC correlations establishing connectivity of the α -substituted- γ -methylbutenolide ring, substructure C, of 1-*O*-methylisulfariellolide (**47**).

The presence of an upfield non-protonated olefinic carbon and a downfield olefinic methine, suggested that it is an α -substituted butenolide ring. The NMR data for the butenolide ring for 1-*O*-isoluffariellolide (**47**) was also compared to that of isoluffariellolide (**46**), 25-*O*-methylluffariellolide (**107**)¹¹³ and 1-*O*-ethylhyrtiolide (**108**)¹¹⁴ to ensure the correct structural isomer of **47** was assigned (Table 5.4). Firstly comparing **46** and **47**, the only significant difference in the ¹³C NMR spectrum is C-1, which is shifted downfield by approximately 6 ppm in **47**. This change in chemical shift is consistent with carbon substitution of the free hydroxyl group. Compound **47** is substituted on the α -position (same in **46** and **108**) while **107** is a β -substituted butenolide ring. In **47**, the olefinic methine proton appears at δ_{H} 6.76 ppm and resonates at δ_{H} 5.91 ppm in **107**. The substitution on the α -position of the butenolide ring, as opposed to the β -position, caused the downfield shift of the olefinic methine in the ¹H NMR spectrum. The substitution position also affected the chemical shifts of the olefinic methine carbon and non-protonated olefinic carbon. In **47**, the olefinic methine carbon appears at δ_{C} 142.2 ppm and resonates at δ_{C} 118.8 ppm in **107**, whilst in **107**, the non-protonated olefinic carbon appears at δ_{C} 170.0 ppm compared to δ_{C} 138.5 ppm in **47**. The substitution of the butenolide ring does not affect the chemical shifts of C-1 and C-25. The ¹H and ¹³C NMR data for **47** were consistent with that of **108**, supporting the substitution on the α -position (C-3). Therefore the structure of 1-*O*-methyisoluffariellolide is given as **47** with NMR data presented in Table 5.4.

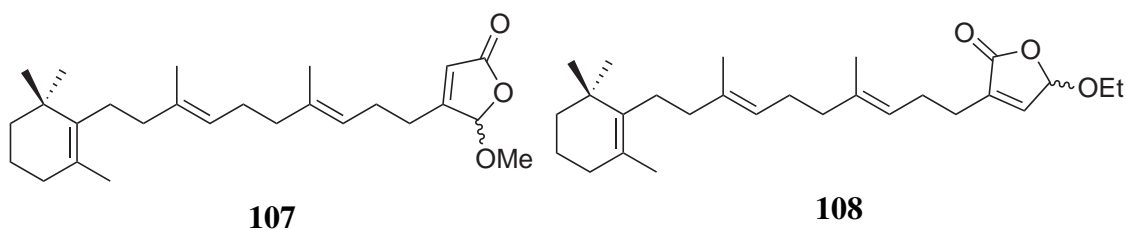
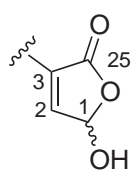
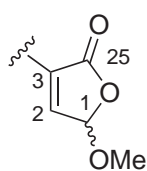


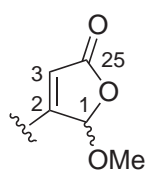
Table 5.4. Comparison of the ^1H and ^{13}C NMR Chemical Shifts of the Butenolide Ring of Isoluffariellolide (**46**), 1-*O*-Methylisoluffariellolide (**47**), 25-*O*-Methylisoluffariellolide (**107**), and 1-*O*-Ethylisoluffariellolide (**108**).



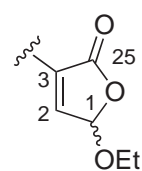
46



47



107



108

Position	^1H				^{13}C			
	46	47	107	108	46	47	107	108
1	6.10	5.72	5.78	5.78	96.9	102.6	106.3	101.5
2	6.84	6.76		6.75	143.6	142.2	170.0	142.2
3			5.91		138.1	138.5	118.8	138.1
25					171.7	171.6	172.0	171.5

Compounds **46**, **47** and **108** were recorded in CDCl_3 whilst **107** was recorded in CD_3OD .

Table 5.5. ^{13}C (150 MHz) and ^1H (600 MHz) NMR data (CDCl_3) for 1-*O*-Methylisoluffariellolide (**47**).

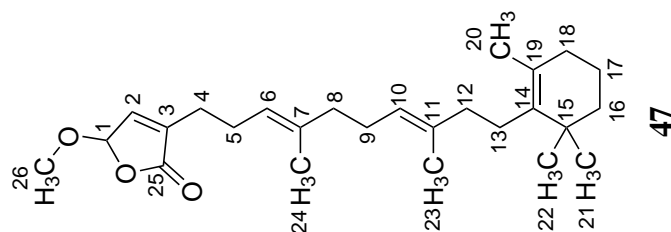
Position	^{13}C		^1H		COSY	HMBC (^1H to ^{13}C)
	$\delta(\text{ppm})$	$^1J_{\text{CH}}(\text{Hz})$	$\delta(\text{ppm})$	$J(\text{Hz})$		
1	102.6	CH	5.73	m	2,4	3,25,26
2	142.2	CH	6.76	m	1,4	1,3,4,25
3	138.5	C				
4	25.5	CH_2	2.34	m	1,2,5	1,2,5,6,25
5	25.6	CH_2	2.27	m	4,6,24	3,4,6,7
6	122.5	CH	5.10 [†]	m	5,24	5,8,24
7	137.2	C				
8	39.8	CH_2	2.00 [‡]	m	9	7,9
9	26.7	CH_2	2.06 [*]	m	8,10	8,10
10	123.5	CH	5.10 [†]	m	9,23	9,12,23
11	136.3	C				
12	40.4	CH_2	1.98 [‡]	m	13	10,11,13,23
13	28.1	CH_2	2.04 [*]	m	12	12,14,15,19
14	137.3	C				
15	35.1	C				
16	40.0	CH_2	1.40	m	17	14,15,17,18,21,22
17	19.7	CH_2	1.55	m	16,18	15,16,18,19
18	32.9	CH_2	1.90	t	6	14,15,16,17,19,20,21,22
19	127.1	C				
20	20.0	CH_3	1.60	s	18	18,19
21	28.8	CH_3	0.99	s		14,15,16,17
22	28.8	CH_3	0.99	s		14,15,16,17
23	16.2 ^{**}	CH_3	1.63	s	10	10,11,12
24	16.3 ^{**}	CH_3	1.60	s	6	6,7,8
25	171.6	C				
26	57.0	CH_3	3.55	s		1

[†]Assignment interchangeable.

[‡]Assignment interchangeable.

^{*}Assignment interchangeable.

^{**}Assignment interchangeable.



5.6 Biological Activity

Isodehydroluffariellolide (**44**), isoluffariellolide (**46**) and 1-*O*-methylisoluffariellolide (**47**) were submitted for cytotoxicity testing at the School of Biological Sciences, VUW. They were tested in a 48 hour MTT assay against HL-60 (leukemia) cells. Compounds **44**, **46** and **47** were found to be moderately cytotoxic with IC₅₀ values in the micromolar range (12.21 μ M, 29.63 μ M and 5.09 μ M respectively).⁸⁶

5.7 Related Compounds

Many primary and secondary metabolites are derived from terpenes, all biosynthesised from the five-carbon isoprene building units.¹¹⁵ Structural modification of these isoprene units leads to a diverse range of derivatives with unique chemical structures and biological properties. Triterpenoids were the first terpenoids reported from marine resources and since then a vast array of derivatives have been documented. Marine sponges have been identified as one of the prime resources of sesterterpenes.¹¹⁶

Manoalide (**109**) is the parent compound of a series of marine sponge metabolites belonging to the sesterterpene class and probably the most well known of all sesterterpene sponge metabolites. Manoalide (**109**) was originally isolated by Scheuer *et al.* in 1980 from the sponge *Luffariella variabilis* collected in Palau.¹¹⁷ One year later, Scheuer *et al.* reported three additional related metabolites from the same Palauan sponge, secomanoalide (**110**), (*E*)-neomanoalide (**111**) and (*Z*)-neomanoalide (**112**).¹¹⁸ All four compounds (**109–112**) exhibit antibiotic activity.¹¹⁹ Later, marine sponges of the family Thorectidae, including species of the genera *Hyrtios*,^{114,120,121} *Cacospongia*,^{122,123} *Thorectandra*,^{124,125} *Fasciospongia*,^{126–129} *Luffariella*,^{108,110,118,130–140} *Aplysinopsis*,¹⁴¹ and *Acanthodendrilla*,¹¹³ were also found to be rich sources of novel bioactive sesterterpenoids closely related to **109**.

Early studies into the pharmacology of **109** revealed an irreversible inhibition of phospholipase A₂.^{142,143} Subsequently, many related metabolites with PLA₂ inhibitory

activity were also reported, which attracted scientific interest to study the structure-activity relationships (SAR) of **109** to understand both PLA₂ function and mechanism of action in the whole cell.^{108,144–150} Several studies revealed the contribution of various functional groups incorporated in **109** and its analogues, such as the γ -hydroxybutenolide, α -hydroxydihydropyran and trimethylcyclohexenyl ring systems, to the efficacy as PLA₂ inhibitors.^{146,150,151}

Manoalide-25-monoacetate (**113**) was reported in 1988 from the marine sponge *Thorectandra excavatus*.¹²⁴ 24-*O*-Ethylmanoalide (**114**) was isolated from *Luffariella* cf. *variabilis* collected from the Indian Ocean,¹⁴⁰ while 24-*O*-propylmanoalide (**115**) was obtained from the Palauan sponge *L. variabilis*.¹³⁸ (4*E*,6*E*)-Dehydromanoalide (**116**) was obtained from the Palauan sponge *L. variabilis* and showed reduced potency but similar efficacy to that of **109** against bee venom PLA₂ (IC₅₀ = 0.28 μ M).^{134,151} Two diastereomers of 24-*O*-methylmanoalide (**117** and **118**) and (6*Z*)-neomanoalide-24,25-diacetate (**119**) were isolated from a sponge of the genus *Luffariella*.¹³⁶ Compounds **117** and **118** exhibited antibacterial activity. Four new antibacterial sesterterpenes (**120–123**) were reported from a marine sponge of the genus *Luffariella* collected from the Australian Great Barrier Reef.¹³³

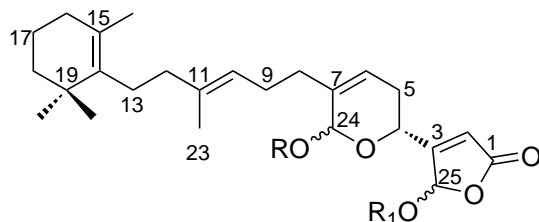
An investigation of the Fijian sponge *F. reticulata* led to the isolation of isodehydroluffariellolide (**44**) and dehydroluffariellolide diacid (**72**).⁹¹ Fasciospongide A (**124**) was obtained from the New Caledonian sponge *Fasciospongia* sp.¹²⁶ Bioassay-directed separation of an extract of a *Thorectandra* sp. sponge led to isolation of 16-oxoluffariellolide (**125**), 16-hydroxyluffariellolide (**126**), and compound **127**, all with phosphatase Cdc25B inhibitory activity.¹²⁵ Compounds **44**, **124** and **125** possessed a substituted trimethylcyclohexenone ring moiety instead of a trimethylcyclohexenyl ring system found in **109** and other analogues. Luffariellolide (**45**) is a sesterterpenoid analogue of **110**, which was first reported by Faulkner *et al.* in 1987 from the Palauan marine sponge *Luffariella* sp.¹⁰⁸ In contrast with the irreversible inhibitory action of **109** towards PLA₂, luffariellolide (**45**) is a slightly less potent, but a partially reversible PLA₂ inhibitor, which meant that **45** became a more preferable anti-inflammatory agent for potential pharmacological investigation.¹⁰⁸

In addition to luffariellolide (**45**), its 25-*O*-methyl (**107**) and 25-*O*-ethyl derivatives (**128**), five cytotoxic acantholides A-E, were isolated from the Indonesian sponge *Acanthodendrilla* sp.¹¹³ Acantholides A (**129**) and B (also reported as 16-oxo-luffariellolide, **125**) possessed both the trimethylcyclohexene and the γ -hydroxybutenolide moieties. Acantholides D (**130**) and E (**131**) are derivatives comprising the 1-acetylcyclopentan-5-ol moiety, and are rare variants for the C₁₄-C₂₀ segment in this type of linear sesterterpenes thus replacing the trimethylcyclohexenyl ring. Luffariellolide (**45**) and its 25-*O*-methyl congener (**107**), as well as acantholide E (**131**), were cytotoxic against the mouse lymphoma L5178Y cell line with ED₅₀ values of 3.3, 0.7, and 7.0 μ g/mL, respectively. Interestingly, these results suggested that the 25-*O*-methyl group in compound **107** and the stereochemistry of 1-acetylcyclopentan-5-ol in **131** play an important role in the cytotoxicity of the compound.¹¹³

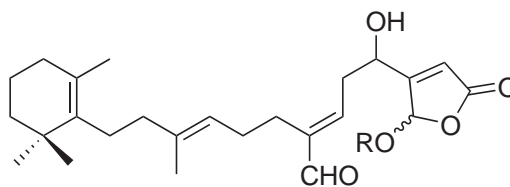
Luffariolides A-J (**132–140**), are a related group of sesterterpenoidal analogues, have been isolated from different collections of the Okinawan marine sponge *Luffariella* sp.^{110,130,139} All luffarieolides exhibited significant cytotoxicity against the murine lymphoma L1210 cell line with IC₅₀ values ranging between 1.1–7.8 μ g/mL. Luffariellins A (**141**) and B (**142**) were isolated from the marine sponge *L. variabilis* collected in Palau.¹³¹ Chemical investigation of the same sponge species collected from the Great Barrier Reef, Australia, yielded three new acetylated compounds, 25-acetoxyluffariellin A (**143**), 25-acetoxyluffariellin B (**144**), and 25-acetoxysecomanoalide (**145**).¹³⁷ Luffariellins C (**146**) and D (**147**) were obtained from the nudibranch *Chromodoris funerea* collected from Palau.¹⁵² Luffariellins (**141–144**) are all characterized by the 1-isoproprenyl-2-methylcyclopentane ring system replacing the trimethylcyclohexenyl moiety in other manoolide analogs. Despite this difference in chemical structure, luffariellins A (**141**) and B (**142**) retain identical functional groups as present in **109** and **110**, respectively. Therefore, not surprisingly, each respective pair was shown to have similar anti-inflammatory properties to **109** and **110**.¹³¹

Hyrtiolide (**148**) and its 1-*O*-ethyl derivatives (**108**) were obtained from sponge *Hyrtios* cf. *erecta*, from Fiji.¹¹⁴ Aplysinoplides A–C (**149–151**) were isolated from the marine sponge *Aplysinopsis digitata*.¹⁴¹ Compounds (**149–151**) exhibited cytotoxic activity against P388

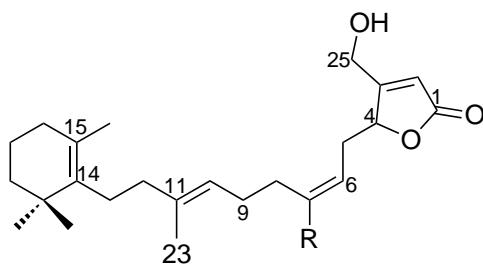
mouse leukemia cell lines with IC₅₀ values of 0.45, 0.45, and 11 $\mu\text{g/mL}$, respectively. In a parallel experiment, aplysinoplides A (**149**) and B (**150**) did not inhibit bovine pancreas PLA₂ at a concentration of 100 μM , whereas manoalide (**109**) exhibited a potent activity. These results suggested the important role of the C-24 aldehyde for inhibition of PLA₂.¹⁵¹



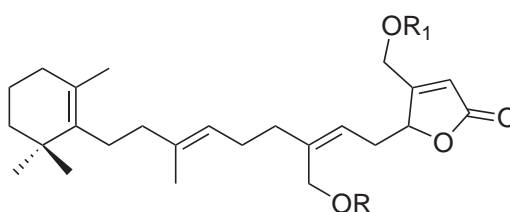
- 109** R = H-*trans* R₁ = H
113 R = H-*trans* R₁ = Ac-*cis*
114 R = Et R₁ = H
115 R = *n*-Pr R₁ = H
117 R = Me-*trans* R₁ = H
118 R = Me-*cis* R₁ = H



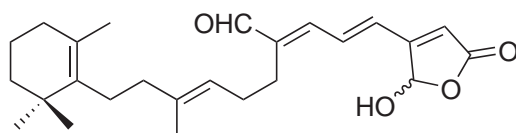
- 110** R = H
145 R = Ac



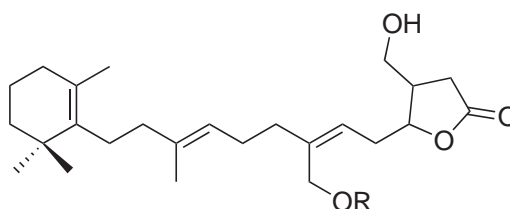
- 111** R = CH₂OH
123 R = CHO



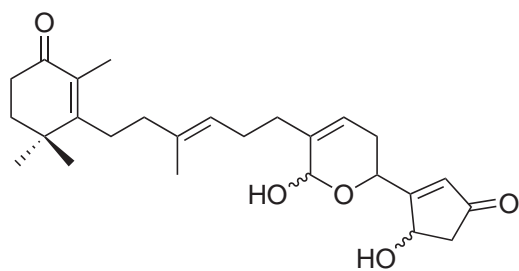
- 112** R = H R₁ = H
119 R = Ac R₁ = Ac
122 R = Ac R₁ = H



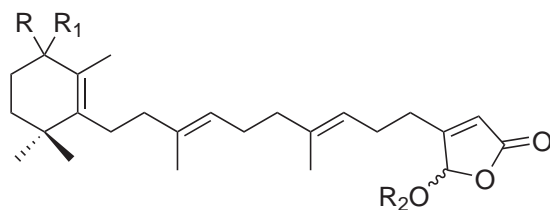
116



- 120** R = OH
121 R = Ac



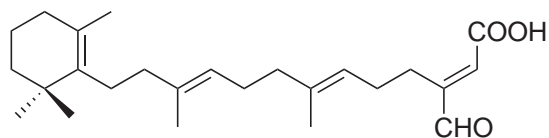
124



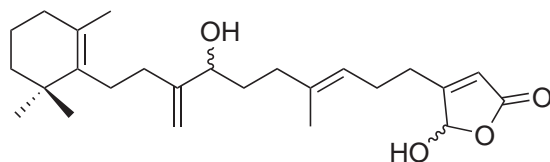
125 R = O R₁ = O R₂ = H

126 R = H R₁ = OH R₂ = H

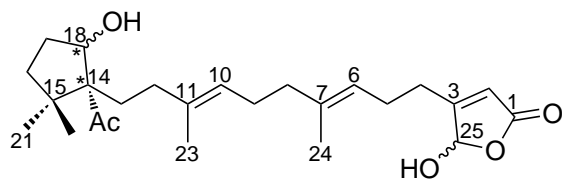
128 R = H R₁ = H R₂ = Et



127

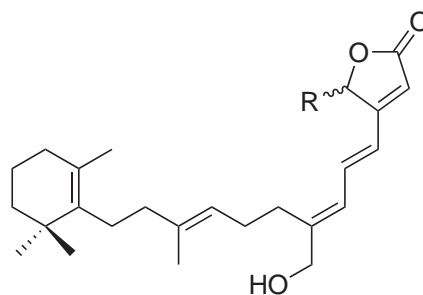


129



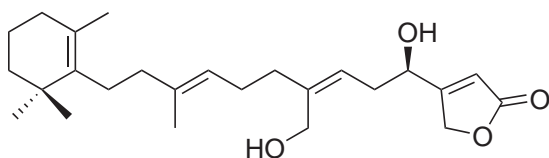
130 R = 18(OH)-*trans*

131 R = 18(OH)-*cis*

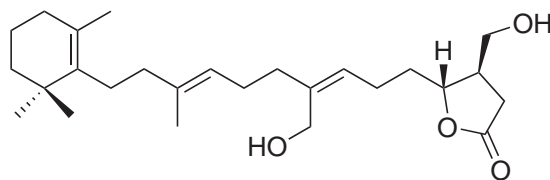


132 R = H

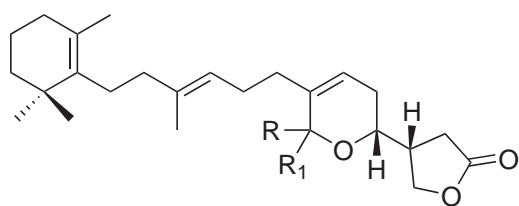
149 R = OH



133

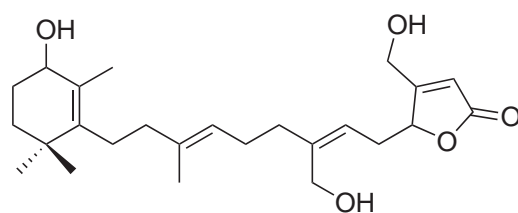


134

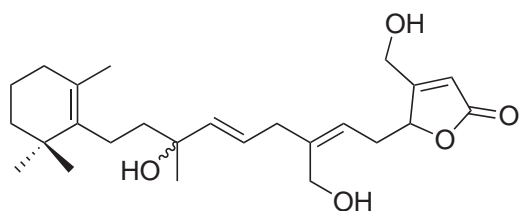


135 R = OH R₁ = H

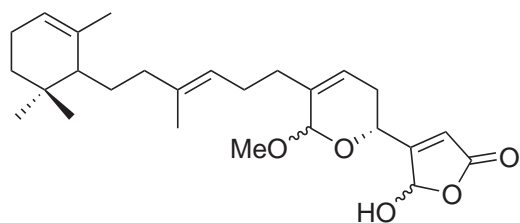
136 R = O R₁ = O



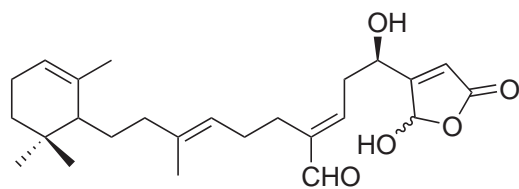
137



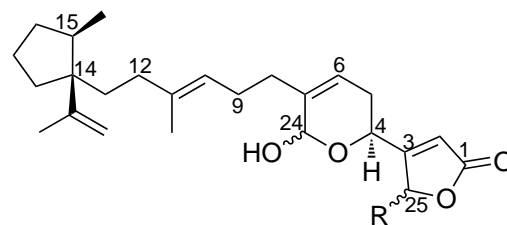
138



139



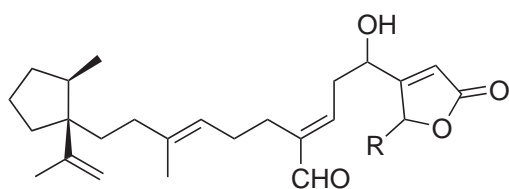
140



141 R = OH

143 R = OAc

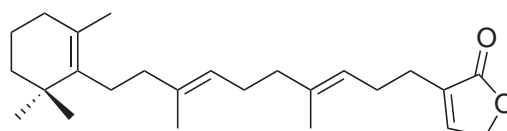
146 R = H



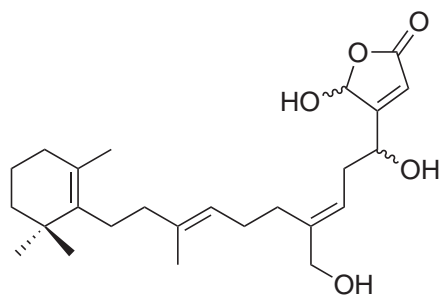
142 R = OH

144 R = OAc

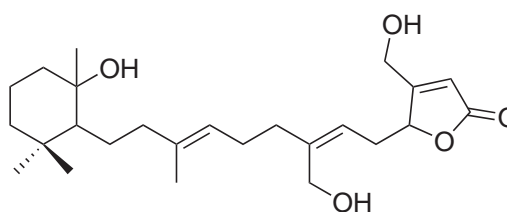
147 R = H



148



150



151

Chapter 6

Investigation of Sponge from the Order Dictyoceratida

6.1 Order Dictyoceratida

The order Dictyoceratida, which belongs to the class Demospongiae, does not have any siliceous spicules, which makes taxonomic identification of the dictyoceratid sponges more difficult. Dictyoceratid sponges are tough and flexible, with typical conulose surface, marked by conules or cone-shaped elevations. These sponges often have a marked difference in external and internal pigmentation with a dark exterior and the interior ranging from white, cream, through to pale brown or yellow. The order consists of four families: Dysideidae, Spongiidae, Irciniidae and Thorectidae (Table 6.1).²¹ In terms of chemotaxonomy, the order is characterised by a diverse range of terpenes and very low sterol content.²¹ The taxonomy of the Dictyoceratida has been revised multiple times,²¹ and a full review of the secondary metabolites isolated from dictyoceratid sponges is beyond the scope of this report.

The sponge investigated in this study (shown in Figure 6.1) was a encrusting sponge with upright fingers. The sponge is soft with a slippery texture. It was pale grey on the surface with mid-brownish interior. It contained no siliceous spicules, and has tentatively been identified as belonging to the order Dictyoceratida.



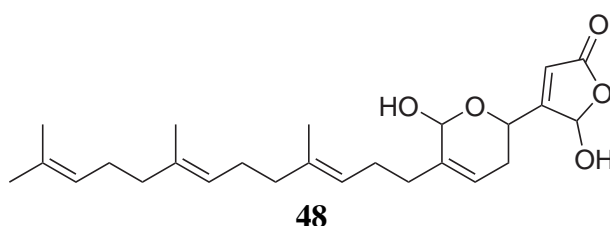
Figure 6.1. Surface photograph of the sponge PTN3_21C.

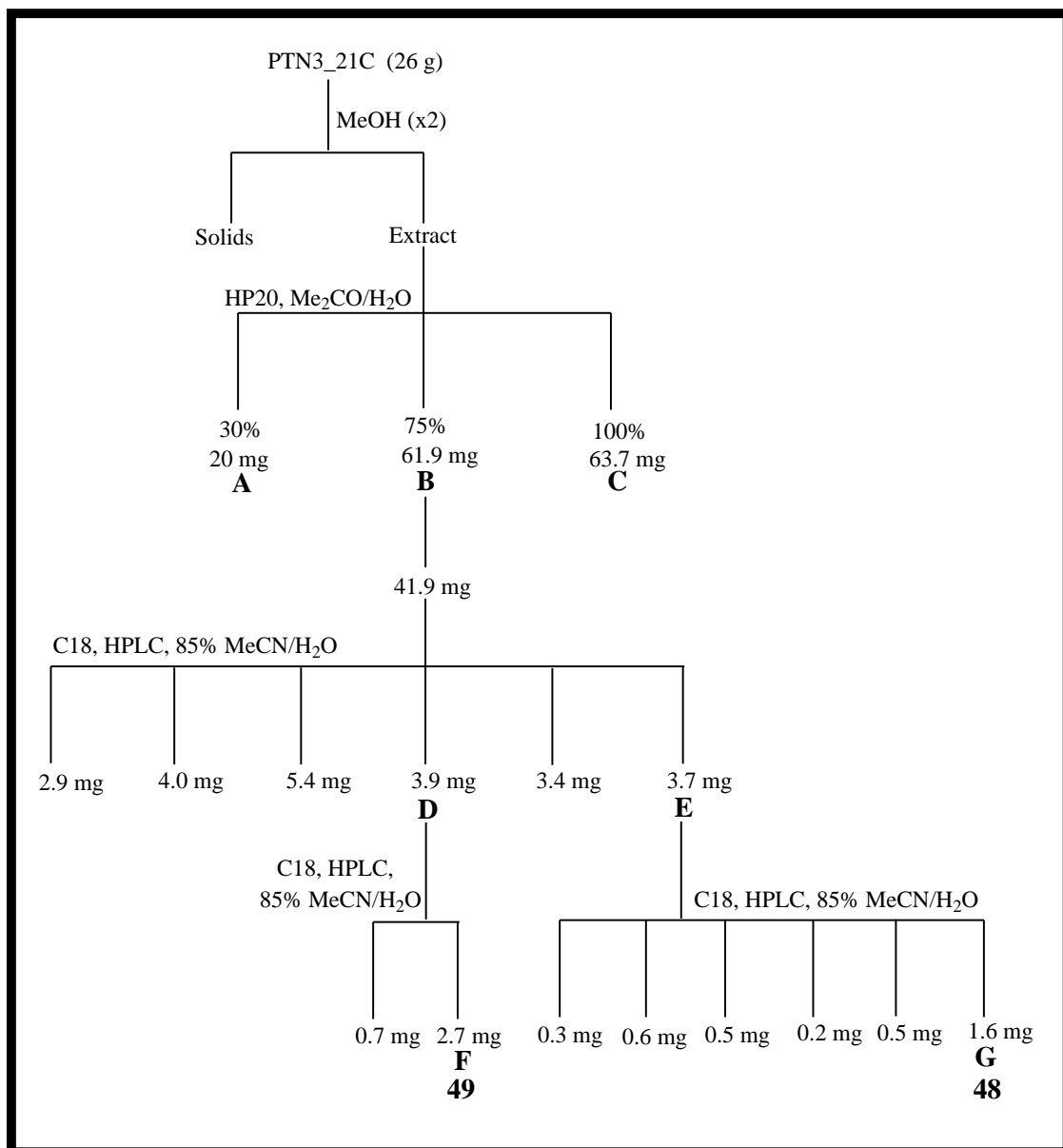
Table 6.1. Taxonomic classification of the order Dictyoceratida.²¹

Class	Order	Family	Genus
Demospongiae	Dictyoceratida	Dysideidae	
		Irciniidae	
		Spongiidae	
		Thorectidae	
			<i>Aplysinopsis</i>
		<i>Cacospongia</i>	
		<i>Fasciospongia</i>	
		<i>Fascaplysinopsis</i>	
		<i>Hytrios</i>	
		<i>Luffariella</i>	
	<i>Thorectandra</i>		

6.2 Isolation

An undescribed dictyoceratid sponge (PTN3_21C), was collected from an underwater cave at the southwest of 'Eua, Tonga. The sponge was extracted twice in MeOH and the extracts were cyclic loaded onto reversed-phase PSDVB beads. The resin was batch eluted with increasing amounts of Me₂CO in H₂O. NMR examination of the screened fractions showed that the interesting signals were confined to the 75% Me₂CO/H₂O fraction. Further chromatographic steps employing reversed-phase HPLC (depicted in Scheme 6.1) led to the isolation of the known thorectolide (**48**), and a novel sesterterpene, secothorectolide (**49**). Use of HPLC led to the isolation of two impure compounds with a very similar chromophore. Preliminary NMR analysis of fractions **D** and **E** (Scheme 6.1) showed similarities to each other, however the aldehyde proton that appears in the ¹H NMR spectrum of fraction **D** was absent in fraction **E**. Mass spectroscopy indicated a molecular formula of C₂₅H₃₆O₅ for fraction **E**, and a literature search of the sesterterpene class and comparison of the NMR data revealed the compound to be thorectolide (**48**). Compound **48** was reported from a New Caledonian sponge *Hyrtios* sp. in 1996.¹²⁰





Scheme 6.1. Isolation of thorecetolide (**48**) and secothorectolide (**49**) from PTN3_21C, collected from 'Eua, Tongatapu.

6.3 Secothorectolide

The observation of a pseudomolecular ion by positive-ion mode HRESIMS indicated a molecular formula of $C_{25}H_{36}O_5$ for compound (**49**) (m/z 439.2460, $[M + Na]^+$, Δ 0.0 ppm), which requires eight double bond equivalents. Examination of the ^{13}C NMR spectrum revealed only 24 resonances, however the carbon signal observed at 170.3 ppm accounted for two different carbons, thereby accounting for all 25 carbons suggested by the molecular formula. The 1H NMR spectrum accounted for 34 protons, suggesting two exchangeable protons. Analysis of the HSQC spectrum confirmed the attachment of these 34 protons to carbon.

Initial analysis of the ^{13}C and multiplicity-edited HSQC spectra revealed 19 protonated carbons; four methyls (δ_C 16.16; 16.20; 17.9, 25.9), seven methylenes (δ_C 24.7; 26.7; 26.88; 26.89; 34.8; 39.8; 39.9), six olefinic methines (δ_C 118.9; 123.0; 124.1; 124.5, 147.7; 194.9), two oxymethines (δ_C 67.0; 97.8), leaving six non-protonated carbons (δ_C 131.6; 135.4; 136.8; 146.1; 170.3, 170.3). The quaternary carbon resonance at δ_C 170.3 is characteristic of an α,β -unsaturated lactone or acid. A highly deshielded carbonyl methine (δ_H 9.41, δ_C 194.9) indicated the presence of an α,β -unsaturated aldehyde. Four quaternary carbon resonances (δ_C 131.6, 135.4, 136.8, 146.1), together with olefinic methines at δ_H 123.0, 124.1, 124.5, 147.7, are typical for four trisubstituted olefins. With five double bonds accounted for, this requires that the molecule be monocyclic.

HMBC correlations observed from two of the methyl singlets CH_3 -20 (δ_H 1.68; δ_C 25.9) and CH_3 -21 (δ_H 1.60; δ_C 17.9) to the same two carbons; olefinic methine carbon CH-18 (δ_H 5.08; δ_C 124.5) and quaternary olefinic carbon C-19 (δ_C 131.6) as well as to each other implied the presence of geminal methyls as part of a trisubstituted double bond. Long-range COSY correlations from H-18 to H_3 -20, in conjunction with HMBC correlations from H-18 to CH_3 -20 and CH_3 -21, confirmed this connectivity. HMBC correlations from H-18 to methylene carbon CH_2 -17 (δ_H 2.05; δ_C 26.9) and a COSY correlation between H_2 -18 and H_2 -17 extended the fragment further, unveiling substructure A (Figure 6.2) as an isoprene unit.

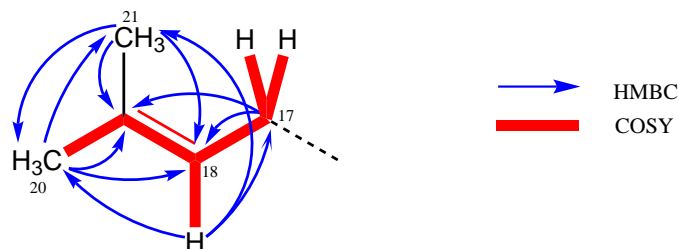


Figure 6.2. COSY and HMBC correlations establishing connectivity of the terminal isoprene unit, substructure A, of secothorectolide (**49**).

COSY and HMBC correlations between CH_2 -17 and methylene CH_2 -16 (δ_{H} 1.96; δ_{C} 39.9), established the connectivity between the two respective carbons. Further HMBC correlations were observed from H_2 -16 to an olefinic quaternary carbon C-15 (δ_{C} 135.4), olefinic methine carbon CH-14 (δ_{H} 5.08; δ_{C} 124.1) and methyl carbon CH_3 -22 (δ_{H} 1.59; δ_{C} 16.2), suggesting the presence of another trisubstituted double bond. HMBC correlations from H_3 -22 to C-16, C-15 and C-14 (δ_{H} 5.08; δ_{C} 124.1), together with COSY correlations between H_3 -22 and H-14 confirmed this connection.

Two further methylenes CH_2 -13 (δ_{H} 2.05; δ_{C} 26.9) and CH_2 -12 (δ_{C} 39.8, δ_{H} 1.96) were placed next to the double bond based on COSY and HMBC correlations observed between CH-14, CH_2 -13 and H_2 -12. CH_2 -12 showed further HMBC correlations to ^{13}C resonances attributed to another trisubstituted double bond— C-11 (δ_{C} 136.8), olefinic methine CH-10 (δ_{H} 5.10; δ_{C} 123.0) and an attached methyl, CH_3 -23 (δ_{H} 1.57; δ_{C} 16.2). COSY and HMBC correlations from H-10 and H_2 -9 (δ_{H} 2.05; δ_{C} 26.9) extended the fragment further, unveiling substructure B (Figure 6.3) as two unfunctionalised isoprene units.

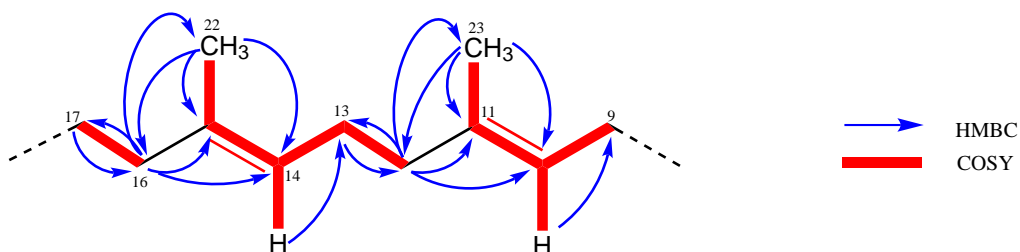


Figure 6.3. COSY and HMBC correlations establishing connectivity of the isoprene units, substructure B, of secothorectolide (**49**).

COSY correlations were observed from H_2 -9 to methylene proton H_2 -8 (δ_{H} 2.30; δ_{C} 24.7) that established two contiguous methylenes, confirmed through HMBC correlations from

H₂-9 to C-8 and H₂-8 to C-9. Further HMBC correlations from H₂-8 to an olefinic quaternary carbon C-7 (δ_C 146.1) and olefinic methine carbon CH-6 (δ_H 6.55; δ_C 147.7) revealed another trisubstituted double bond. CH-6 has an unusual, highly deshielded chemical shifts compared to the two previous trisubstituted double bonds. The H-6 proton appeared at δ_H 6.55 ppm while its carbon C-6 resonated at δ_C 147.7 ppm and the C-7 carbon resonance appeared at δ_C 146.1. With all four methyls accounted for, this trisubstituted double bond was considered to have a different chemical environment. The H₂-8 proton showed an extra HMBC correlation to the aldehyde carbon C-24 (δ_H 9.41; δ_C 194.9). The aldehyde proton H-24 showed HMBC correlations to three carbons, C-7, C-6, and C-8, establishing its connection to the polarised trisubstituted double bond. Further analysis of the COSY spectrum revealed a long-range correlation between H-6 and H₂-8, together with HMBC correlations from H-6 to C-24 and C-7, and confirmed the connectivity of the trisubstituted double bond (Figure 6.5). The deshielding effect on aldehyde carbon C-24 was consistent with the presence of a conjugated double bond (C-6 and C-7). In addition, the stereochemistry of the double bond $\Delta_{6,7}$ was assigned as *E*, based on the chemical shift of the aldehyde proton, δ_H 9.41 ppm, corresponding to the slightly shielded values recognised for the *E* configuration (*E*: 9.3–9.4 ppm; *Z*: 10.0–10.1 ppm) of this functional group.^{118,131,153}

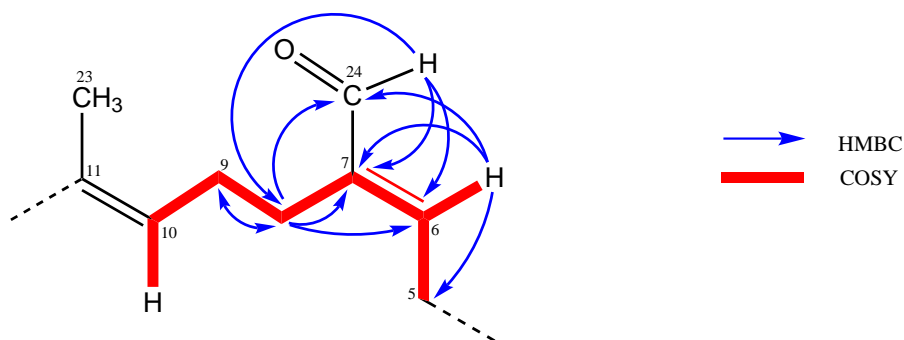


Figure 6.4. COSY and HMBC correlations establishing connectivity of the isopropene unit, substructure C, of secothorectolide (**49**).

Further analysis of the HMBC spectrum showed extra correlations from H-6 to methylene CH₂-5 (δ_H 2.81, 2.86; δ_C 34.8) and oxymethine carbon CH-4 (δ_H 4.82; δ_C 67.0), assigning a methylene carbon CH₂-5 between the polarised double bond (C-6 and C-7), and the oxymethine CH-4. The difference in chemical shift of the two protons of this methylene CH₂-5 is consistent with an adjacent chiral centre (CH-4). HMBC correlations

from the H₂-5 protons to C-7, C-6 and C-4 are consistent with this assignment. In the coupled HSQC spectrum, the oxymethine CH-4 has ¹J_{CH} of 147 Hz which is typical for that of a *sp*³ carbon attached to oxygen. COSY correlations were observed from H₂-5 to H-4 and H-6 that confirmed this skeletal arrangement. This connectivity was further supported by the triplet signal observed in the ¹H NMR spectrum for olefinic methine proton H-6 which indicated a methylene proton CH₂-5 adjacent.

With 21 of the 25 carbons and 33 of the 36 protons accounted for, a fragment containing four carbons, three oxygens, three hydrogens including an exchangeable proton, remained to be assigned (C₄H₃O₃). The chemical shift of the C-1 (δ_C 170.3) carbonyl was typical of an α,β-unsaturated lactone. Also supporting this assumption was the fact that five of the double bond equivalents were accounted for, leaving three double bond equivalents. These requirements are consistent with that of a butenolide ring system. The oxymethine proton H-4 showed weak HMBC correlations to three carbons, C-6, C-2 (δ_H 6.11; δ_C 118.9), and C-5. The olefinic methine proton H-2 also showed HMBC correlations to C-1 (δ_C 170.3), C-25 (δ_H 6.18; δ_C 97.8), and C-4. Weak COSY correlations between H-2 and H-4 but not between H-25 and H₂-4 (in the case of **46** and **47**) was observed, which suggested a β-substituted-γ-hydroxybutenolide. With aid from the literature, the ring system was assigned as a β-substituted-γ-hydroxybutenolide ring, which is also encountered in luffariellolide,¹⁰⁸ luffariolides,^{110,130} manoalide,^{117,119} luffariellins,^{118,131} cacospongiolides,^{122,123} fasciospongides,¹²⁶ and sarcotins.¹⁵⁴ In addition, the *E*-configuration of the C-6–C-7 prevents ring closure between the C-24 aldehyde and the hydroxyl group at C-4 which lead to the formation of thorectolide (**48**). Therefore the structure of secothorectolide is given as **49** with NMR data presented in Table 6.2.

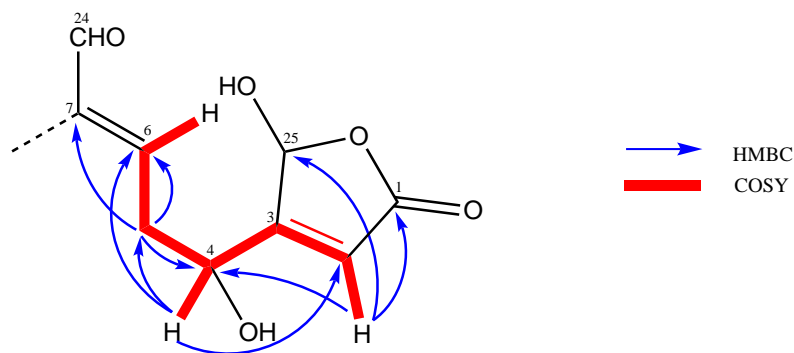
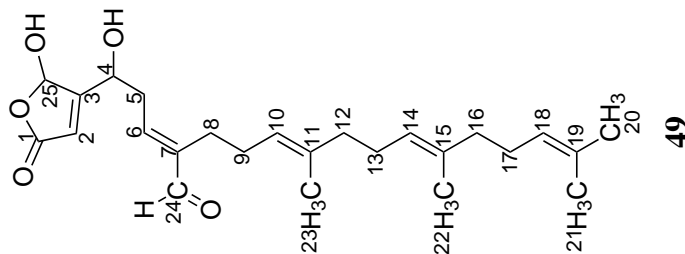


Figure 6.5. COSY and HMBC correlations establishing connectivity of the isopropene unit, substructure D, of secothorectolide (**49**).

Table 6.2. ^{13}C (150 MHz) and ^1H (600 MHz) NMR Data (CDCl_3) for Secothorectolide (**49**).

Position	^{13}C		^1H		COSY	HMBC (^1H to ^{13}C)
	δ (ppm)	mult	$^1J_{\text{CH}}$ (Hz)	δ (ppm)	mult	J (Hz)
1 [†]	170.3	C				
2	118.9	CH	183	6.11	s	
3 [†]	170.3	C			4*, 25*	1, 3, 25
4	67.0	CH_2	147	4.82	br s	
5a	34.8	CH_2	129	2.81	m	2, 5, 6
5b	34.8	CH_2	129	2.86	m	4, 6, 7
6	147.7	CH	153	6.55	t	4, 6
7	146.1	C			7.2	8
8	24.7	CH_2	129	2.31	t	7.8
9 [†]	26.89	CH_2	123	2.05	m	9
10	123.0	CH	150	5.10 [†]	m	8, 10
11	136.8	C			9, 23	9
12 ^{**}	39.9	CH_2	122	1.96	m	13
13 [†]	26.88	CH_2	123	2.05	m	10, 11, 12
14	124.1	CH	151	5.08 [†]	m	12
15	135.4	C			13, 22	13
16 ^{**}	39.8	CH_2	122	1.96	m	17
17 [†]	26.7	CH_2	123	2.06	m	14, 15, 16
18	124.5	CH	151	5.08	m	15, 16, 22
19	131.6	C			17, 20	17, 20, 21
20	25.9	CH_3	125	1.68	s	18, 19, 21
21	17.9	CH_3	125	1.60	s	18, 19, 20
22 [†]	16.16	CH_3	126	1.59	s	14, 15, 16
23 [†]	16.20	CH_3	125	1.57	s	10, 11, 12
24	194.9	CH	175	9.41	s	6, 7, 8
25	97.8	CH	177	6.18	s	2*



[†]Assignment interchangeable.

[‡]Assignment interchangeable.

**Assignment interchangeable.

*Weak correlations.

6.4 Biological Activity

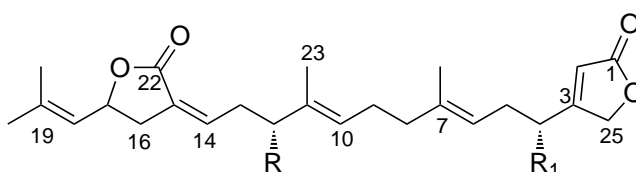
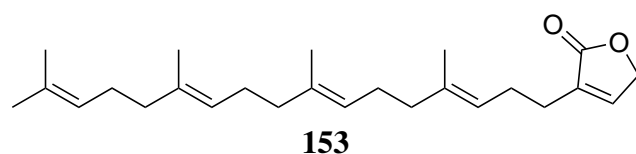
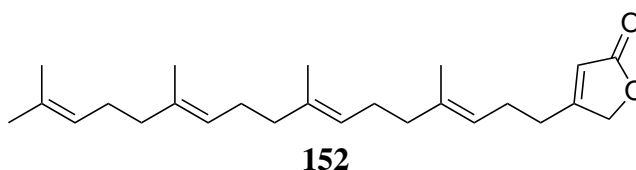
The biological activity profile of thorectolide (**48**) and secothorectolide (**49**) against human cancer cell lines has undergone preliminary investigation. An MTT assay on ovarian cancer (1A9) cells was performed at the School of Biological Sciences, VUW. Compounds **48** and **49** were found to be moderately cytotoxic with IC₅₀ values of 3.74 and 2.45 μ M respectively.⁸⁶

6.5 Related Compounds

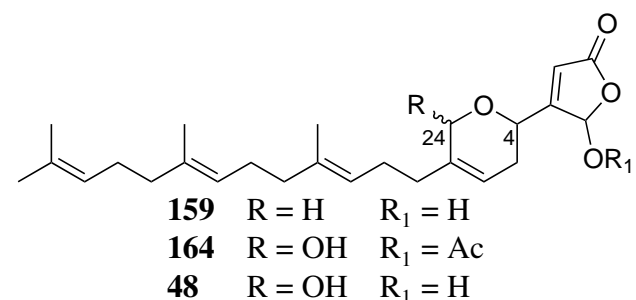
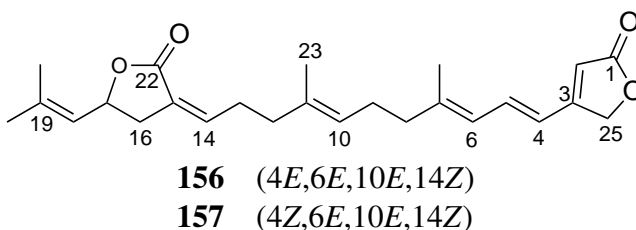
Two isomeric linear sesterterpenes (**152** and **153**) were isolated from the Caribbean sponge *Thorecta horridus*.¹⁵⁵ Compound **152** shown a marked inflammatory activity, inducing the release of histamine and causing oedema in the paw of test animals. Luffarins A-Z have been reported from the Australian marine sponge *Luffariella geometrica* and they are classified into 14 bicyclic sesterterpenes based on their chemical structures;¹¹⁸ luffarins A-N; one bicyclic bisnorsesterterpene, luffarin O; one monocyclic sesterterpene, luffarin P; and six acyclic sesterterpenes, luffarins Q-V (**152–158**), in addition to four diterpenoidal derivatives, luffarin W-Z. Luffarin Q and compound **152**, have similar structures and both compounds were reported to have *E* geometry for the three double bonds. For this reason, it was suggested that **152** and luffarin Q are the same compound. Luffarin T (**156**) is a *dehydro* analogue of luffarin S (**155**) while luffarin V (**158**) is a *dihydro* analogue of both luffarins T and U (**156** and **157**). Cacospongionolide D (**159**) and (6*Z*)-luffarin V (**160**) were isolated from the marine sponge *Fasciospongia cavernosa* from the Bay of Naples.¹⁵⁵ Despite the structural relationship with luffarins, cacospongionolide D (**159**) exhibited significant cytotoxicity.¹⁵⁶ This notion suggested a possible relation between the presence of the α -hydroxybutenolide moiety and the cytotoxicity.

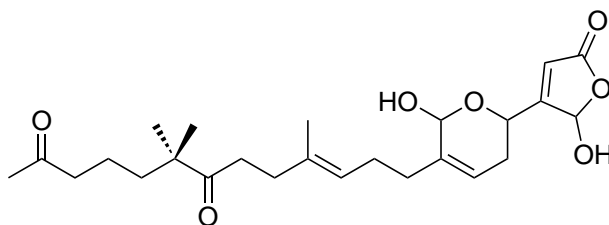
A new sesterterpene (**161**), related to luffarins, has been isolated from the sponge *Fasciospongia cavernosa* from the Adriatic Sea.¹²⁹ The absolute stereochemistry of **161** was determined by application of Mosher's method. Fasciospongides B and C (**162** and

163) were obtained from the New Caledonian sponge *Fasciospongia* sp.¹²⁶ Compounds **162** and **163** possess a new oxidized variant of the cyclohexenyl ring found in manoalide (**109**) and other analogues. Thorectolide monoacetate (**164**) was first obtained from the marine sponge *Thorectandra excavatus*.¹²⁴ The absolute configuration of C-24 and C-4 were assigned following re-isolation of **164** from a New Caledonian marine sponge of the genus *Hyrtios*, together with thorectolide (**48**).¹²⁰ The hydroxyl group at C-24 was established as axial and the absolute configuration of C-4 was assigned as *R* by measuring the Cotton Effect of the diol, obtained by reduction of **164**.

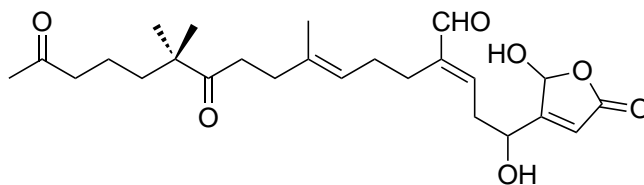


154	(6 <i>E</i> ,10 <i>E</i> ,14 <i>Z</i>)	R = H	R ₁ = OH
155	(6 <i>E</i> ,10 <i>E</i> ,14 <i>Z</i>)	R = H	R ₁ = OAc
158	(6 <i>E</i> ,10 <i>E</i> ,14 <i>E</i>)	R = H	R ₁ = H
160	(6 <i>Z</i> ,10 <i>E</i> ,14 <i>E</i>)	R = H	R ₁ = H
161	(6 <i>Z</i> ,10 <i>E</i> ,14 <i>E</i>)	R = OAc	R ₁ = H





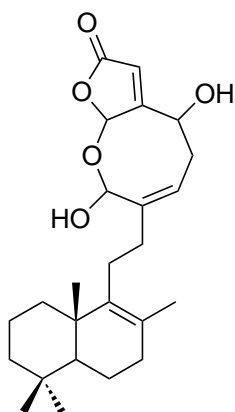
162



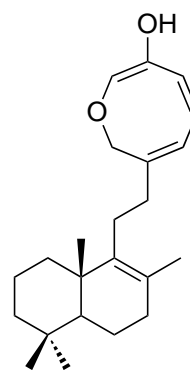
163

6.5.1 Biosynthetic relationship between all *Luffarella* metabolites

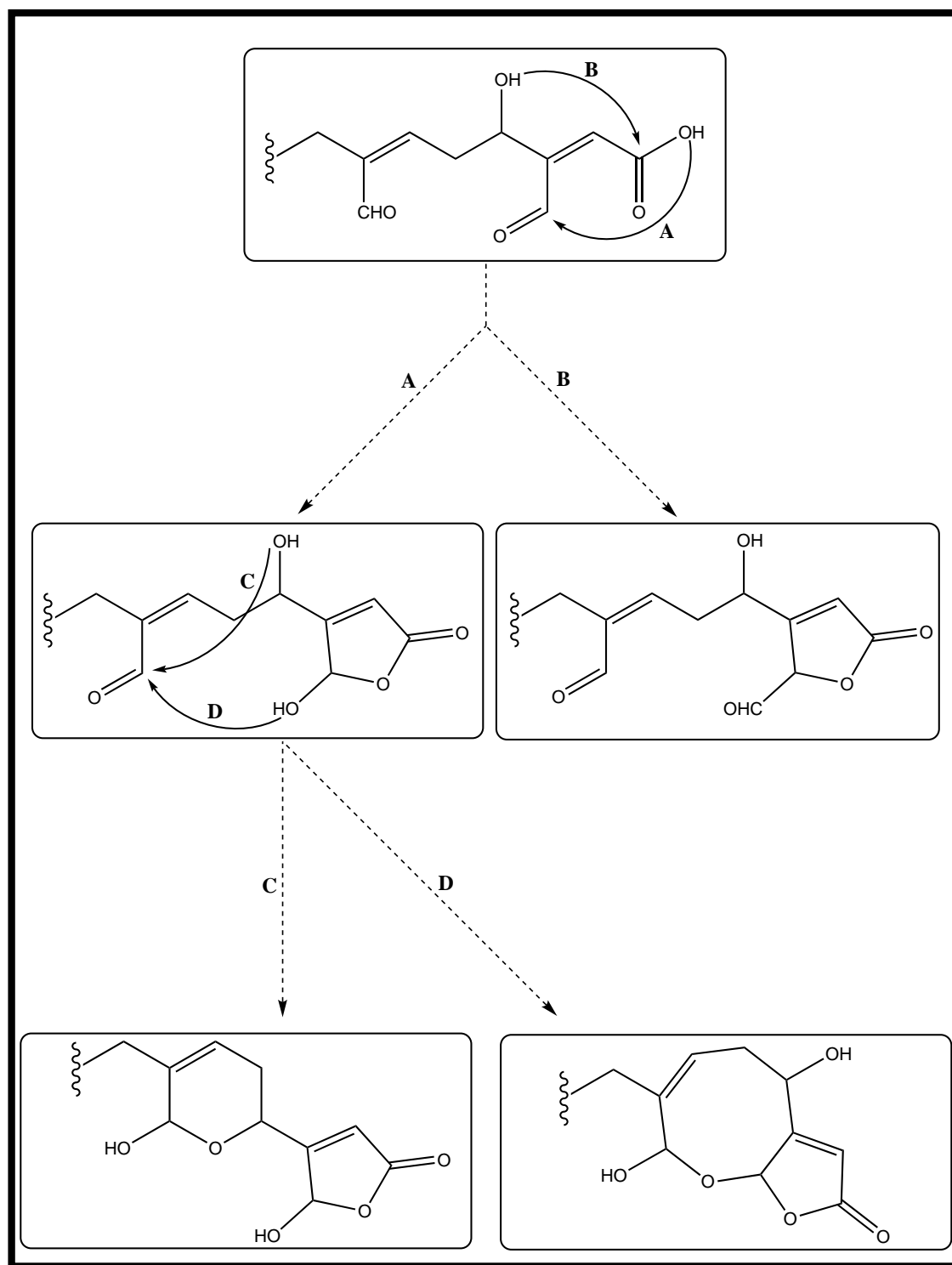
Biosynthetically, a relationship could be recognized between the various luffarins as illustrated in Scheme 6.2. Luffarins appear to belong to the same enantiomeric series as reported for manoalide-type marine natural products. It is also curious to note that none of the acyclic luffarins incorporated the hydroxylated butenolide functionality. Perhaps the most interesting luffarins from a biosynthetic point of view are luffarins B (**165**) and O (**166**), which were the first examples of a hitherto unknown cyclization pattern in compounds of this class.¹¹⁸ The *E*-configuration of the C-6–C-7 in secothorectolide (**49**) prevents ring closure between the C-24 aldehyde and the hydroxyl group at C-4 that lead to the formation of thorectolide (**48**), as illustrated in pathway C (Scheme 6.2).



165



166



Scheme 6.2. Postulated biosynthetic relationship between all known *Luffariella* metabolites.¹¹⁸

Chapter 7

Conclusion

Marine biomedicine is one of the most recent focal points in assessing the role of the oceans in human health. There is simply no question that the vast diversity of plants and animals in the sea will contribute toward the amelioration of human suffering.

Marine sponges do not have physical means of defense and so have developed a rich chemical arsenal that can be exploited in the search for new pharmaceutical leads. Not surprisingly, marine sponges are still the most prolific producers of biologically active marine natural products.

Over the course of this study, various species of Tongan marine sponge were examined using an NMR-based screening method, in order to identify which sponge extracts were worthy of further investigation. The isolation of metabolites from selected sponges was then guided by NMR analysis, which led to isolation of three new chemical structures from two different species, together with 11 known compounds.

The two novel sesterterpenes, isoluffariellolide (**46**) and 1-*O*-methyisoluffariellolide (**47**) share the same backbone pattern as the known luffariellolide (**45**) and 25-*O*-methylluffariellolide (**107**) respectively, and differ only in the substitution on the butenolide ring. In the literature, the majority of the secondary metabolites that have the butenolide ring are β -substituted with only few α -substituted (in the case of **46** and **47**). Isoluffariellolide (**46**) was found to be approximately six times less cytotoxic than 1-*O*-methyisoluffariellolide (**47**). Interestingly, these results suggested that the 1-*O*-methyl group in compound **47** plays an important role in the cytotoxicity of the compound.

Secothorectolide (**49**) is a ring-opened and geometric isomer of the known compound thorectolide (**48**). This ring closure and opening relationship was also observed between manoalide (**109**) and secomanoalide (**110**), as well as luffariellins A (**141**) and B (**142**). Despite the different carbon skeleton, the functional groups in **141** and **142** are similar with those in **109** and **110**, respectively, and not surprisingly the biological properties are

almost identical. The biological activities of compounds **48** and **49** were almost the same, which would give an insight into the structure-activity relationship (SAR) between these types of compounds.

In addition, the structurally related known bromotyrosines (**52–54**) and pyrroloquinoline metabolites (**55–56**) isolated in this research can be tested in screening libraries, that are unbiased by specific biological activity (as in bioassay guided studies), in order to understand their SAR and mode of action.

In New Zealand sponges, primary metabolites dominate the 75% Me₂CO/H₂O fraction (the mass window). Even though most primary metabolites were discarded in both the 30% Me₂CO/H₂O and 100% Me₂CO fractions, the levels of secondary metabolites were very low. The screening technique was adapted to find the approximately one in ten sponges that contained enough secondary metabolites to detect. Using this general methodology on tropical sponges we found that the 75% Me₂CO/H₂O was predominantly secondary metabolites in every sponge examined. The problem was not finding secondary metabolites, but finding novel compounds. While some of the techniques developed in this study have helped find novel compounds, more sophisticated methods will have to be developed to rapidly identify well known secondary metabolites and detect the presence of novel compounds.

Furthermore, sponges that are abundant in Tongan waters have been investigated before by other marine natural groups (collected from Fiji, Vanuatu, Papua New Guinea, Solomon Islands, etc.). Not surprisingly, their chemical content is quite similar to that from Tongan sponges. From our experience from these collecting trips, the less abundant sponges (which might be ignored by other research groups) tend to have higher probability of containing novel secondary metabolites. Therefore, on future collecting trips, these sponges can be targeted, and with the Tongan sponges proved to have higher secondary metabolites content compared to New Zealand sponges, isolation of novel compounds from smaller amount of sponges can be achieved using the VUW screening method.

Chapter 8

Experimental

8.1 General Experimental

NMR spectra were obtained using a Varian Direct Drive spectrometer equipped with a triple resonance HCN cryogenic probe, operating at 600 MHz for the ^1H nucleus, 150 MHz for the ^{13}C nucleus and 60 MHz for ^{15}N nucleus. All HSQC spectra were obtained as coupled HSQC. Chemical shifts δ (ppm) were internally referenced to the residual solvent peak.¹⁵⁷ For acid sensitive compounds, a catalytic amount (1-2 μL) of d_5 -pyridine is added to each NMR sample performed in CDCl_3 to prevent compound degradation due to acidity associated with the solvent. ^1H NMR quantification of samples was performed with an internal CH_3NO_2 standard (100 μL in 5 mL CDCl_3), using the acquisition parameters described by West.⁵² High-resolution mass spectra were obtained using a Micromass Q-TOF Premier mass spectrometer. TLC analyses were performed on Machery-Nagel Alugram SIL G/UV₂₅₄ normal-phase silica plates using a mobile phase of 5% $\text{MeOH}/\text{CH}_2\text{Cl}_2$ unless otherwise stated. The TLC plates were visualised by either (1) fluorescence quenching under UV light ($\lambda = 254$ nm), (2) fluorescence under UV light ($\lambda = 350$ nm), (3) dipping in 5% H_2SO_4 (conc.)/ MeOH solution, followed by dipping in a solution of 0.1% vanillin in EtOH (% wt/vol) then heating, or a combination of the above.

Normal-phase column chromatography was performed using YMC Co. LTD 2,3-dihydropropoxypropyl-derivatised silica (DIOL), or silica (SiO_2). Reversed-phase column chromatography was carried out using Supelco Diaion HP20 or HP20SS poly(styrene divinylbenzene) (PSDVB) resin. All solvents used in bench-top chromatography were glass-distilled. All other reagents were purchased commercially (at least reagent grade) and distilled prior to use when necessary. High-pressure liquid chromatography (HPLC) was performed using a Rainin Dynamax SD-200 solvent delivery module with 25 mL pump heads (analytical scale), or a Varian PrepStar 210 solvent delivery module with 100 mL pump heads (preparative and semi-preparative scale). UV detection for HPLC runs

was obtained with a Varian Prostar 335 photodiode array detector. All organic solvents used were HPLC grade and H₂O was glass-distilled and deionised using a MilliQ system. Solvent mixtures are reported as % vol/vol, unless otherwise stated.

8.2 Investigation of Genus *Fascaplysinopsis*

8.2.1 Initial Fractionation of *Fascaplysinopsis* sp.

The sponge (PTN3_19A and PTN3_22B) was collected by hand using SCUBA from an underwater cave at the southwest of Eua, Tonga in late November 2008. The sample was frozen immediately and kept at -18 °C until extraction. Voucher samples (PTN3_19A and PTN3_22B) have been deposited and stored in 100% EtOH, at the School of Chemical and Physical Sciences, Victoria University of Wellington, New Zealand.

The sponge (200 g frozen weight) was cut into small pieces and extracted with MeOH (2 × 1 L each) for 24 hours. The second then first methanolic extracts were cyclic loaded* onto a glass column packed with HP20 beads (200 mL) pre-equilibrated in MeOH. The combined eluent was then diluted with H₂O (2 L) and passed through the same column. This eluent was further diluted with H₂O (4 L) and passed again through the same column. The loaded column was then washed with 600 mL of H₂O and fractionated with 600 mL of increasing concentrations of Me₂CO in H₂O; (i) 30% (fraction **A**), (ii) 40% (fraction **B**), (iii) 60% (fraction **C**), (iv) 80% (fraction **D**), (v) 100% Me₂CO (fraction **E**). Fractions **A** to **D** were each individually back-loaded onto glass columns packed with HP20 beads (80 mL) pre-equilibrated in MeOH. The columns were then washed with H₂O (240 mL) and eluted with Me₂CO (240 mL). The eluents were then concentrated to dryness to give 149.1 mg of fraction **A**, 92.9 mg of fraction **B**, 379.8 mg of fraction **C** and 648.9 mg of fraction **D**. Fraction **E** was also concentrated to dryness (614.7 mg).

*For a detailed discussion of cyclic loading and back loading, please see Chapter 2, Section 2.1.1.

8.2.2 Isolation of Homofascaplysin A

Fraction **A** (~96.1 mg) was dissolved in 2 mL HPLC grade MeOH. The sample was then injected onto a semi-preparative (250 mm × 10 mm) C18 HPLC column pre-equilibrated with 50% MeCN/0.5M HCOOH_(aq), with a flow rate of 5 mL/min and UV detection set to λ_{245nm} and λ_{280nm} . The column was then eluted with 50% MeOH/0.1M HCOOH_(aq). The fractions eluted between 1.5–2.0 minutes (fraction **F**), 2.2–3.3 minutes (fraction **G**) were collected. Fraction **F** was back-loaded onto a 3 mL HP20SS column. The column was eluted with 15 mL of Me₂CO and then concentrated to dryness. ¹H NMR analysis showed that fraction **F** contained 13.7 mg homofascaplysin A. Fraction **G** was back-loaded onto a 3 mL HP20SS column. The column was eluted with 15 mL of Me₂CO and then concentrated to dryness. ¹H NMR analysis showed that fraction **G** contained 10.8 mg of homofascaplysin A. Fraction **F** and **G** were combined to yield 24.5 mg of homofascaplysin A (**43**).

Homofascaplysin A (**43**)

Amorphous yellow solid; all spectroscopic data as previously published.⁹¹

8.2.3 Isolation of Luffariellolide, Isoluffariellolide, 1-*O*-Methylisoluffariellolide

Fraction **D** (~336 mg) was dissolved in a minimum amount of CH₂Cl₂ and loaded onto a glass column packed with silica gel (60 mL) pre-equilibrated in CH₂Cl₂. The loaded column was then eluted with 100 mL portions of: (i) 100% CH₂Cl₂, (ii) 5% EtOAc/CH₂Cl₂, (iii) 15% EtOAc/CH₂Cl₂, (iv) 30% EtOAc/CH₂Cl₂, (v) 50% EtOAc/CH₂Cl₂, (vi) 100% EtOAc, all fractions were collected across 129 test-tubes and were concentrated to dryness. The fractions were analysed by TLC and fractions 8–16 were combined to give fraction **H** (9 mg) and fractions 37–46 were combined to give fraction **I** (75.7 mg). ¹H NMR analysis showed that fraction **H** contained impure 1-*O*-methylisoluffariellolide, while fraction **I** revealed three structurally related compounds.

Fraction **H** (9 mg) was dissolved in a minimum amount of pet. ether and loaded onto a glass column packed with silica gel (10 mL) pre-equilibrated in pet. ether. The loaded column was then eluted with 30 mL portions of; (i) 100% pet. ether, (ii) 5% CH₂Cl₂/pet. ether, (iii) 10% CH₂Cl₂/pet. ether, (iv) 15% CH₂Cl₂/pet. ether, (v) 20% CH₂Cl₂/pet. ether, (vi) 25% CH₂Cl₂/pet. ether, (vii) 30% CH₂Cl₂/pet. ether, (viii) 50% CH₂Cl₂/pet. ether, (ix) 70% CH₂Cl₂/pet. ether, (x) 100% CH₂Cl₂, all fractions were collected across 48 test-tubes and were concentrated to dryness. The fractions were analysed by TLC and fractions 33–36 (fraction **J**) were combined. ¹H NMR analysis showed that fraction **J** contained 0.2 mg of 1-*O*-methylisoluffariellolide (**47**).

Fraction **I** (~10 mg) was dissolved in 300 μL of HPLC grade MeOH. Fifteen 20 μL samples were then injected onto an analytical (250 mm × 4.6 mm) C18 HPLC column pre-equilibrated with 95% MeCN/H₂O, with a flow rate of 1 mL/min and UV detection set to λ_{245nm} and λ_{280nm}. The eluent between 4.7–5.0 minutes (fraction **K**) was collected and then concentrated to dryness. ¹H NMR analysis showed that fraction **K** contained 1.2 mg of isodehydroluffariellolide (**44**). The eluent between 8.2–8.8 minutes (fraction **L**) was collected and concentrated to dryness. ¹H NMR analysis showed that fraction **L** contained 3.3 mg mixture of isoluffariellolide (**46**) and accompanied by small amount of luffariellolide (**45**).

Isodehydroluffariellolide (44)

Colourless oily residue; all spectroscopic data as previously published.⁹¹

Luffariellolide (45)

Yellowish oily residue; all spectroscopic data as previously published.¹⁰⁸

Isoluffariellolide (46)

Yellowish oily residue; NMR data see Table 5.3; HRESIMS, observed *m/z* 409.3471 [M + Na]⁺, C₂₅H₃₈O₃Na requires 409.2719, Δ 0.0752 ppm.

1-*O*-Methylisoluffariellolide (47)

Yellowish oily residue; NMR data see Table 5.5; HRESIMS, observed m/z 423.2867 $[M + Na]^+$, $C_{26}H_{40}O_3Na$ requires 423.2875, Δ 0.0008 ppm.

8.3 Investigation of Dictyoceratid Sponge

8.3.1 Isolation of Secothorectolide and Thorectolide

The sponge (PTN3_21C) was collected by hand using SCUBA from an underwater cave at the southwest of 'Eua, Tonga in late November 2008. The sample was frozen immediately and kept at -18°C until extraction. Voucher sample (PTN3_21C) has been deposited and stored in 100% EtOH, at the School of Chemical and Physical Sciences, Victoria University of Wellington, New Zealand.

The sponge (26 g frozen weight) was cut into small pieces and extracted with MeOH (2×100 mL each) for 24 hours. The second then first methanolic extracts were cyclic loaded onto a glass column packed with HP20 beads (25 mL) pre-equilibrated in MeOH. The combined eluent was then diluted with H_2O (200 mL) and passed through the same column. This eluent was further diluted with H_2O (400 mL) and passed through the column. The column was then washed with 75 mL of H_2O . The loaded column was eluted with 75 mL of increasing concentrations of Me_2CO in H_2O : (i) 30% (fraction **A**), (ii) 75% (fraction **B**) and (iii) 100% Me_2CO (fraction **C**). Fractions **A** and **B** were each individually back-loaded onto glass columns packed HP20 beads (75 mL) pre-equilibrated in MeOH. The columns were then washed with H_2O (75 mL) and eluted with Me_2CO (75 mL). The eluents were then concentrated to dryness to give 20 mg of fraction **A**, 61.9 mg of fraction **B**. Fraction **C** was also concentrated to dryness (63.7 mg).

The TLC and NMR examination of the resulting fractions showed that the interesting signals were confined to the 75% Me_2CO/H_2O fraction. Fraction **B** (~ 41.9 mg) was dissolved in 1.5 mL of HPLC grade MeOH. Fifteen 100 μL samples were then injected

into a semi-preparative (250 mm × 10 mm) C18 HPLC column pre-equilibrated with 85% MeCN/H₂O, with a flow rate of 4 mL/min and UV detection set to λ_{245nm} and λ_{280nm} . The eluent between 7.6-8.6 minutes (fraction **D**) and 11.3–12.3 minutes (fraction **E**) was collected and then concentrated to dryness. ¹H NMR analysis showed that fraction **D** contained 3.9 mg of secothorectolide and fraction **E** contained 3.7 mg impure thorectolide.

Fraction **D** (3.9 mg) was dissolved in 140 μ L of HPLC grade MeOH. Seven 20 μ L samples were then injected onto an analytical (250 mm × 4.6 mm) C18 HPLC column pre-equilibrated with 85% MeCN/H₂O, with a flow rate of 1 mL/min and UV detection set to λ_{245nm} and λ_{280nm} . The eluent between 6.6-7.6 minutes (fraction **F**) was collected and then concentrated to dryness. ¹H NMR analysis showed that fraction **F** contained 2.7 mg of secothorectolide (**49**).

Fraction **E** (3.7 mg) was dissolved in 140 μ L of HPLC grade MeOH. Seven 20 μ L samples were then injected onto an analytical (250 mm x 4.6 mm) C18 HPLC column pre-equilibrated with 85% MeCN/H₂O, with a flow rate of 1 mL/min and UV detection set to λ_{245nm} and λ_{280nm} . The eluent between 9.3-9.9 minutes (fraction **G**) was collected and then concentrated to dryness. ¹H NMR analysis showed that fraction **G** contained 1.6 mg of thorectolide (**48**).

Thorectolide (48)

Colourless oily residue; all spectroscopic data as previously published.¹²⁰

Secothorectolide (49).

Colourless oily residue; NMR data see Table 6.2; HRESIMS, observed m/z 439.2460 [M + Na]⁺, C₂₅H₃₆O₅Na requires 439.2460, Δ 0.0 ppm.

8.4 Investigation of a Verongiid Sponge

8.4.1 Isolation of Aplysamine-2 and Aerophobin-1

The sponge (PTN3_33F) was collected by snorkel from Ano Beach, Vava'u, Tonga in late November 2009. The sample was frozen immediately and kept at -18°C until extraction. A voucher sample (PTN3_33F) has been deposited and stored in 100% EtOH, at the School of Chemical and Physical Sciences, Victoria University of Wellington, New Zealand.

The sponge (27 g wet weight) was cut into small pieces and extracted with MeOH (2 x 100 mL each) for 24 hours. The second then first methanolic extracts were loaded onto a glass column packed with HP20 beads (30 mL) pre-equilibrated in MeOH. The combined eluent was then diluted with H_2O (200 mL) and passed through the same column. This eluent was further diluted with H_2O (400 mL) and passed again through the same column. The loaded column was then washed with 120 mL of H_2O and fractionated with 120 mL of increasing concentrations of Me_2CO in H_2O : (i) 30% (fraction **A**), (ii) 75% (fraction **B**) and (iii) 100% (fraction **C**). Fractions **A** and **B** were each individually back loaded onto glass columns packed with HP20 beads (30 mL) pre-equilibrated in MeOH. The columns were then washed with H_2O (120 mL) and eluted with Me_2CO (120 mL). The eluents were then concentrated to dryness to give 80.6 mg of fraction **A**, 86.7 mg of fraction **B**. Fraction **C** was also concentrated to dryness (75.8 mg).

Fraction **B** (~34.4 mg) dissolved in 10 mL of MeOH and cyclic loaded onto a glass analytical column packed with 5 mL HP20SS pre-equilibrated in MeOH. The loaded column was eluted with 30 mL of increasing concentrations of Me_2CO in H_2O : (i) 30%, (ii) 40%, (iii) 50%, (iv) 60%, (v) 80% (fraction **D**) and (vi) 100%. NMR examination of the eluted fractions showed that fraction **D** contained impure aplysamine-2 (9.7 mg). Fraction **D** was dissolved in a minimum amount of pet. ether and loaded onto a glass column packed with DIOL (10 mL) pre-equilibrated in pet. ether. The loaded column was then eluted with 30 mL portions of; (i) 100% pet. ether (ii) 50% CH_2Cl_2 /pet. ether, (iii) 75% CH_2Cl_2 /pet. ether, (iv) 100% CH_2Cl_2 , (v) 5% EtOAc/ CH_2Cl_2 , (vi) 15%

EtOAc/CH₂Cl₂, (vii) 30% EtOAc/CH₂Cl₂, (viii) 50% EtOAc/CH₂Cl₂, (ix) 100% EtOAc, (x) 100% MeOH. All fractions were collected across 41 test-tubes, and based on TLC examination, test-tubes 39–41 were combined to give 5.1 mg of impure aplysamine-2 (fraction **E**). Fraction **E** (5.1 mg) was dissolved in 300 μ L of HPLC grade MeOH. Ten 30 μ L samples were then injected onto an analytical (250 mm \times 4.6 mm) C18 HPLC column pre-equilibrated with 85% MeCN/H₂O, with a flow rate of 1 mL/min and UV detection set to λ_{245nm} and λ_{280nm} . The eluent between 2.5-2.6 minutes (fraction **F**) was collected and then concentrated to dryness. ¹H NMR analysis showed that fraction **F** contained 0.6 mg of aplysamine-2 (**50**).

Fraction **B** (~52.3 mg) was dissolved in a minimum amount of pet. ether and loaded onto a glass column packed with DIOL (30 mL) pre-equilibrated in pet. ether. The loaded column was then eluted with 50 mL portions of; (i) 100% pet. ether (ii) 100% CH₂Cl₂, (iii) 50% EtOAc/CH₂Cl₂, (iv) 100% EtOAc, (v) 10% EtOAc/MeOH, (vi) 30% EtOAc/MeOH, (vii) 50% EtOAc/MeOH, (viii) 100% MeOH. All fractions were collected across 60 test-tubes. Based on NMR and TLC examination, test-tubes 46–52 were combined to give 7.1 mg of impure aerophobin-1 (fraction **G**). Fraction **G** (7.1 mg) was dissolved in 300 μ L of HPLC grade MeOH. Ten 30 μ L samples were then injected onto an analytical (250 mm \times 4.6 mm) C18 HPLC column pre-equilibrated with 85% MeCN/H₂O, with a flow rate of 1 mL/min and UV detection set to λ_{245nm} and λ_{280nm} . The eluent between 2.0-2.7 minutes (fraction **H**) was collected and then concentrated to dryness. ¹H NMR analysis showed that fraction **G** contained 1.2 mg of aerophobin-1 (**51**).

Aplysamine-2 (50)

A pale tan semicrystalline solid; all spectroscopic data as previously published.⁷²

Aerophobin-1 (51)

A pale white semicrystalline solid; all spectroscopic data as previously published.⁷³

8.5 Investigation of Verongiid Sponge

8.5.1 Isolation of Fistularin-3, Aeroplysinin-1 and LL-PAA216

The sponge (PTN3_46E) was collected by hand using SCUBA from Tu‘ungasika Island, Vava‘u, Tonga in late November 2009. The sample was frozen immediately and kept at -18°C until extraction. A voucher sample (PTN3_46E) has been deposited and stored in 100% EtOH, at the School of Chemical and Physical Sciences, Victoria University of Wellington, New Zealand.

The sponge (27 g wet weight) was cut into small pieces and extracted with MeOH (2 x 100 mL each) for 24 hours. The second then first methanolic extracts were loaded onto a glass column packed with HP20 beads (30 mL) pre-equilibrated in MeOH. The combined eluent was then diluted with H_2O (100 mL) and passed through the same column. This eluent was further diluted with H_2O (200 mL) and passed through the column. The column was then washed with 75 mL of H_2O . The loaded column was eluted with 120 mL of increasing concentrations of Me_2CO in H_2O : (i) 30% (fraction **A**), (ii) 75% (fraction **B**) and 100% (fraction **C**). Fractions **A** and **B** were each individually back loaded onto glass columns packed with HP20 beads (30 mL) pre-equilibrated in MeOH. The columns were then washed with H_2O (120 mL) and eluted with Me_2CO (120 mL). The eluents were then concentrated to dryness to give 136 mg of fraction **A**, 726.5 mg of fraction **B**. Fraction **C** was also concentrated to dryness (105.5 mg). TLC and NMR examination of the resulting fractions showed that the interesting signals were confined to the 30% and 75% $\text{Me}_2\text{CO}/\text{H}_2\text{O}$ fractions.

Fraction **A** (~32.8 mg) was dissolved in a minimum amount of CH_2Cl_2 and loaded onto a glass column packed with silica gel (10 mL) pre-equilibrated in CH_2Cl_2 . The loaded column was then eluted with 30 mL portions of; (i) 100% CH_2Cl_2 , (ii) 5% EtOAc/ CH_2Cl_2 , (iii) 15% EtOAc/ CH_2Cl_2 , (iv) 30% EtOAc/ CH_2Cl_2 , (v) 50% EtOAc/ CH_2Cl_2 , (vi) 100% EtOAc, (vii) 5% MeOH/EtOAc, (viii) 15% MeOH/EtOAc, (ix) 30% MeOH/EtOAc, (x) 100% MeOH, all fractions were collected in 48 test-tubes and were concentrated to dryness. The fractions were analysed by TLC and fractions 12–17 (fraction **D**) and

fractions 28–33 (fraction **E**) were combined. ^1H NMR analysis showed that fraction **D** contained 8.6 mg of aeroplysinin-1 (**53**) and fraction **E** contained 6.2 mg LL-PAA216 (**54**).

Fraction **B** (~57.9 mg) dissolved in 10 mL of MeOH and cyclic loaded onto a glass analytical column packed with 5 ml HP20SS pre-equilibrated in MeOH. The loaded column was eluted with 25 mL of increasing concentrations of Me_2CO in H_2O : (i) 30% (fraction **F**), (ii) 40% (fraction **G**), (iii) 50%, (iv) 60% (fraction **H**), (v) 80%, and (vi) 100%. All fractions were collected in test-tubes and were concentrated to dryness to give 5.3 mg of fraction **F**, 7.4 mg of fraction **G**, 3.3 mg (50% $\text{Me}_2\text{CO}/\text{H}_2\text{O}$ fraction), 24.3 mg of fraction **H**, 11.1 mg (80% $\text{Me}_2\text{CO}/\text{H}_2\text{O}$ fraction) and 0.8 mg (fraction 100% Me_2CO).

Fraction **F** (5.3 mg) was dissolved in a minimum amount of CH_2Cl_2 and loaded onto a glass column packed with silica gel (10 mL) pre-equilibrated in CH_2Cl_2 . The loaded column was then eluted with 30 mL portions of; (i) 100% CH_2Cl_2 , (ii) 5% EtOAc/ CH_2Cl_2 , (iii) 15% EtOAc/ CH_2Cl_2 , (iv) 30% EtOAc/ CH_2Cl_2 , (v) 50% EtOAc/ CH_2Cl_2 , (vi) 75% EtOAc/ CH_2Cl_2 , (vii) 100% EtOAc, (viii) 10% MeOH/EtOAc, (ix) 100% MeOH, all fractions were collected across 42 test-tubes and were concentrated to dryness. The fractions were analysed by TLC and fractions 13–17 (fraction **I**) and fractions 31–37 (fraction **J**) were combined. ^1H NMR analysis showed that fraction **I** contained 2.2 mg of aeroplysinin-1 and fraction **J** contained 1.8 mg of LL-PAA216 (**54**).

Fraction **G** (7.4 mg) was dissolved in a minimum amount of CH_2Cl_2 and loaded onto a glass column packed with silica gel (10 mL) pre-equilibrated in CH_2Cl_2 . The loaded column was then eluted with 30 mL portions of; (i) 100% CH_2Cl_2 , (ii) 5% EtOAc/ CH_2Cl_2 , (iii) 15% EtOAc/ CH_2Cl_2 , (iv) 30% EtOAc/ CH_2Cl_2 , (v) 50% EtOAc/ CH_2Cl_2 , (vi) 100% EtOAc, (vii) 5% MeOH/EtOAc, (viii) 10% MeOH/EtOAc, (ix) 100% MeOH, all fractions were collected in 42 test-tubes and were concentrated to dryness. The fractions were analysed by TLC and fractions 7–17 (fraction **K**) and 25–32 (fraction **L**) were combined. ^1H NMR analysis showed that fraction **K** contained 0.7 mg of aeroplysinin-1 and fraction **L** contained 0.8 mg of LL-PAA216.

Fraction **H** (24.3 mg) was dissolved in a minimum amount of CH_2Cl_2 and loaded onto

a glass column packed with silica gel (10 mL) pre-equilibrated in CH₂Cl₂. The loaded column was then eluted with 30 mL portions of; (i) 100% CH₂Cl₂, (ii) 5% EtOAc/CH₂Cl₂, (iii) 10% EtOAc/CH₂Cl₂, (iv) 15% EtOAc/CH₂Cl₂, (v) 30% EtOAc/CH₂Cl₂, (vi) 50% EtOAc/CH₂Cl₂, (vii) 100% EtOAc, (viii) 5% MeOH/EtOAc, (ix) 100% MeOH, all fractions were collected across 43 test-tubes and were concentrated to dryness. The fractions were analysed by TLC and fractions 26–31 (fraction **M**) were combined. ¹H NMR analysis showed that fraction **M** contained 18 mg of fistularin-3 (**52**). Fractions **D**, **I**, and **K** were combined to yield 11.5 mg of aeroplysinin-1 (**53**) and fractions **E**, **J**, and **L** were combined to give 8.8 mg of LL-PAA216 (**54**).

Fistularin-3 (52**)**

Colourless solid; all spectroscopic data as previously published.⁶⁴

Aeroplysinin-1 (53**)**

Colourless solid; all spectroscopic data as previously published.⁷⁴

LL-PAA216 (54**)**

Colourless solid; all spectroscopic data as previously published.⁷⁵

8.6 Investigation of a Poecilosclerid Sponge

8.6.1 Isolation of of Makaluvamine G and Prianosin B

Unidentified black sponge (PTN4_10A), was collected by hand using SCUBA from Fakafotulā, Vava'u, Tonga in late November 2009. The sample was frozen immediately and kept at -18 °C until extraction. A voucher sample (PTN4_10A) has been deposited and stored in 100% EtOH, at the School of Chemical and Physical Sciences, Victoria University of Wellington, New Zealand.

The sponge (21 g wet weight) was cut into small pieces and extracted with MeOH (2 ×

100 mL each) for 24 hours. The second then first methanolic extracts were loaded onto a glass column packed with HP20 beads (30 mL) pre-equilibrated in MeOH. The combined eluent was then diluted with H₂O (200 mL) and passed through the same column. This eluent was further diluted with H₂O (400 mL) and passed through the column. The column was then washed with 100 mL of H₂O. The loaded column was eluted with 100 mL of increasing concentrations of Me₂CO in H₂O: (i) 30% (fraction **A**), (ii) 75% (fraction **B**) and (iii) 100% (fraction **C**). Fraction **A** and **B** were each individually back-loaded onto glass columns packed HP20 beads (30 mL) pre-equilibrated in MeOH. The columns were then washed with H₂O (100 mL) and eluted with Me₂CO (100 mL). The eluents were then concentrated to dryness to give 90.6 mg of fraction **A**, 68 mg of fraction **B**. Fraction **C** was also concentrated to dryness (60.8 mg). TLC and NMR examination of the resulting fractions showed that the interesting signals were confined to the 75% Me₂CO in H₂O fraction.

Fraction **B** (~17.9 mg) was dissolved in 10 mL of MeOH and cyclic loaded onto a glass analytical column packed with 5 mL HP20SS pre-equilibrated in MeOH. The loaded column was eluted with 30 mL of increasing concentrations of MeOH in H₂O: (i) 30%, (ii) 40%, (iii) 50% , (iv) 60%, (v) 80% and (vi) 100%. All fractions were concentrated to dryness and based on TLC, the 80% MeOH/H₂O and 100% MeOH fractions were combined to give 9.2 mg (fraction **D**). Fraction **D** was dissolved in a minimum amount of CH₂Cl₂ and loaded onto a glass column packed with DIOL (10 mL) pre-equilibrated in CH₂Cl₂. The loaded column was then eluted with 30 mL portions of; (i) 100% CH₂Cl₂, (ii) 5% EtOAc/CH₂Cl₂, (iii) 10% EtOAc/CH₂Cl₂, (iv) 15% EtOAc/CH₂Cl₂, (v) 30% EtOAc/CH₂Cl₂, (vi) 50% EtOAc/CH₂Cl₂, (vii) 100% EtOAc, (viii) 5% EtOAc/MeOH, (ix) 30% EtOAc/MeOH, (x) 50% EtOAc/MeOH, (xi) 100% MeOH. All fractions were collected across 60 test-tubes. The fractions were analysed by TLC and fractions 45–56 (fraction **E**) were combined. NMR analysis showed that fraction **D** contained impure 3.8 mg of makaluvamine G. Fraction **E** (3.8 mg) was dissolved in 300 μ L of HPLC grade MeOH. Ten 30 μ L samples were then injected onto a analytical (250 mm \times 4.6 mm) C18 HPLC column pre-equilibrated with 85% MeCN/H₂O, with a flow rate of 1 mL/min and UV detection set to λ_{245nm} and λ_{280nm} . The eluent between 4.3-4.7 minutes (fraction **F**) was collected and then concentrated to dryness. ¹H NMR analysis showed that fraction **F**

contained 0.8 mg of makaluvamine G (**55**).

Fraction **B** (~50 mg) was dissolved in a minimum amount of CH₂Cl₂ and loaded onto a glass column packed with DIOL (30 mL) pre-equilibrated in CH₂Cl₂. The loaded column was then eluted with 50 mL portions of; (i) 100% CH₂Cl₂, (ii) 50% EtOAc/CH₂Cl₂, (iii) 75% EtOAc/CH₂Cl₂, (iv) 100% EtOAc, (v) 10% MeOH/EtOAc, (vi) 20% MeOH/EtOAc, (vii) 40% MeOH/EtOAc, (viii) 60% MeOH/EtOAc, (ix) 80% MeOH/EtOAc, (x) 100% MeOH, all fractions were collected across 78 test-tubes and were concentrated to dryness. The fractions were analysed by TLC and fractions 21–22 (fraction **G**) were combined. NMR analysis showed that fraction **G** contained 0.6 mg of prianosin B (**56**).

Makaluvamine G (55)

Greenish-black solid; all spectroscopic data as previously published.⁷⁹

Prianosin B (56)

Red crystalline solid; all spectroscopic data as previously published.⁸²

Appendix A

Existing Marine Chemistry Sponge Screening Protocol

Preparation

Equipment Needed (per Screen)

- 1 x Screen column loaded with 80 mL of HP20 equilibrated in distilled MeOH
- 1 x Backloading column loaded with 40 mL of HP20 equilibrated in distilled MeOH

NMR Standard Preparation

Prepare a standard of 1,3,5-tribromobenzene in CDCl_3 by dissolving 78.9 mg of 1,3,5-tribromobenzene in 5 mL of CDCl_3 .

Procedure

1. Voucher Sample Preparation

- Take a voucher specimen of ca. 10 g of sponge material ensuring that both the ectoderm and the endoderm are represented.
- Label and store the voucher sample in 75% IPA in H_2O .

2. Extraction

- Extract ca. 100 g of sponge material in 400 mL of distilled MeOH overnight.

- Filter the first extract and set aside. Re-extract the sponge material (and any filter paper/celite as necessary) in 400 mL of distilled MeOH overnight.
- Filter the second extract.
- Keep all sponge material (and any filter paper/celite as necessary) until the screen is complete at which time it may be discarded.

3. Cyclic Loading

- Pass the second extract through the screen column with a flow rate of ca. 10 mL/min.
- Pass the first extract through the screen column with a flow rate of ca. 10 mL/min. Combine the eluent with that of the second extract.
- Dilute the combined eluents with 800 mL of distilled H₂O. Pass the diluted eluents back through the screen column at a flow rate of ca. 10 mL/min.
- Dilute the eluent with 1.6 L of distilled H₂O. Pass the diluted eluent back through the screen column at a flow rate of ca. 10 mL/min.
- The eluent should be kept until the screen is complete at which time it may be discarded.

4. Elution

- Elute the screen column with 250 mL of distilled H₂O at a flow rate of ca. 10 mL/min. The H₂O eluent can be discarded immediately.
- Elute the screen column with 250 mL of 30% distilled Me₂CO in distilled H₂O (75 mL Me₂CO to 175 mL H₂O) at a flow rate of ca. 10 mL/min.
- Elute the screen column with 250 mL of 75% distilled Me₂CO in distilled H₂O (187.5 mL Me₂CO to 62.5 mL H₂O) at a flow rate of ca. 10 mL/min.

- Elute the screen column with 250 mL of distilled Me₂CO at a flow rate of ca. 10 mL/min.

5. Backloading the 75% Acetone Fraction

- Dilute the 75% Me₂CO fraction with 250 mL of distilled H₂O. Pass the diluted eluent through the backloading column at a flow rate of ca. 8 mL/min.
- Dilute the eluent with 500 mL of distilled H₂O. Pass the diluted eluent back through the backloading column at a flow rate of ca. 8 mL/min.
- The eluent should be kept until the screen is complete at which time it may be discarded.
- Elute the backloading column with 150 mL of distilled Me₂CO.

6. Processing the 75% Acetone Fraction

- Evaporate the Me₂CO eluent of the backloading column to dryness and transfer to a pre-weighed sample vial. Evaporate to dryness and record the mass.
- Sub-sample approximately 30 mg of material for NMR analysis if necessary.
- Prepare an NMR sample in ca. 700 μL of CD₃OD in a 5 mm NMR tube.
- Add 10 μL of the 1,3,5-tribromobenzene standard (representing 507 nmol of 1,3,5-tribromobenzene) to the NMR tube.

7. NMR Analysis of the 75% Acetone Fraction

- Run a ¹H spectrum of the sample on the 600 MHz instrument using the standard Screen1H parameter set. (Experiment time: ca. 4 min)
- Make a note Standard Added in the sample text.

- Run a COSY spectrum of the sample using the standard ScreenCOSY parameter set. (Experiment time: ca. 20 min)
- Run an HSQC spectrum of the sample using the standard ScreenHSQC parameter set. (Experiment time: ca. 4 h)
- Process appropriately and export HSQC phasefile.
- Add HSQC phasefile to HSQC mask.
- Apply HSQC mask to HSQC phasefile.

8. Assigning Hit Values to the Screen

- Threshold set at 3%.
- Signal strength
 - An arbitrary value indicating how the strength of the interesting peaks.
 - Weak – 1. Medium – 2. Strong – 3 (remember to consider the subsampling factor if necessary).
- Number of interesting peaks
 - Indicates how many red peaks in the HSQC. Something exhibiting more than 20 non-masked peaks will score a 10.
- Uniqueness of interesting peaks
 - An arbitrary value indicating whether non-masked peaks represent something interesting (1–10).
- Available mass

– The total mass of the available sponge material (including that used for the screen) in kg is multiplied by 10 and rounded to the nearest integer. If more than 1 kg of sponge material is available the score is 10.

- Recollectability

– Collected locally – 3. Collected from Northland – 2. Other – 1.

- Sum all 5 hit values. A score of 20 would be considered average.

9. Backloading the 30% Acetone Fraction

- Dilute the 30% Me₂CO fraction with 250 mL of distilled H₂O. Pass the diluted eluent through the backloading column at a flow rate of ca. 8 mL/min.
- Dilute the eluent with 500 mL of distilled H₂O. Pass the diluted eluent back through the backloading column at a flow rate of ca. 8 mL/min.
- The eluent should be kept until the screen is complete at which time it may be discarded.
- Elute the backloading column with 150 mL of distilled MeOH.

10. Processing the 30% Acetone Fraction

- Evaporate the MeOH eluent of the backloading column to dryness and transfer to a pre-weighed sample vial. Evaporate to dryness and record the mass.
- Sub-sample approximately 30 mg of material for NMR analysis if necessary.
- Prepare an NMR sample in ca. μ 700 L of CD₃OD in a 5 mm NMR tube.

11. NMR Analysis of the 30% Acetone Fraction

- Run a ^1H spectrum of the sample on the 600 MHz instrument using the standard Screen ^1H parameter set. (Experiment time: ca. 4 min)

12. Processing the 100% Acetone Fraction

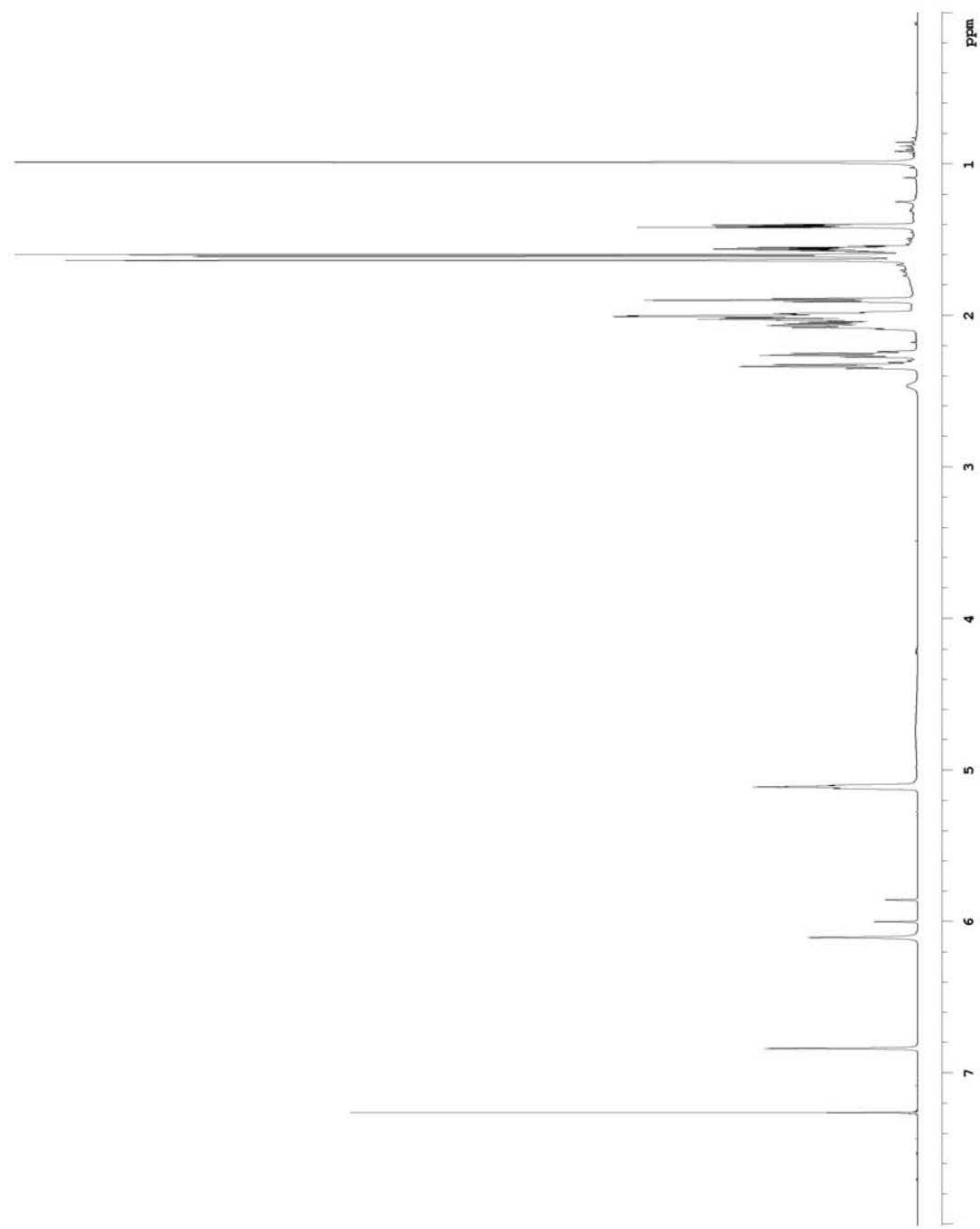
- Evaporate the Me_2CO eluent of the screen column to dryness and transfer to a pre-weighed sample vial. Evaporate to dryness and the record mass.
- Sub-sample approximately 30 mg of material for NMR analysis if necessary.
- Prepare an NMR sample in ca. 700 μL of CDCl_3 in a 5 mm NMR tube.

13. NMR Analysis of the 100% Acetone Fraction

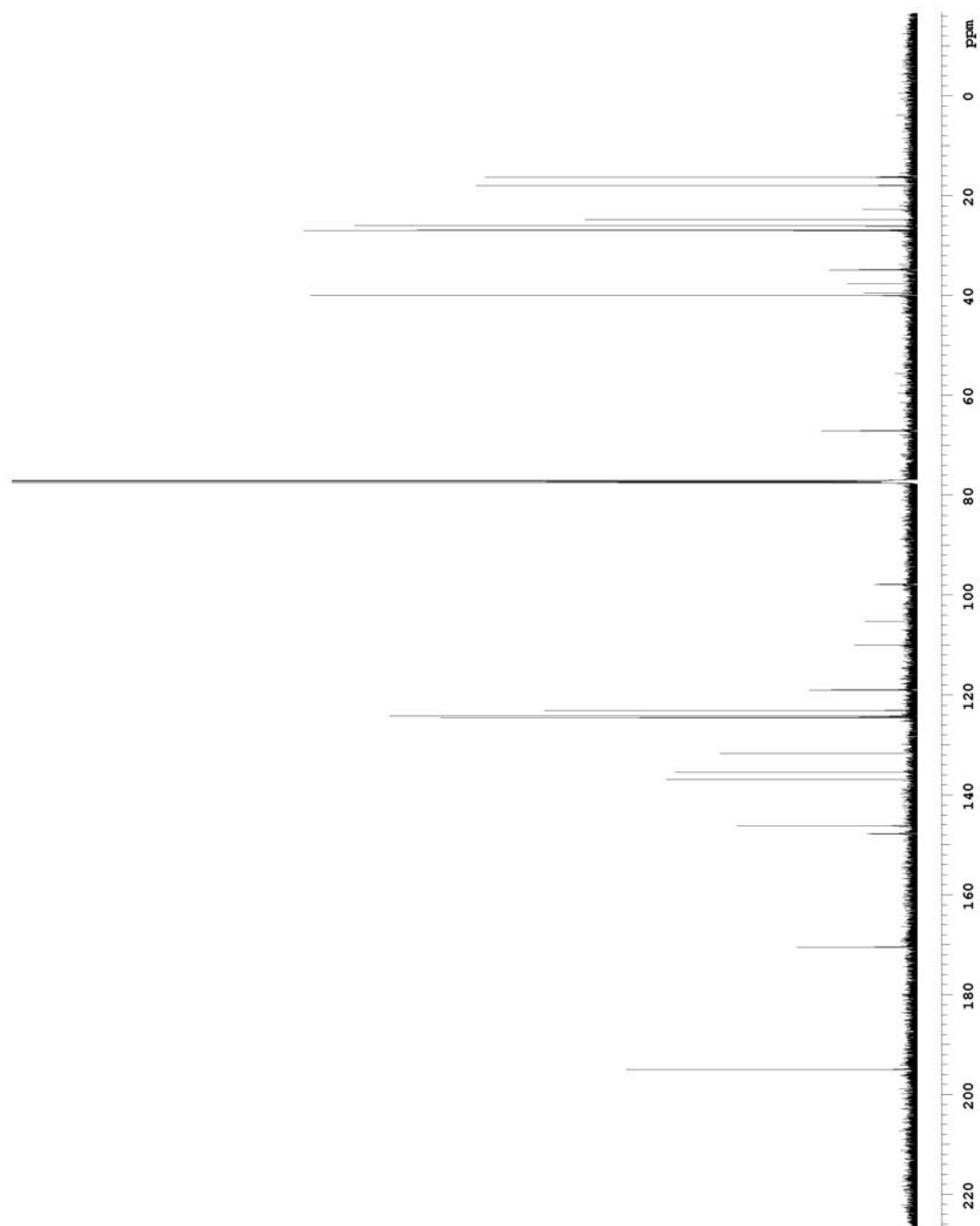
- Run a ^1H spectrum of the sample on the 600 MHz instrument using the standard Screen ^1H parameter set. (Experiment time: ca. 4 min)

Appendix B

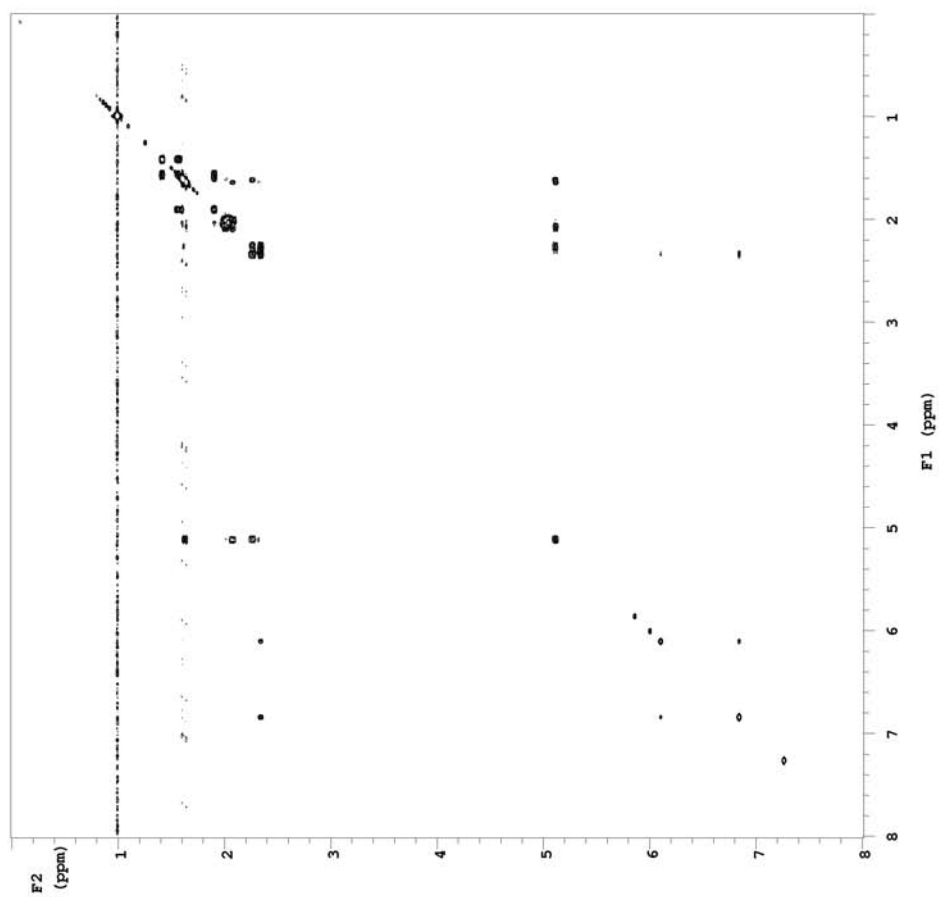
Isoluffariellolide Spectra



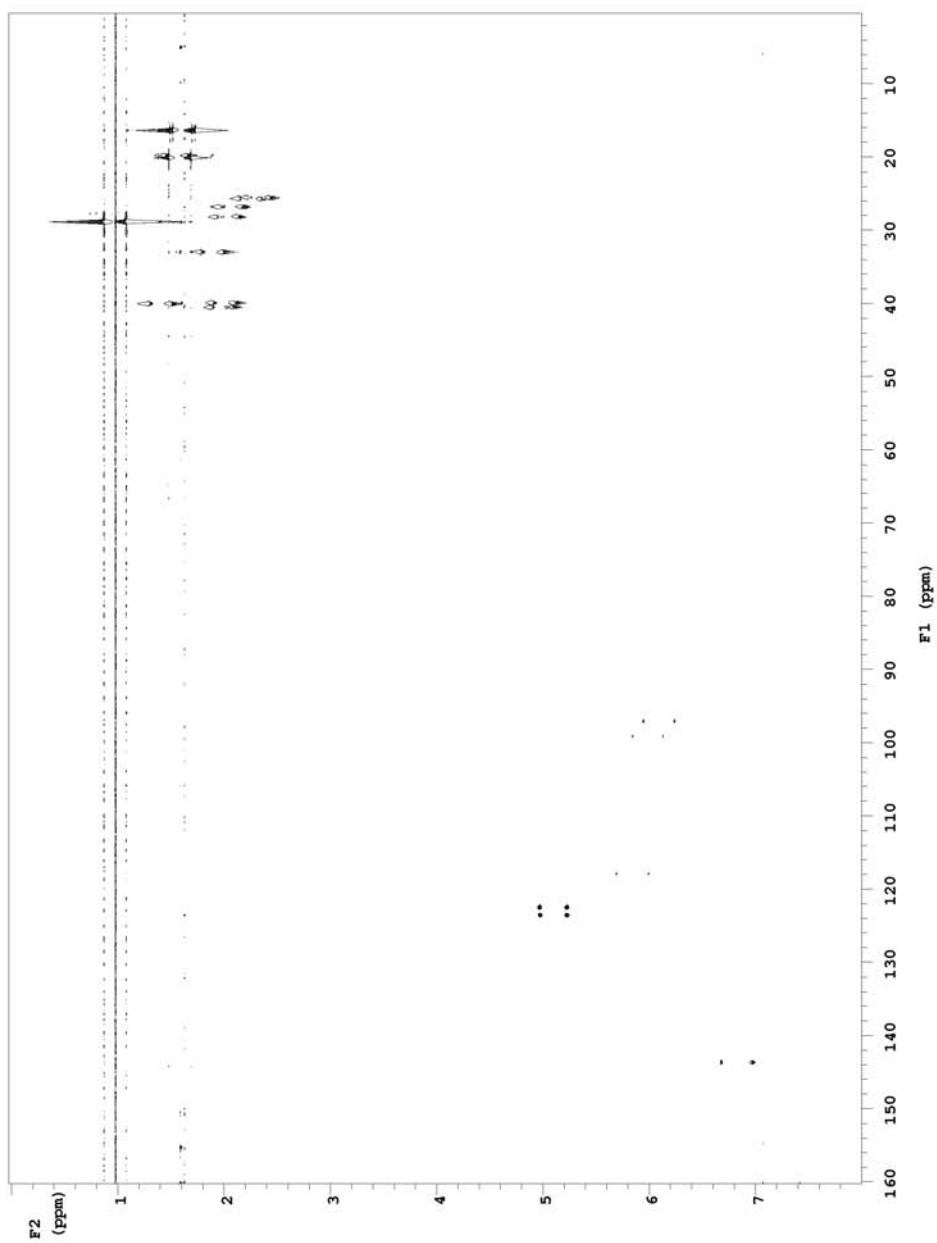
^1H NMR spectrum of isoluffariellolide (**46**) (600 MHz, CDCl_3)



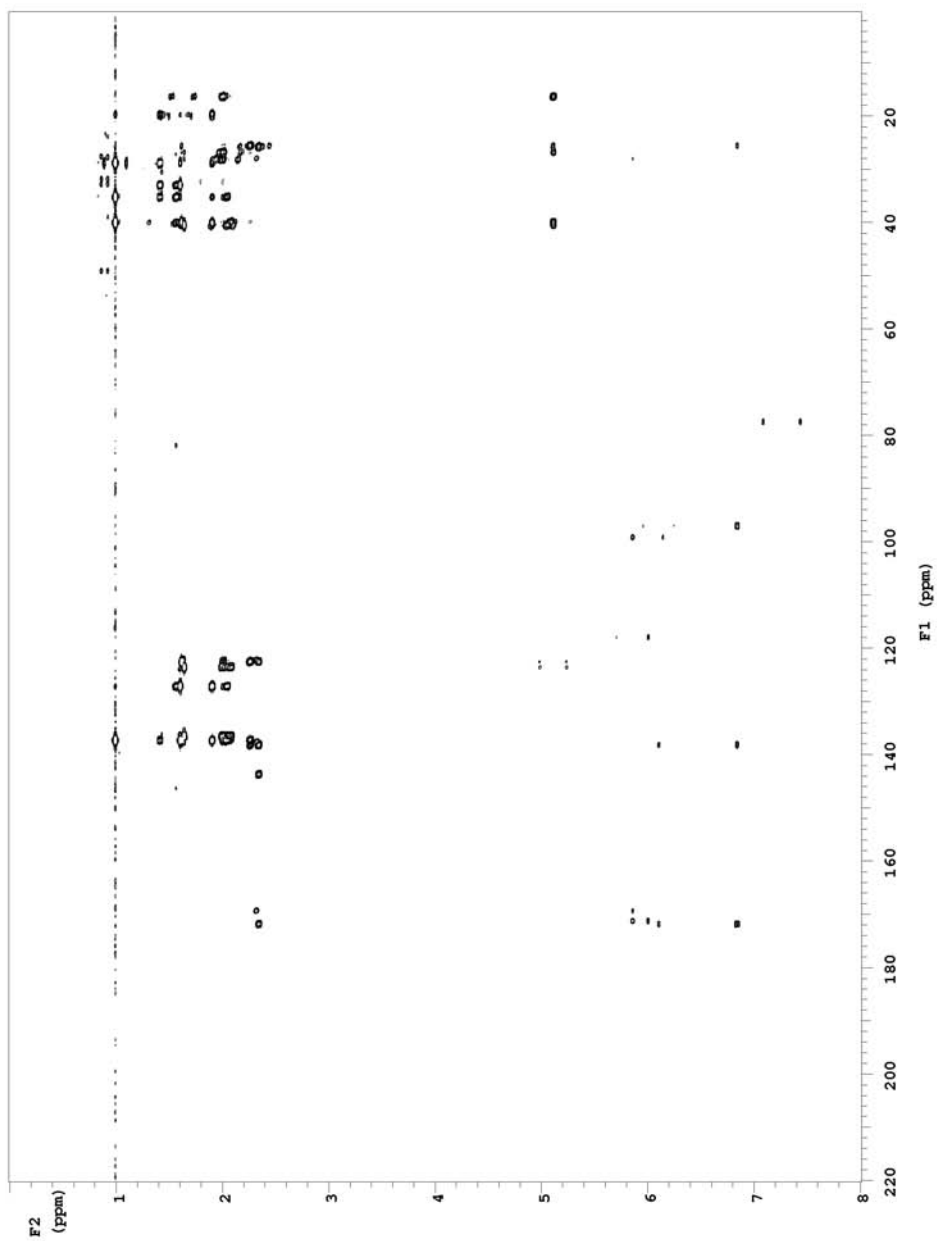
^{13}C spectrum of isoluffariellolide (**46**) (150 MHz, CDCl_3)



COSY spectrum of isoluffariellolide (**46**) (600 MHz, CDCl₃)



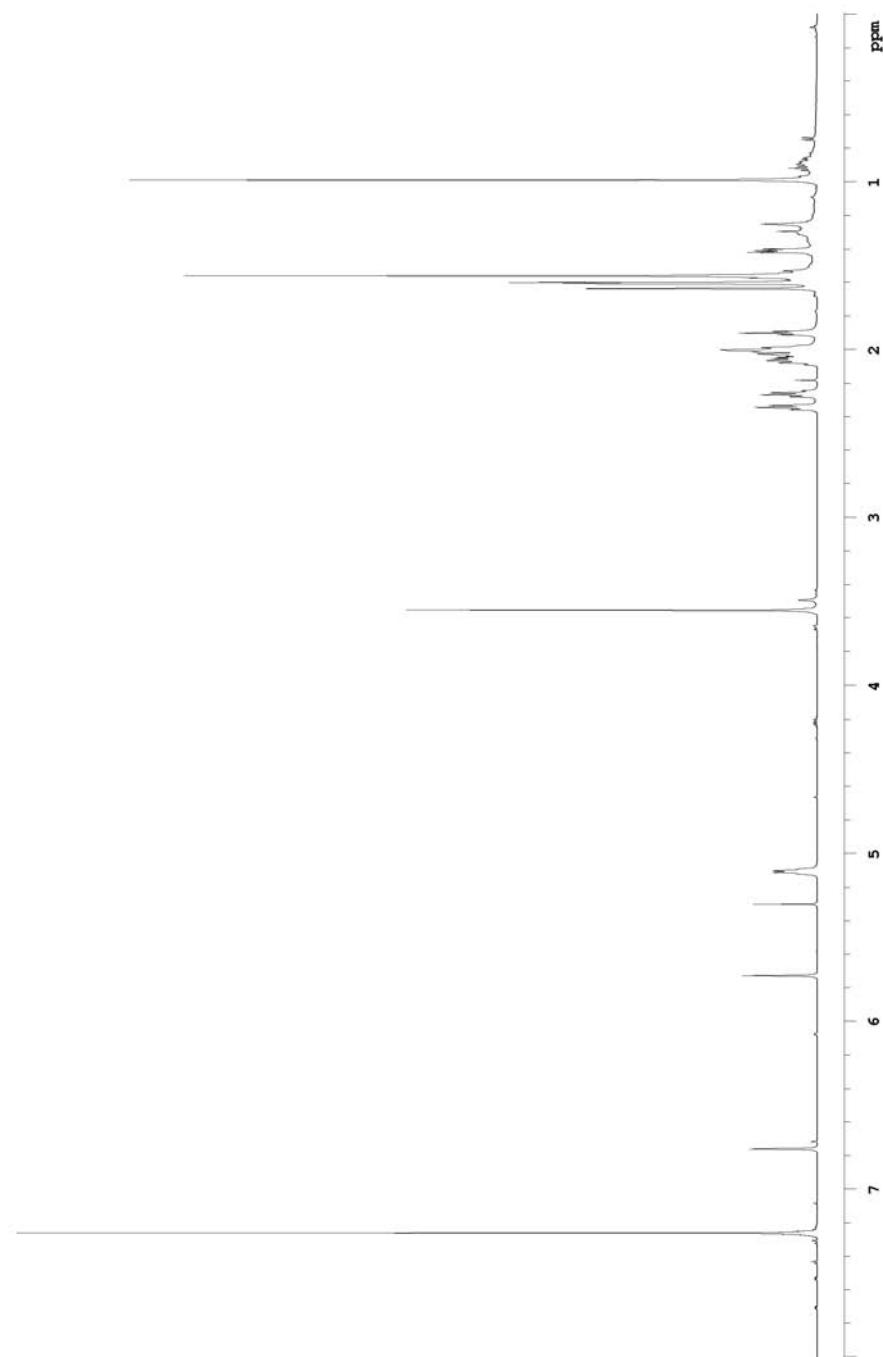
Coupled HSQC spectrum of isoluffariellolide (**46**) (600 MHz, CDCl_3)



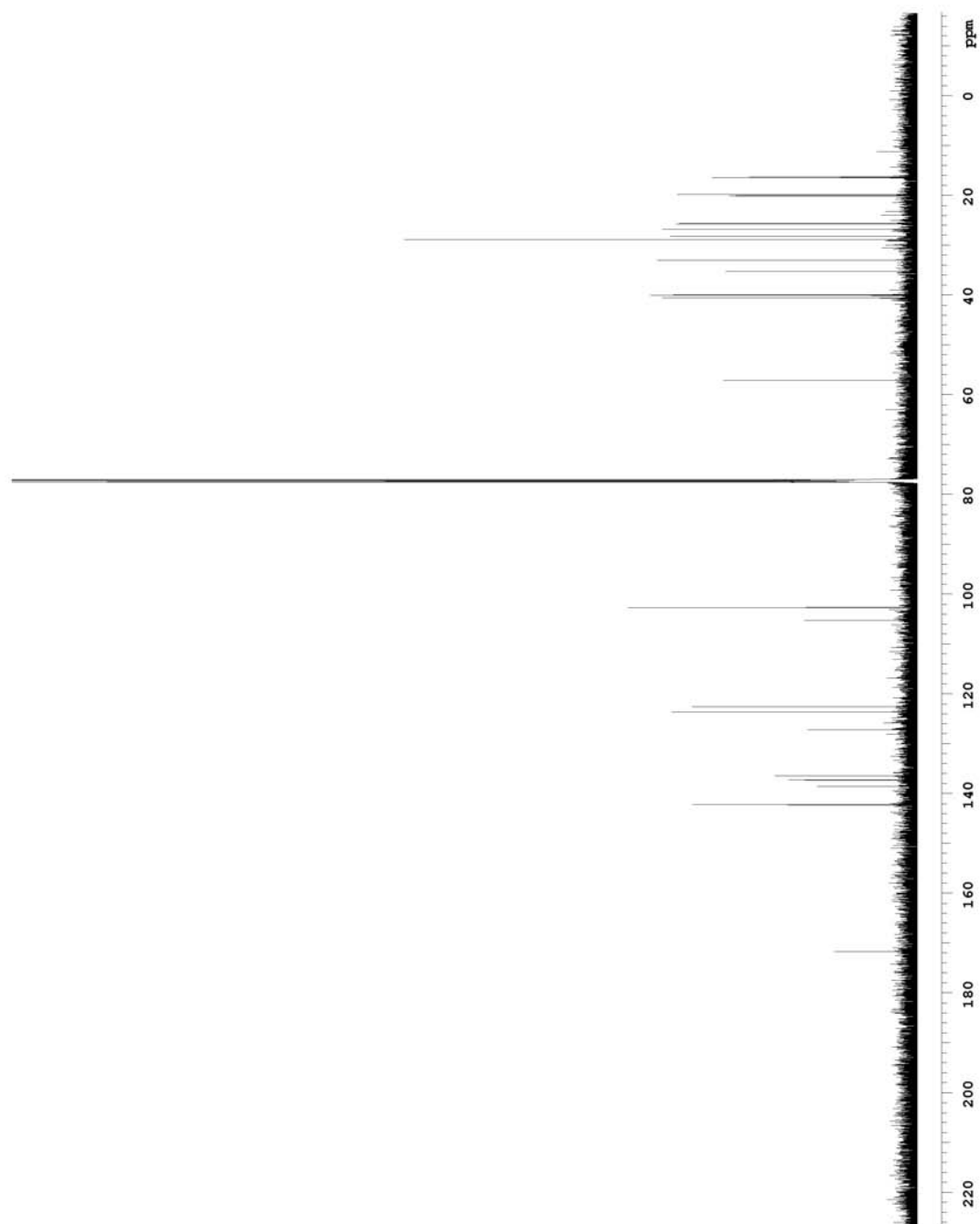
HMBC spectrum of isoluffariellolide (**46**) (600 MHz, CDCl₃)

Appendix C

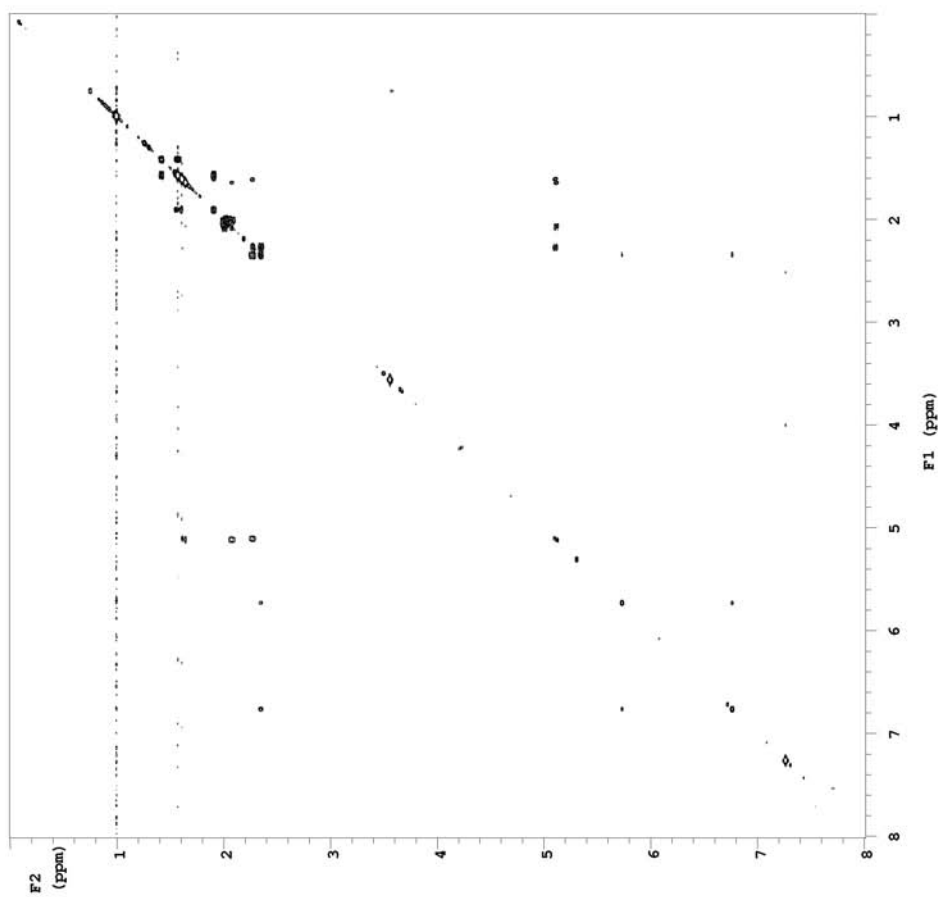
1-*O*-Methylisoluffariellolide Spectra



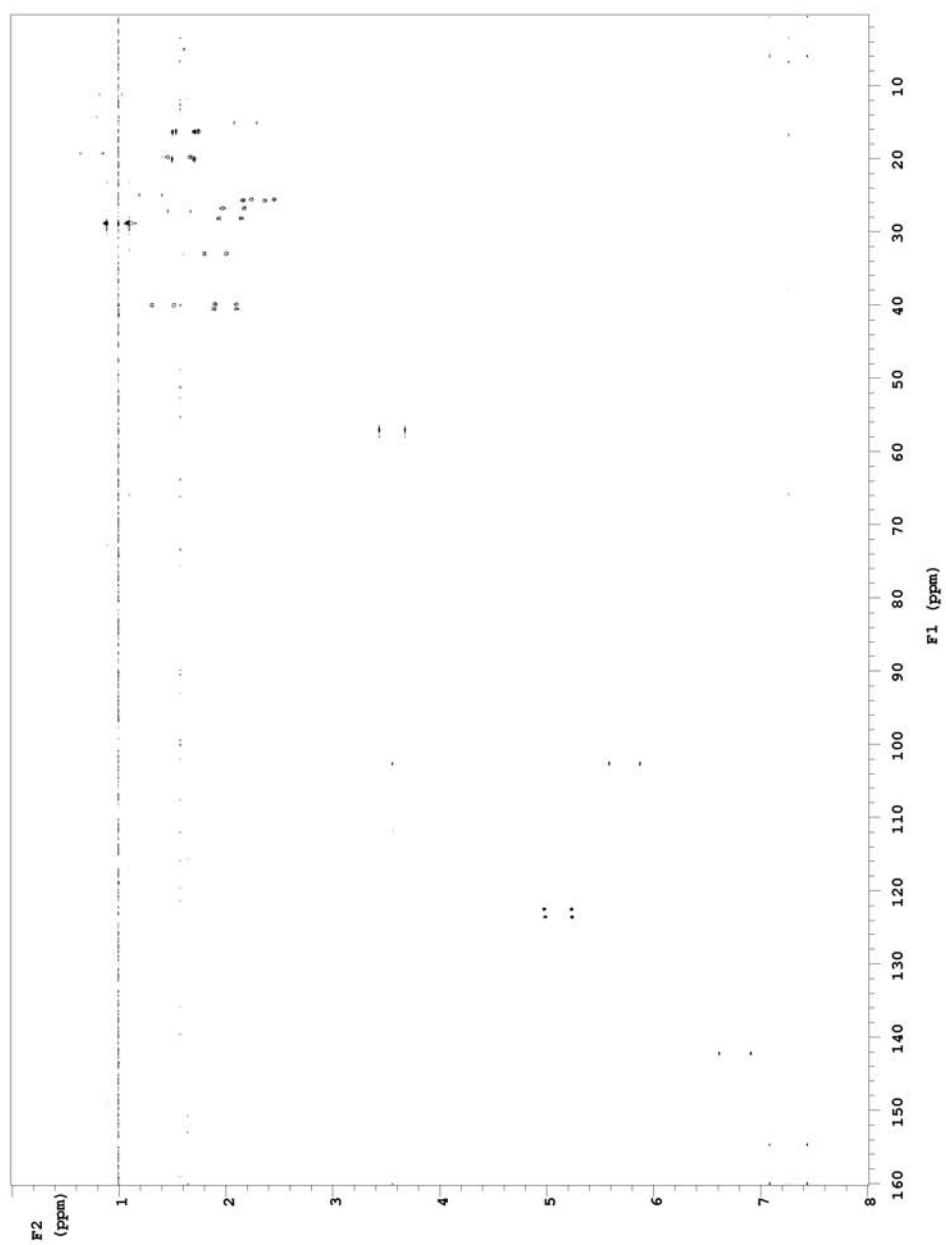
^1H NMR spectrum of 1-*O*-methylisoluffariellolide (**47**) (600 MHz, CDCl_3)



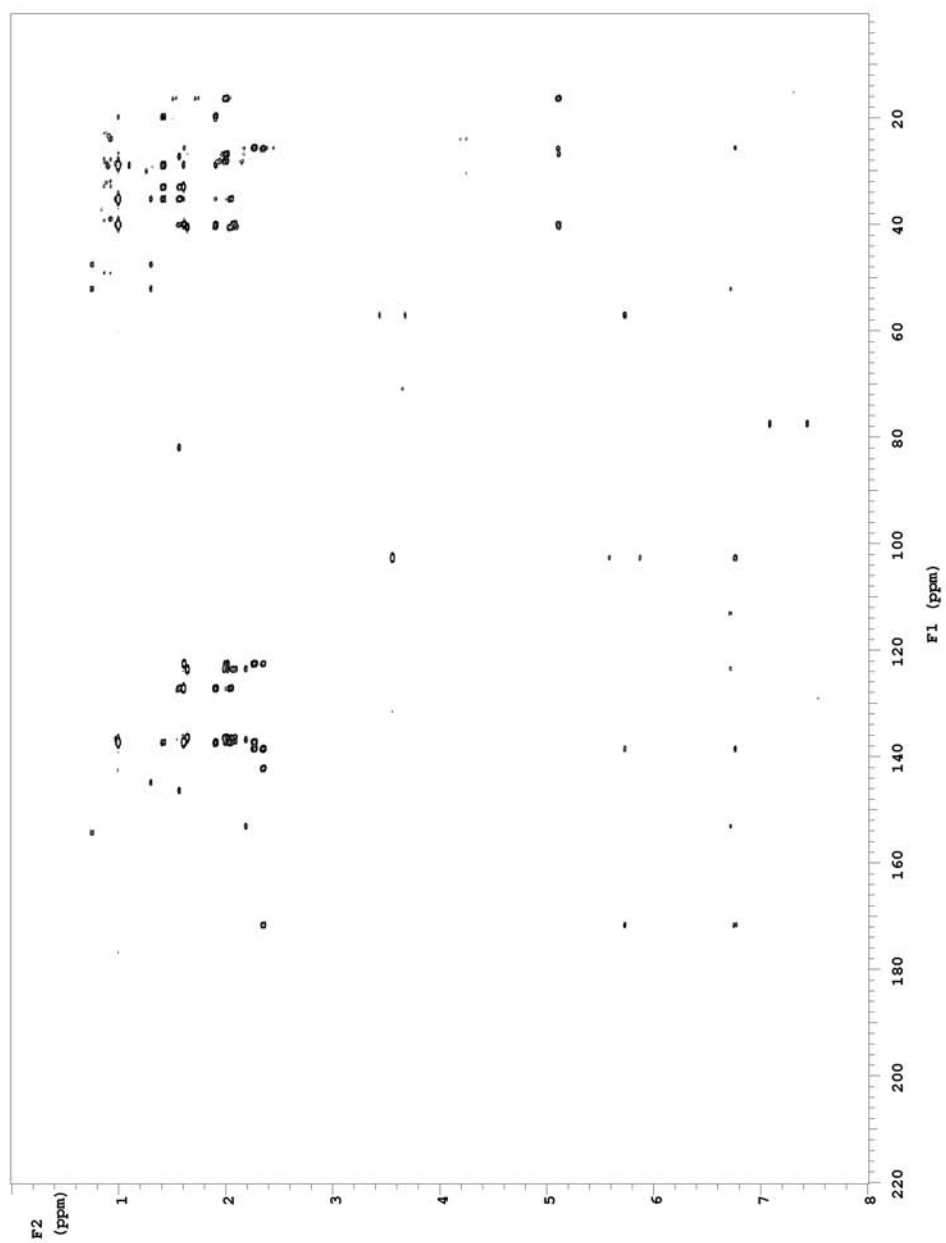
^{13}C spectrum of 1-*O*-methylisulfariellolide (**47**) (150 MHz, CDCl_3)



COSY spectrum of 1-*O*-methylisuluffariellolide (**47**) (600 MHz, CDCl₃)



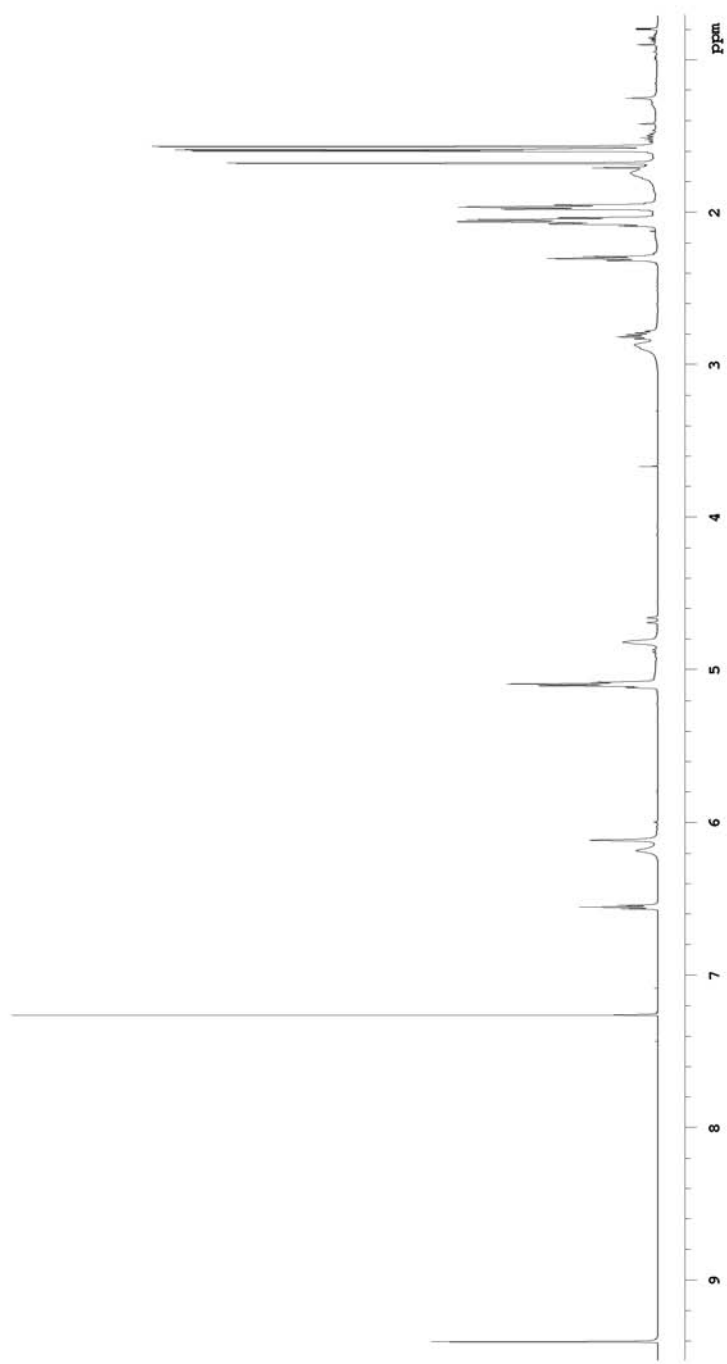
Coupled HSQC spectrum of 1-*O*-methylisoluffariellolide (**47**) (600 MHz, CDCl₃)



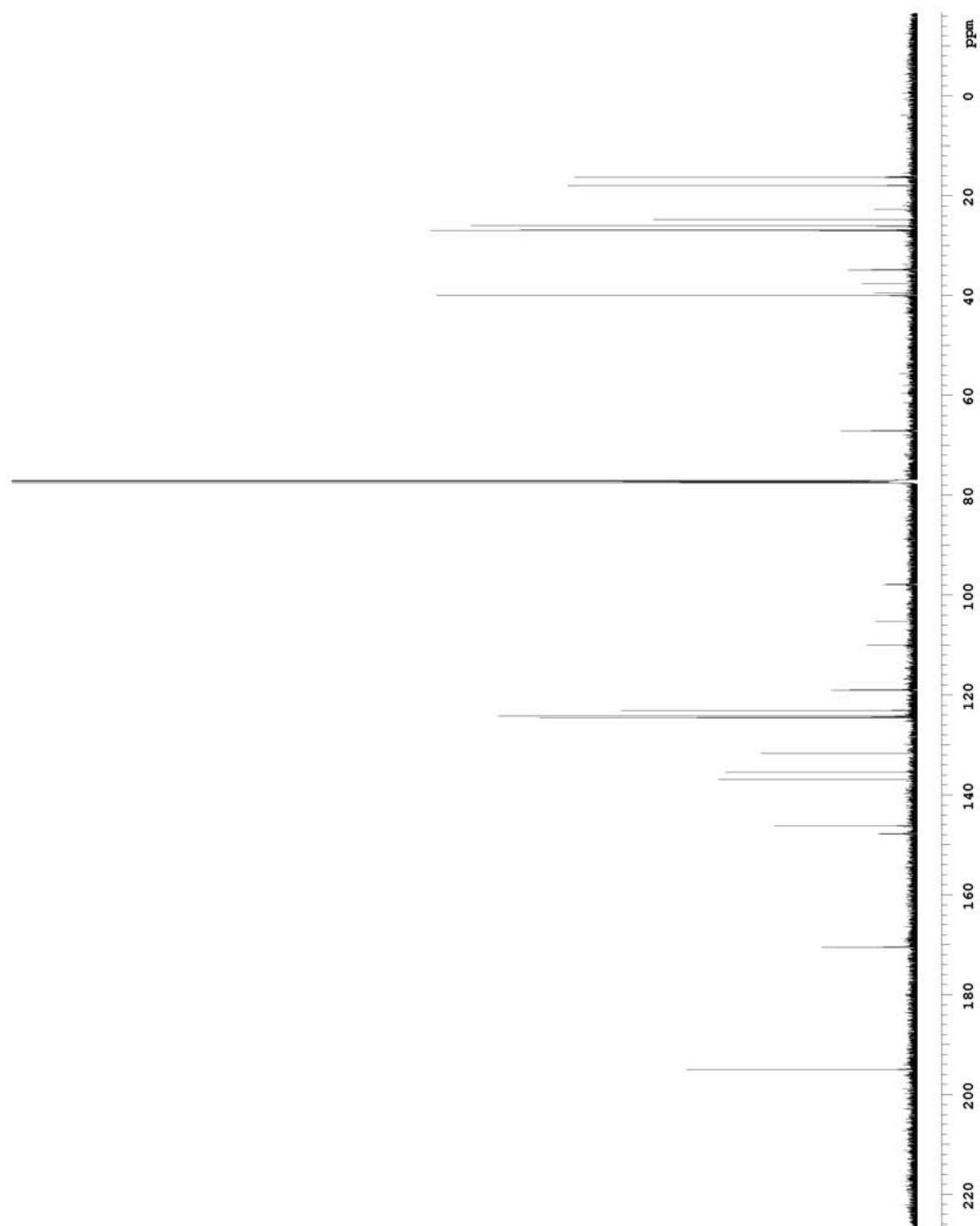
HMBC spectrum of 1-*O*-methylisulfariellolide (**47**) (600 MHz, CDCl_3)

Appendix D

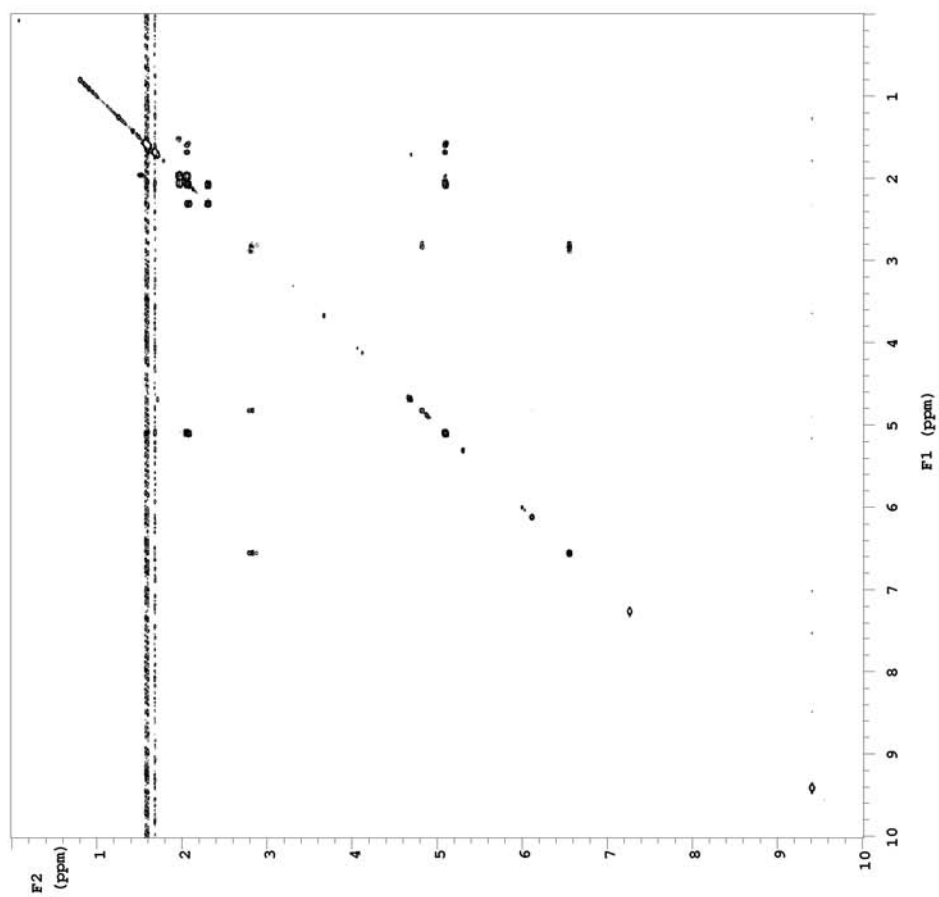
Secothorectolide Spectra



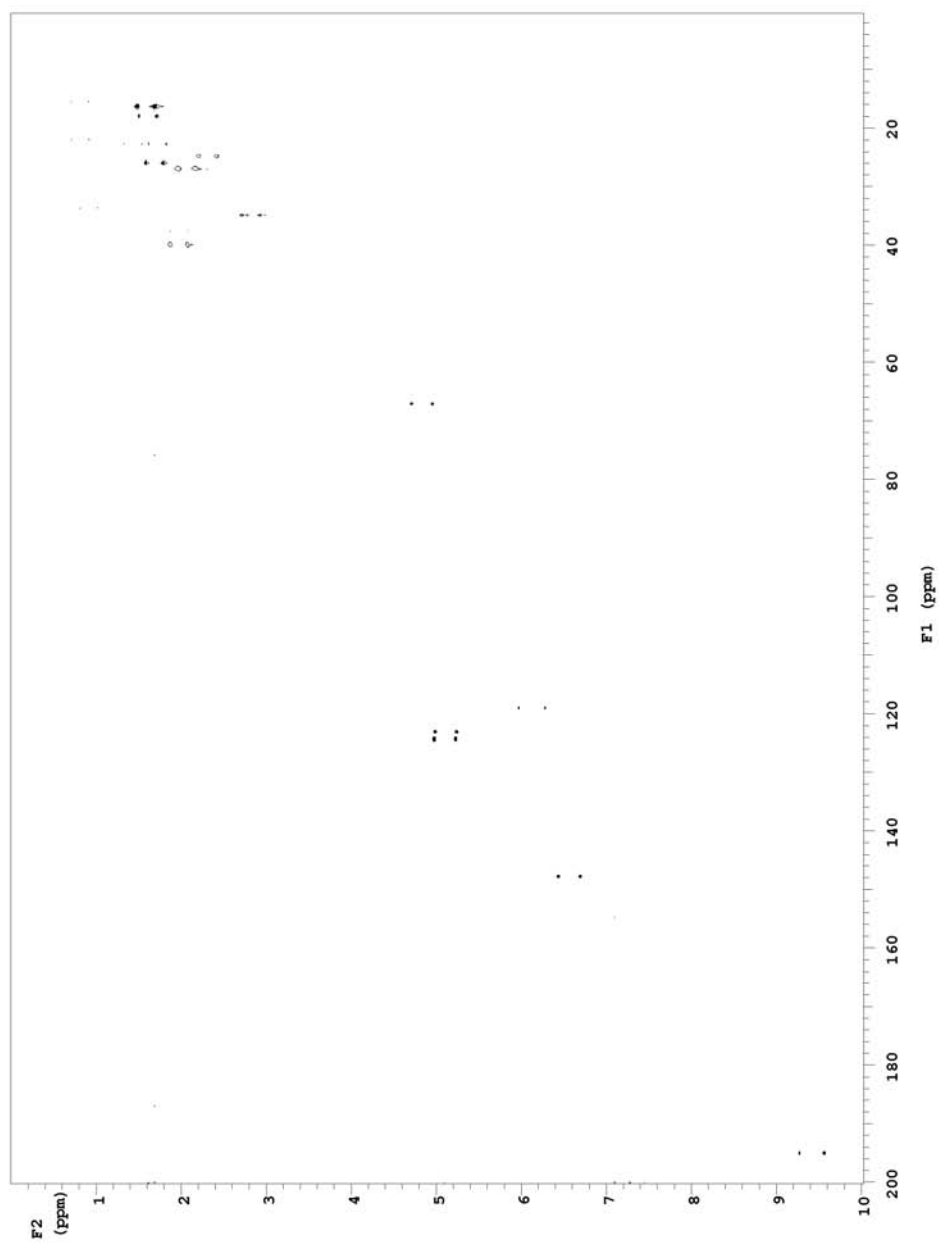
^1H NMR spectrum of secothorectolide (**49**) (600 MHz, CDCl_3)



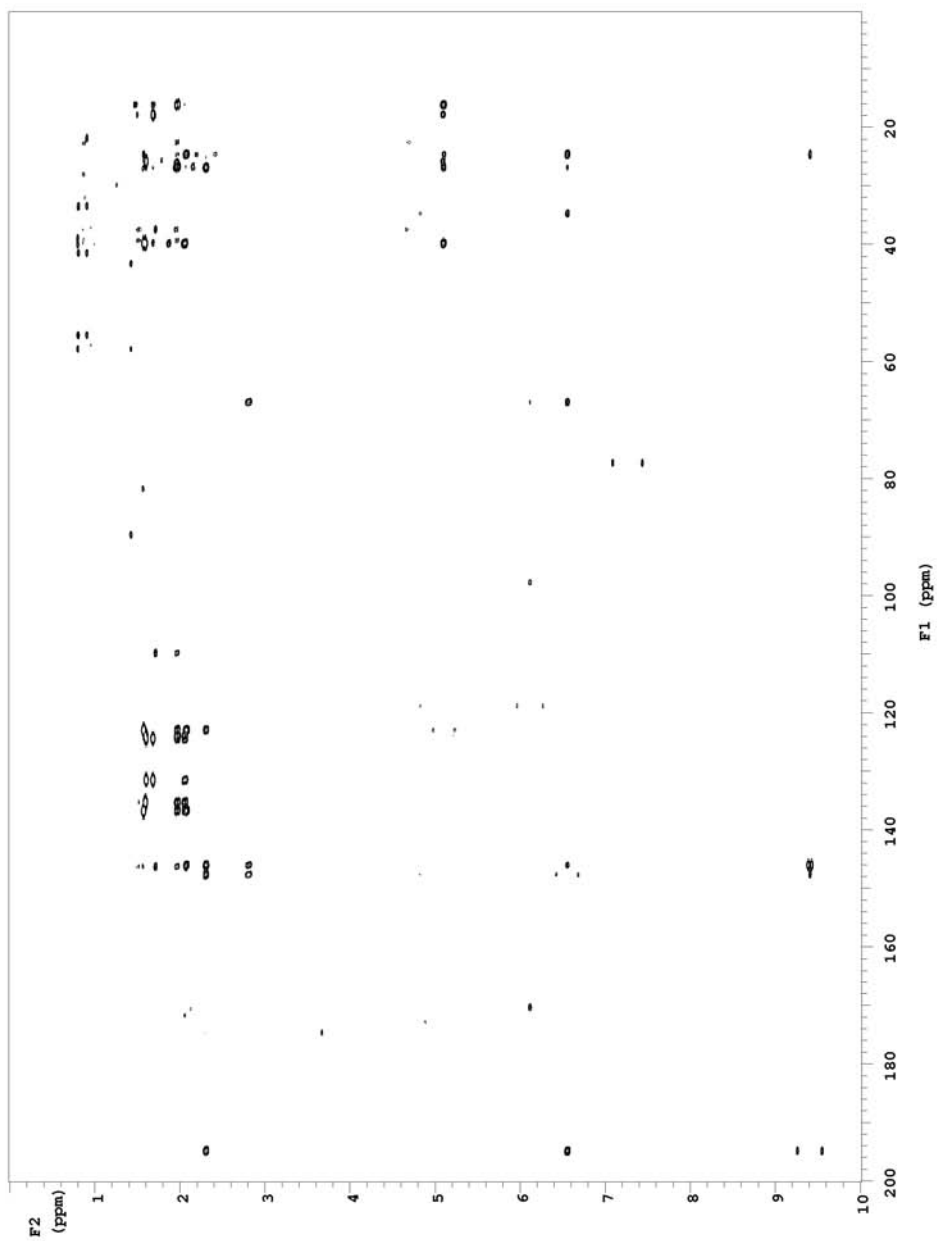
^{13}C spectrum of secothorectolide (**49**) (150 MHz, CDCl_3)



COSY spectrum of secothorectolide (**49**) (600 MHz, CDCl_3)



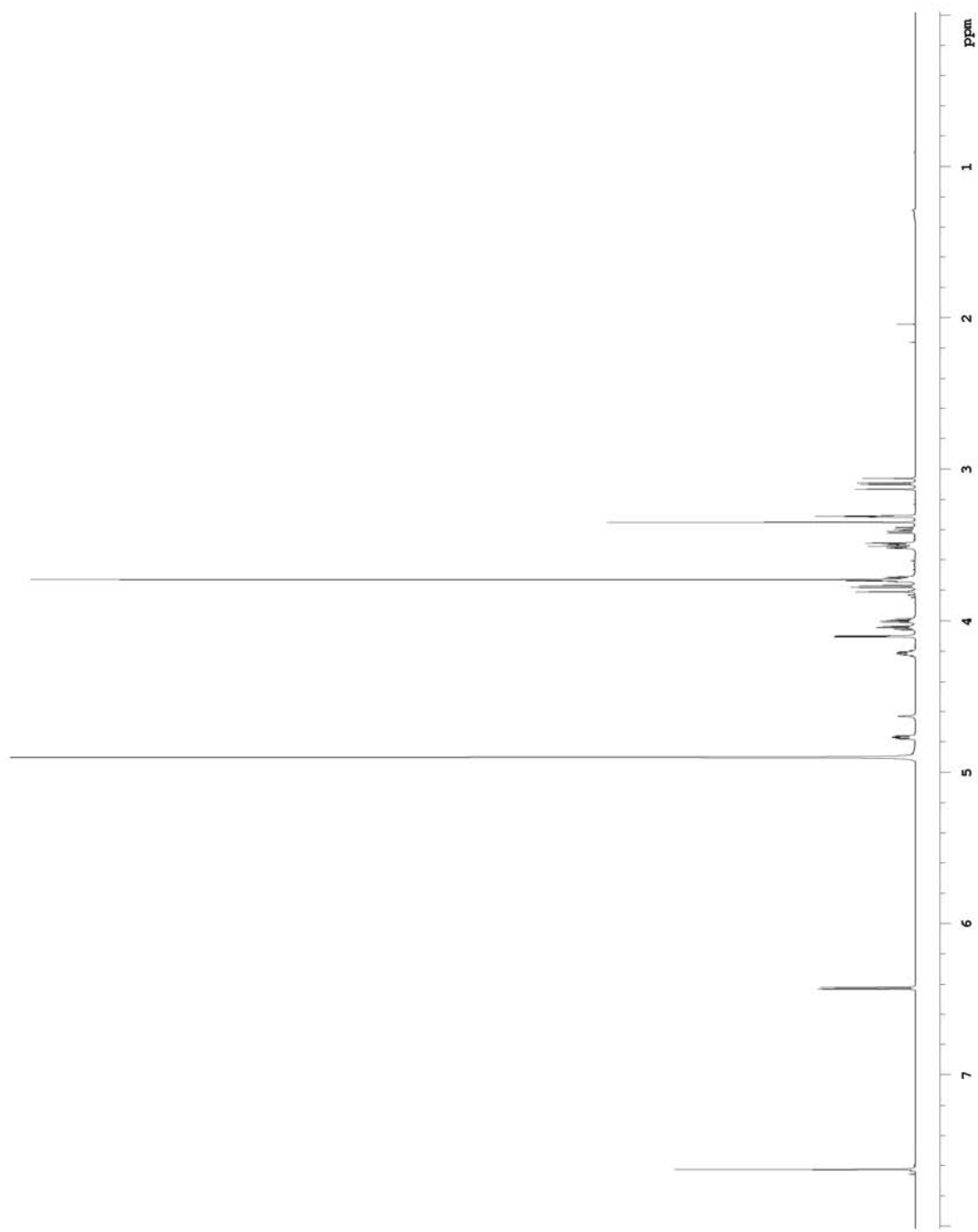
Coupled HSQC spectrum of secothorectolide (**49**) (600 MHz, CDCl_3)



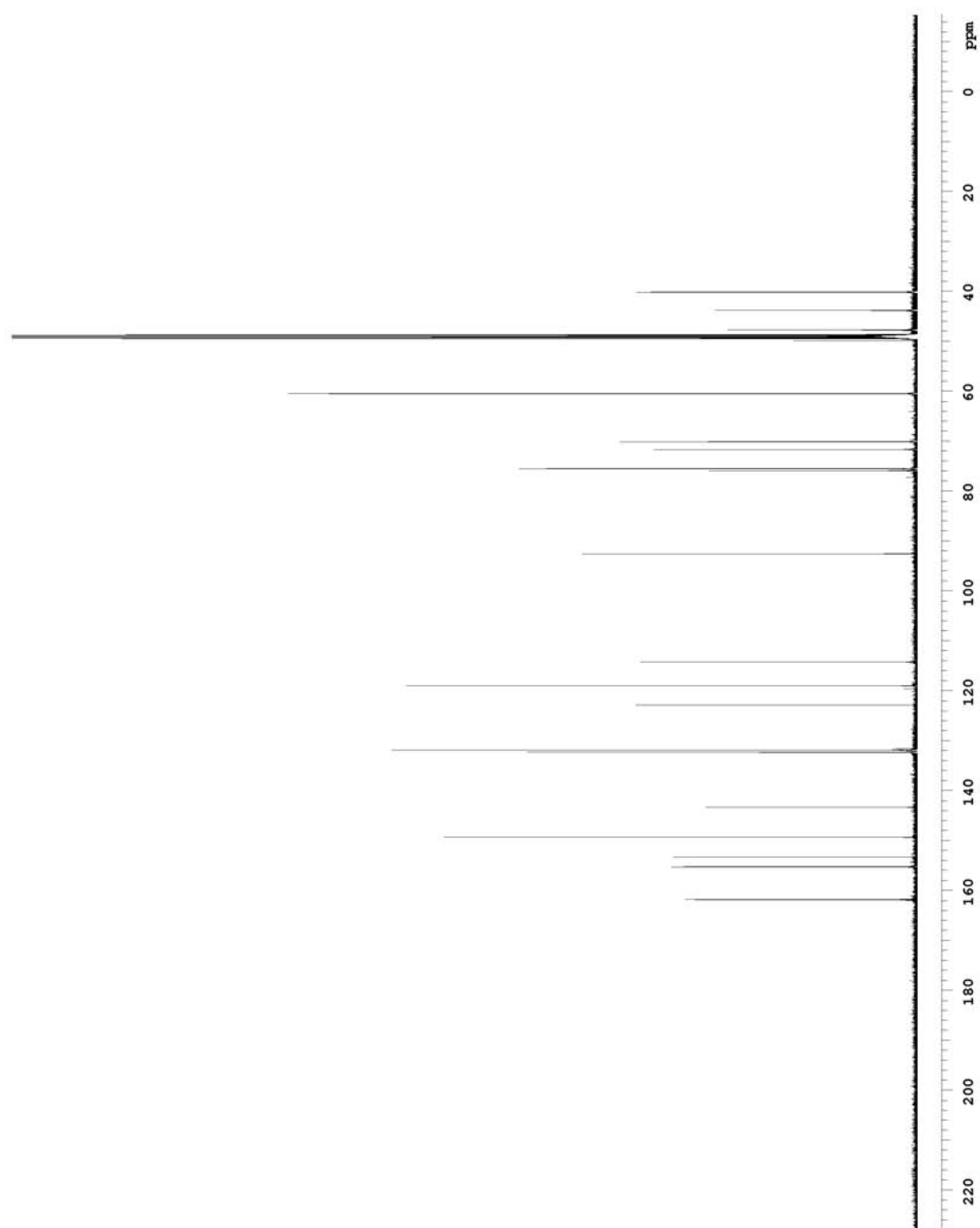
HMBC spectrum of secothorectolide (**49**) (600 MHz, CDCl_3)

Appendix E

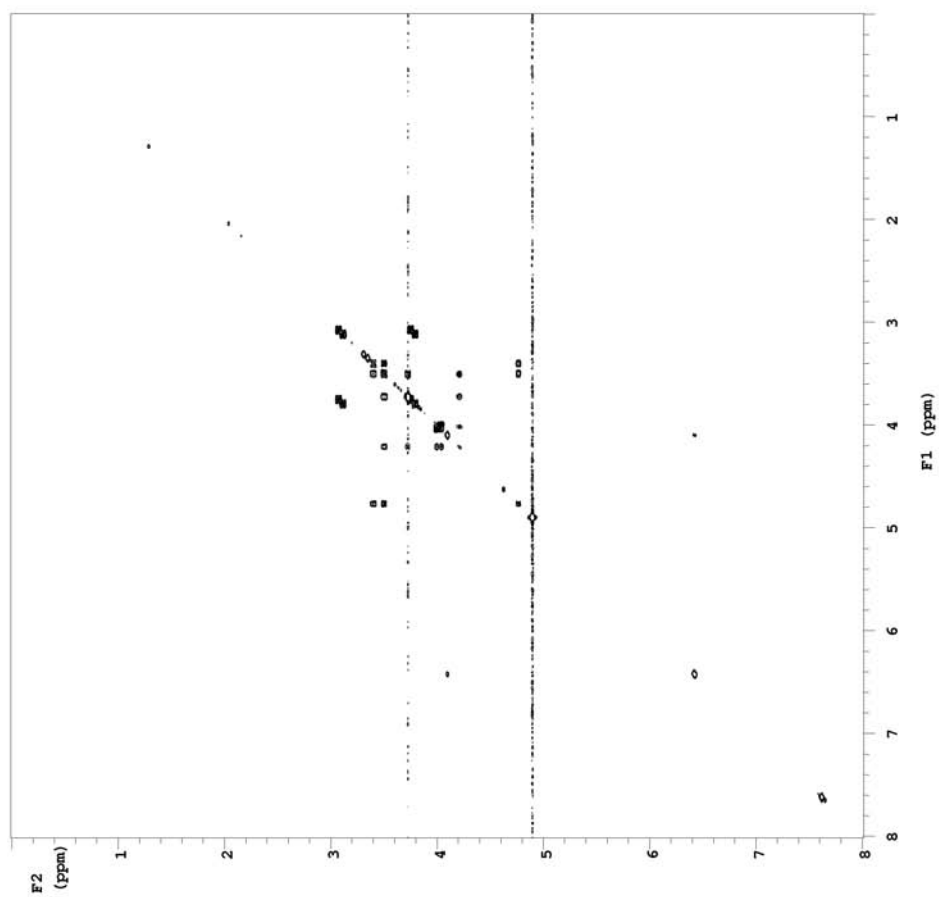
Fistularin-3 Spectra



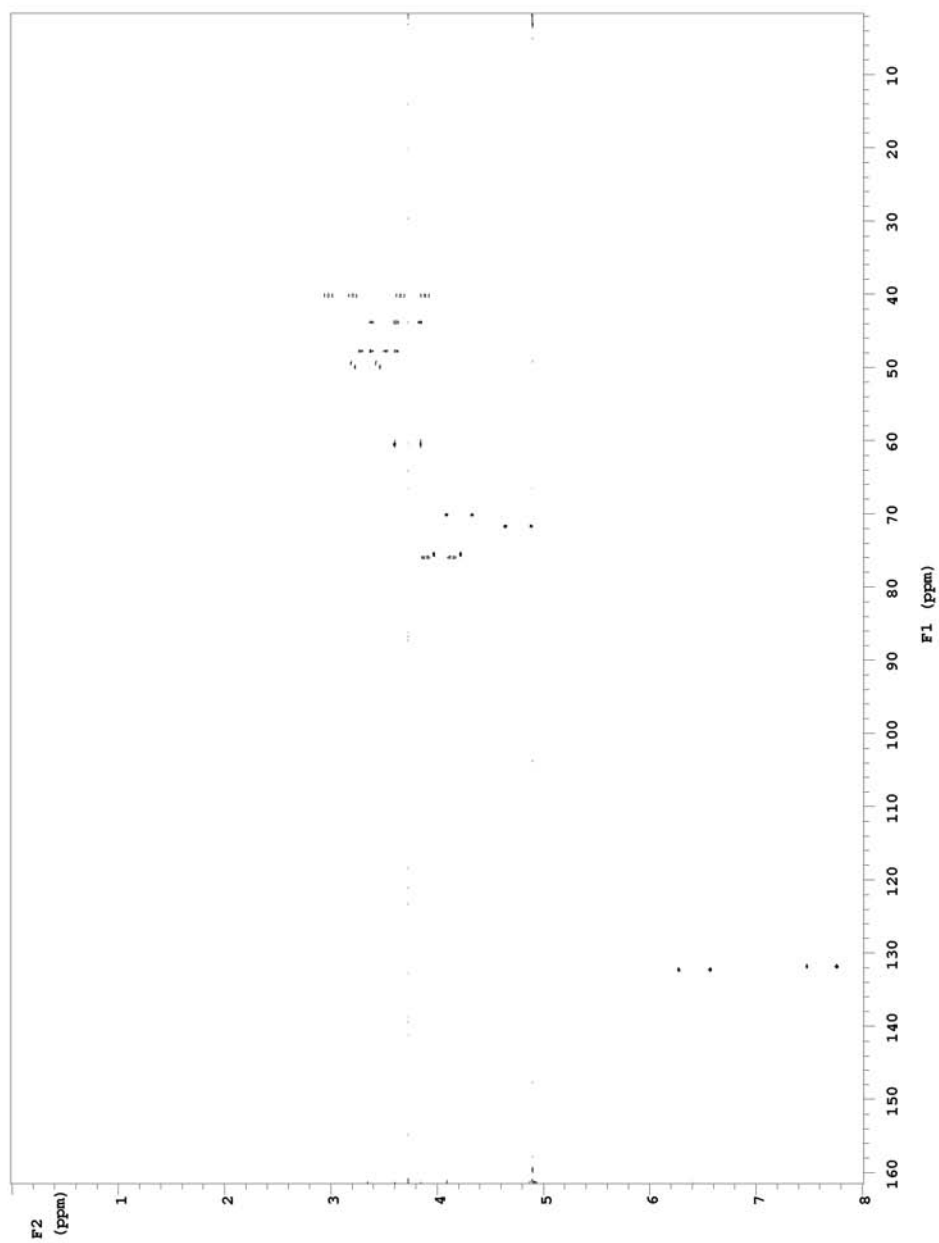
^1H NMR spectrum of fistularin-3 (**52**) (600 MHz, CD_3OD)



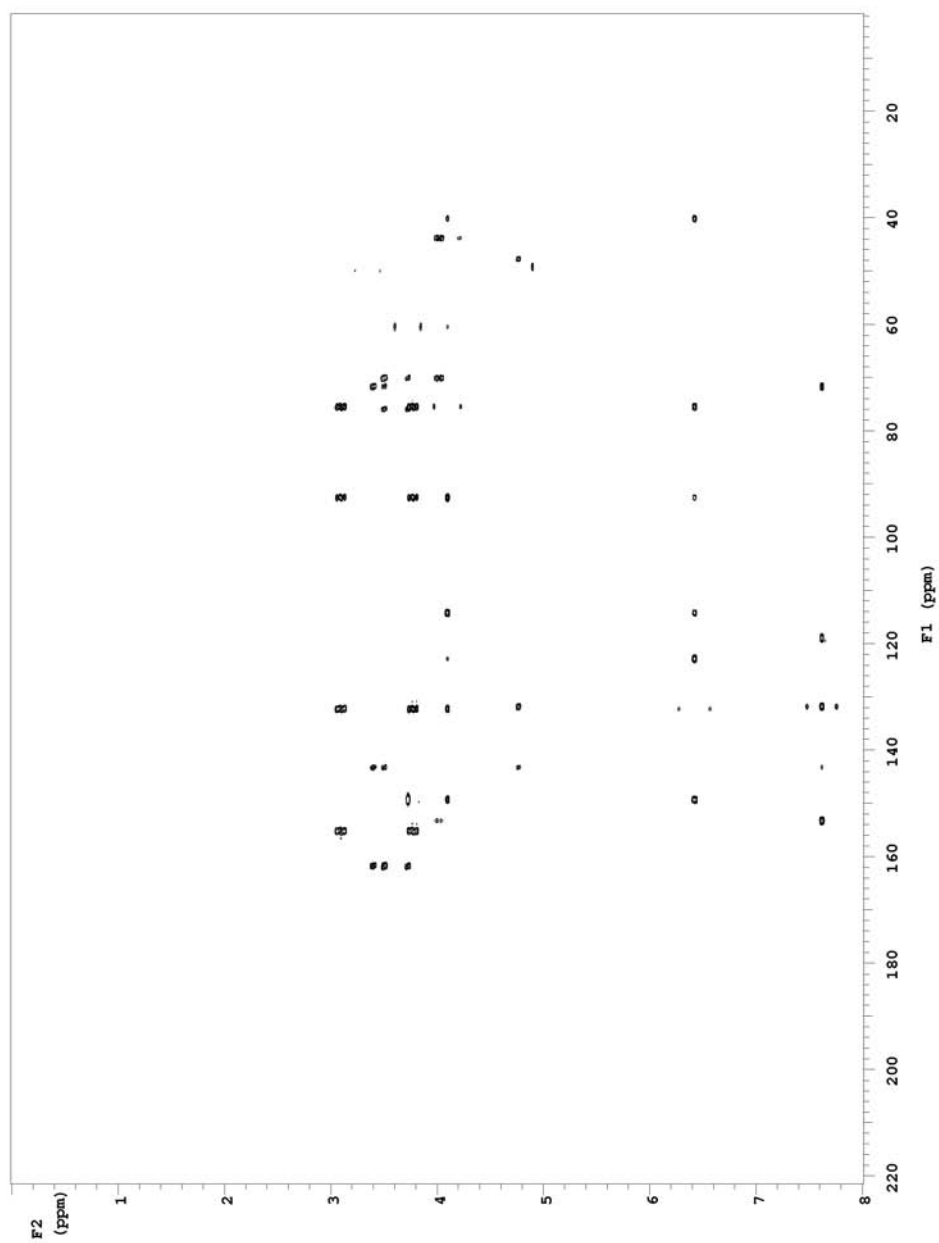
^{13}C spectrum of fistularin-3 (**52**) (150MHz, CD_3OD)



COSY spectrum of fistularin-3 (**52**) (600 MHz, CD₃OD)



Coupled HSQC spectrum of fistularin-3 (**52**) (600 MHz, CD_3OD)

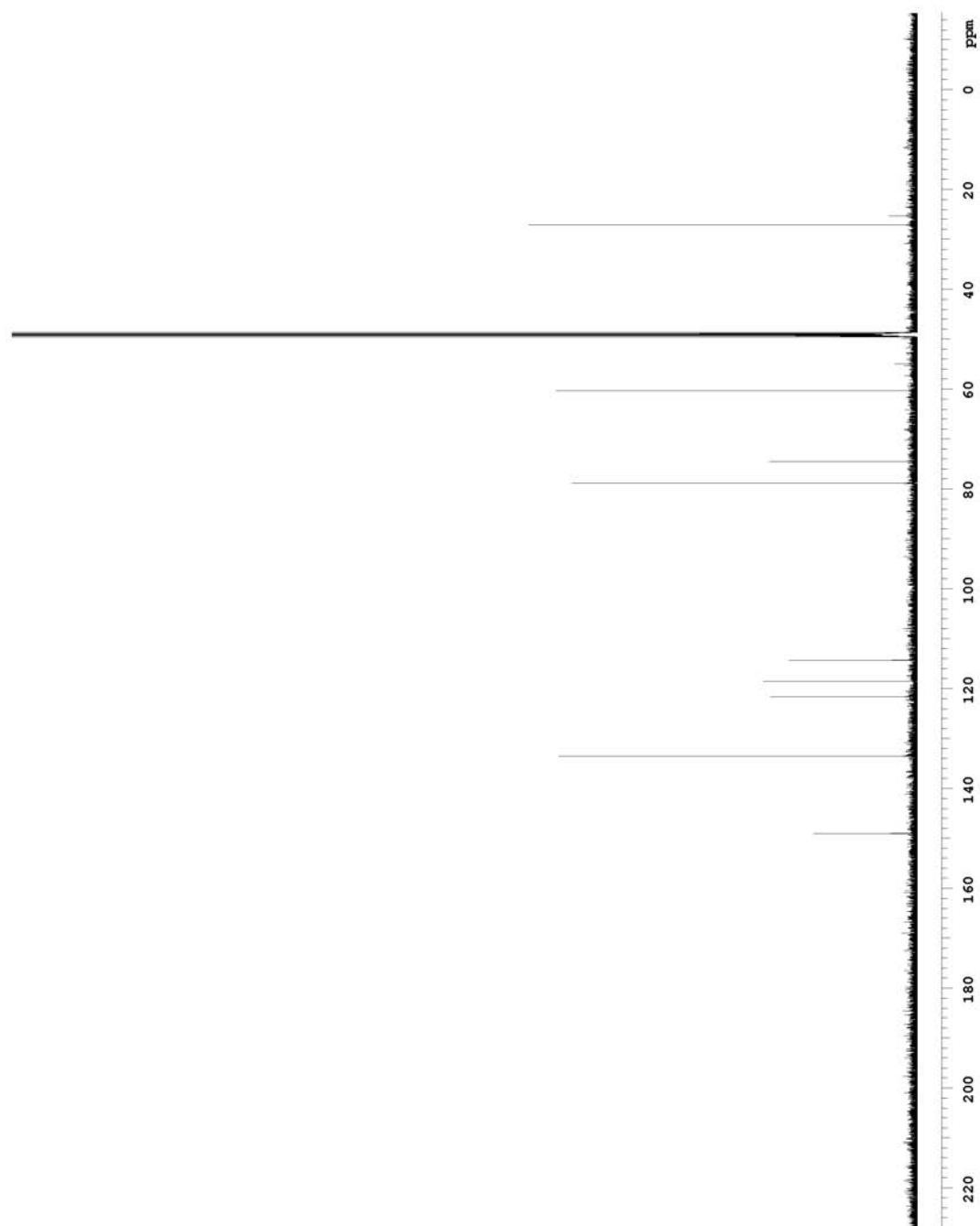


HMBC spectrum of fistularin-3 (**52**) (600 MHz, CD_3OD)

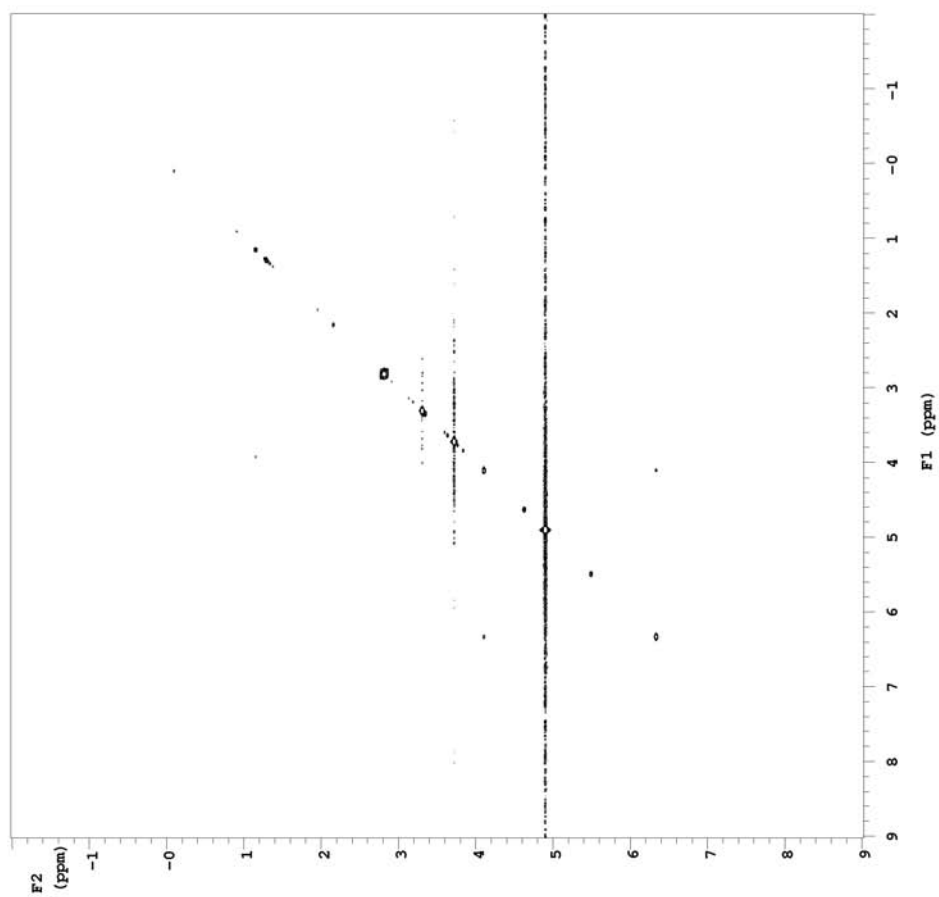
Appendix F

Aerophysinin-1 Spectra

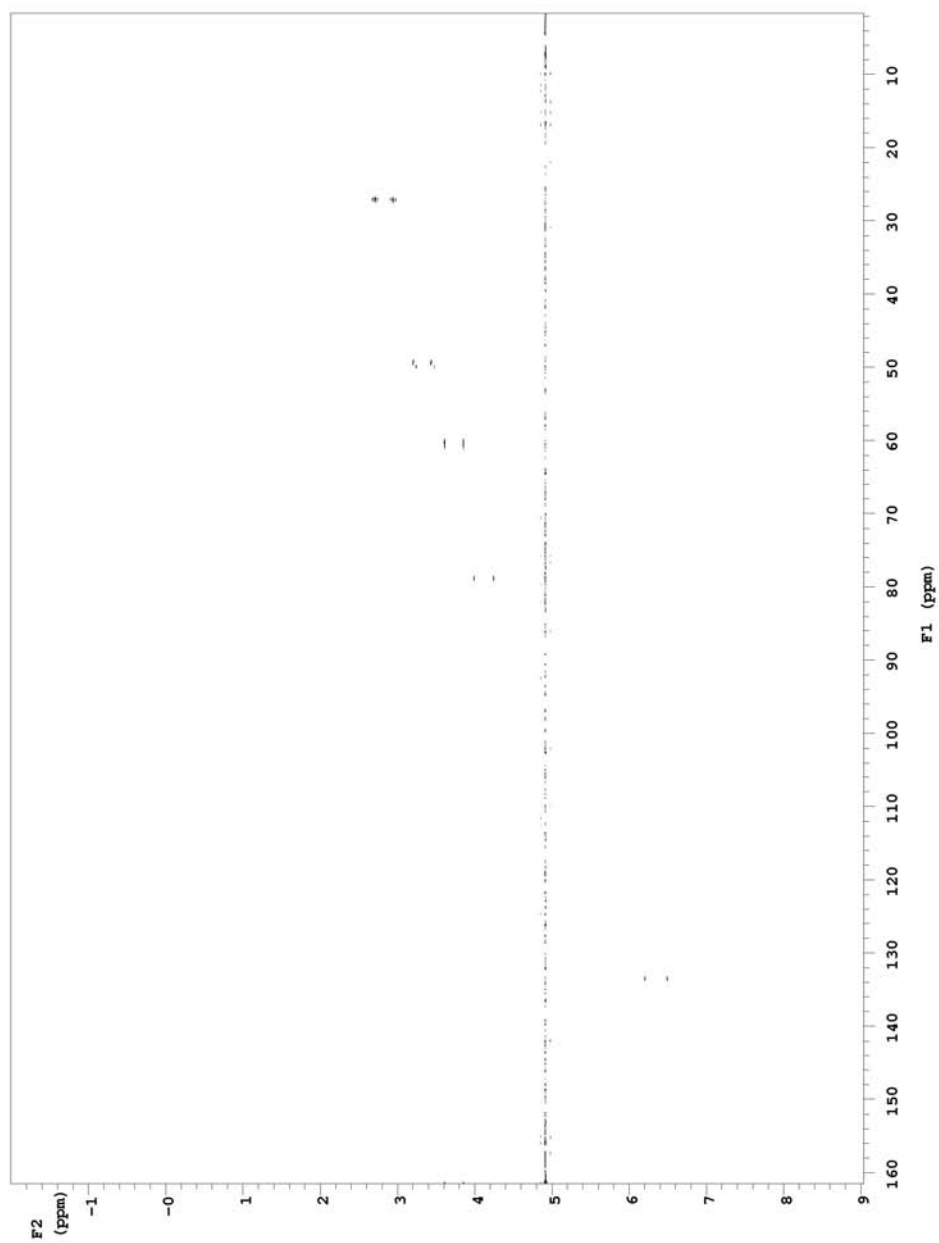
¹H NMR spectrum of aeroplysinin-1 (**53**) (600 MHz, CD₃OD)



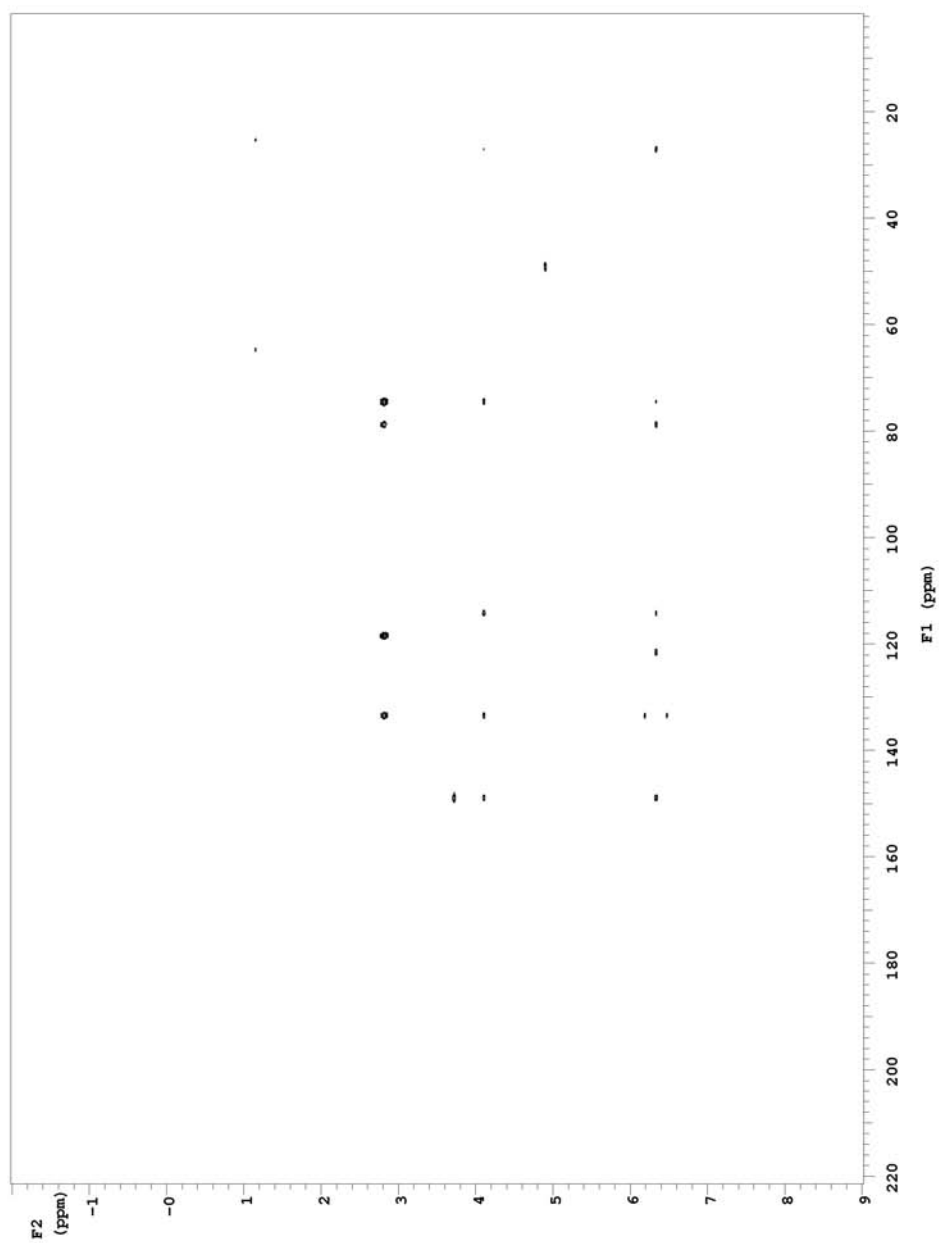
^{13}C spectrum of aeroplysinin-1 (**53**) (150 MHz, CD_3OD)



COSY spectrum of aeroplysinin-1 (**53**) (600 MHz, CD₃OD)



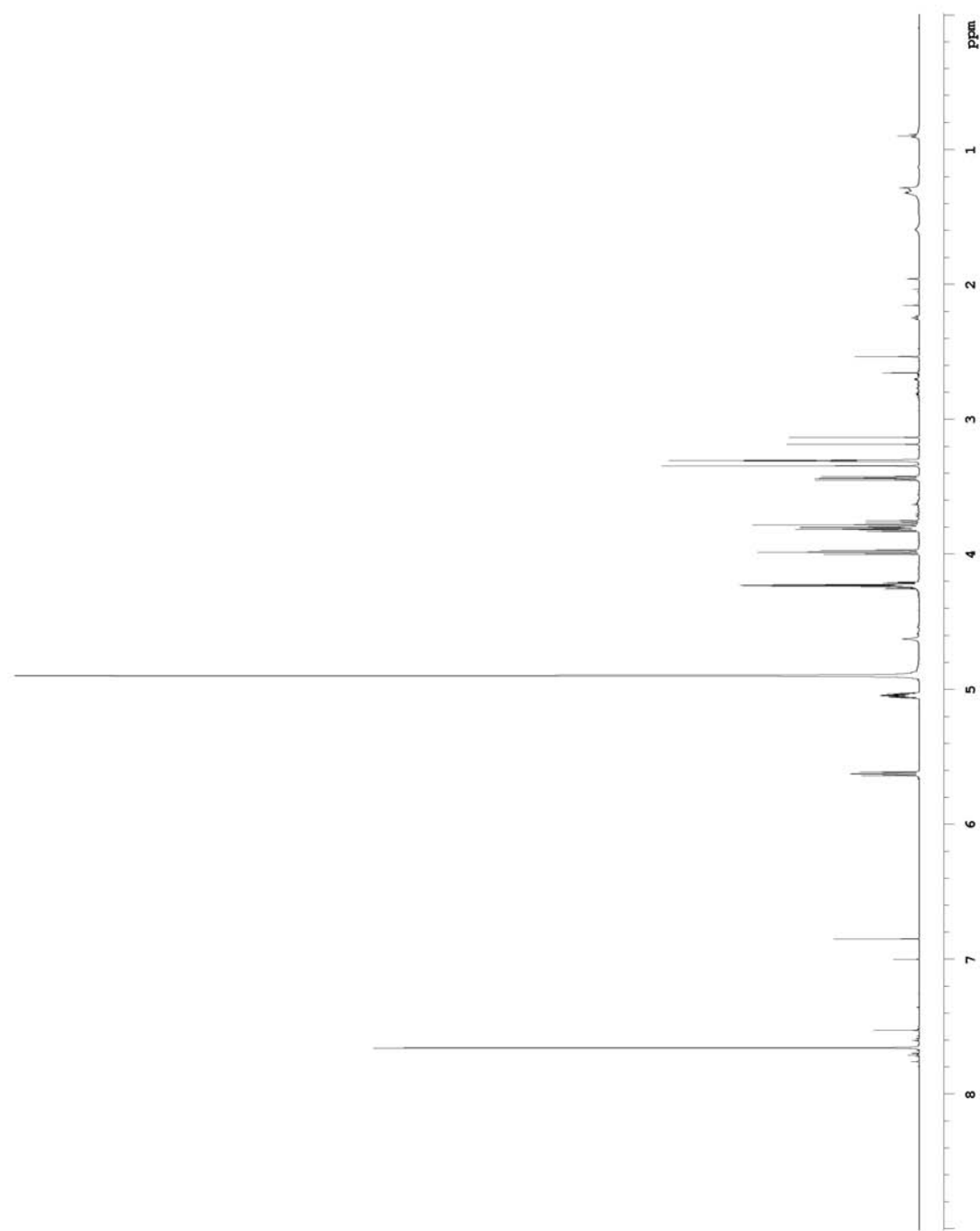
Coupled HSQC spectrum of aeroplysinin-1 (**53**) (600 MHz, CD_3OD)



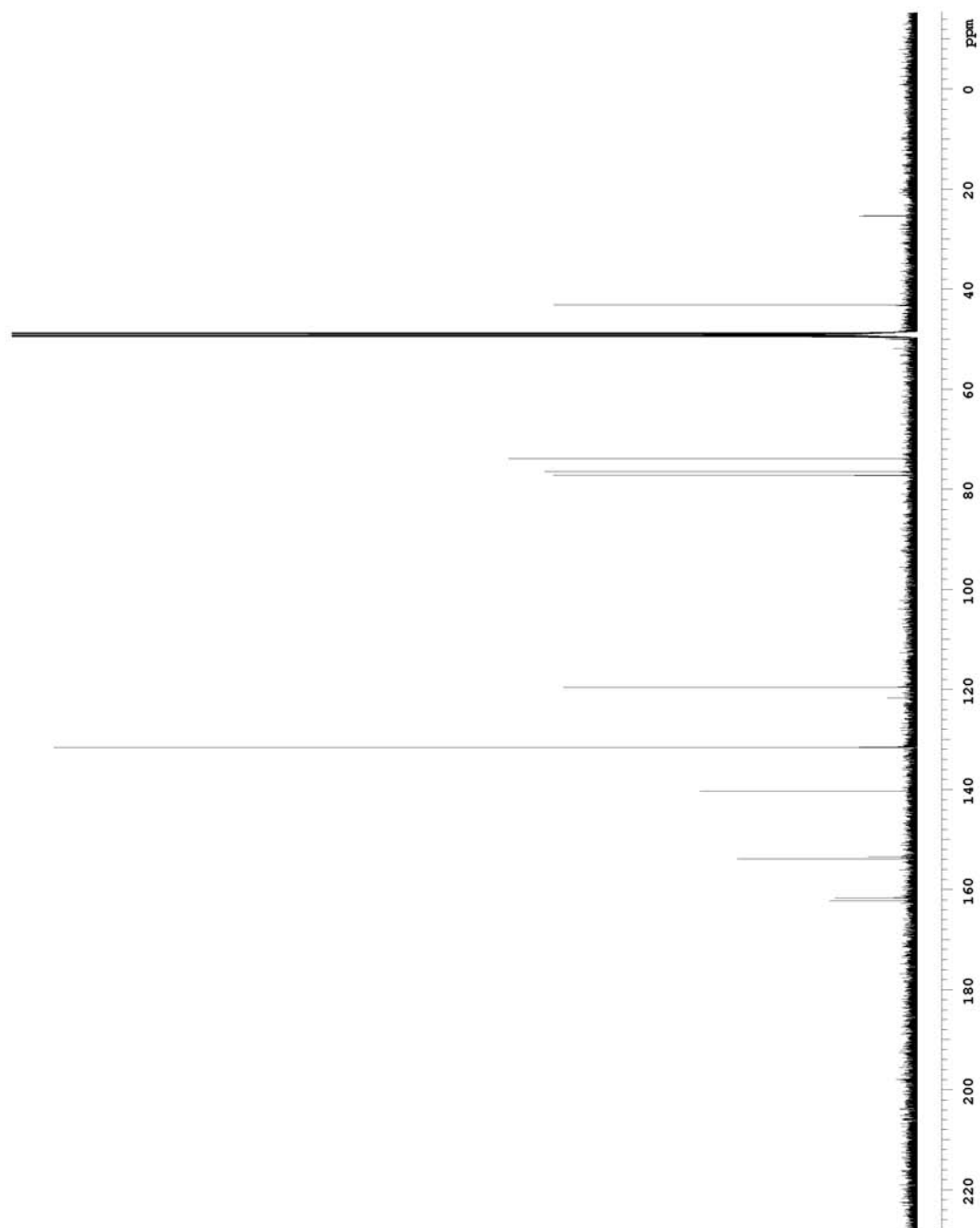
HMBC spectrum of aerophysinin-1 (**53**) (600 MHz, CD_3OD)

Appendix G

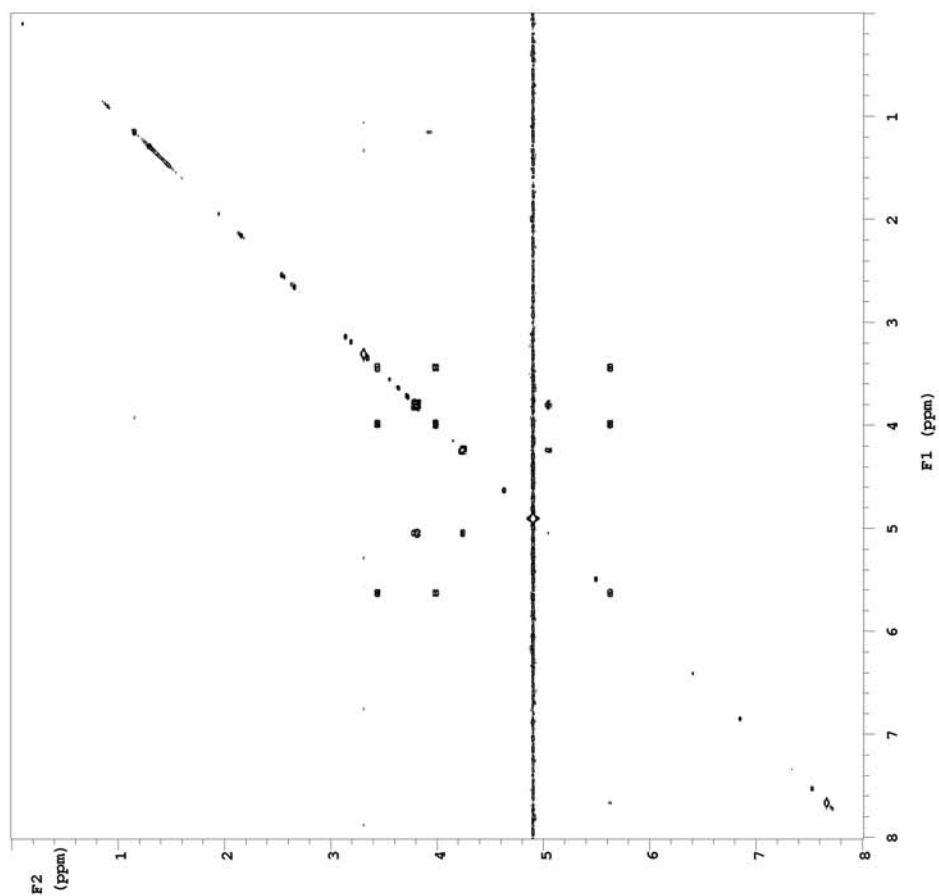
LL-PAA216 Spectra



^1H NMR spectrum of LL-PAA216 (**54**) (600 MHz, CD_3OD)

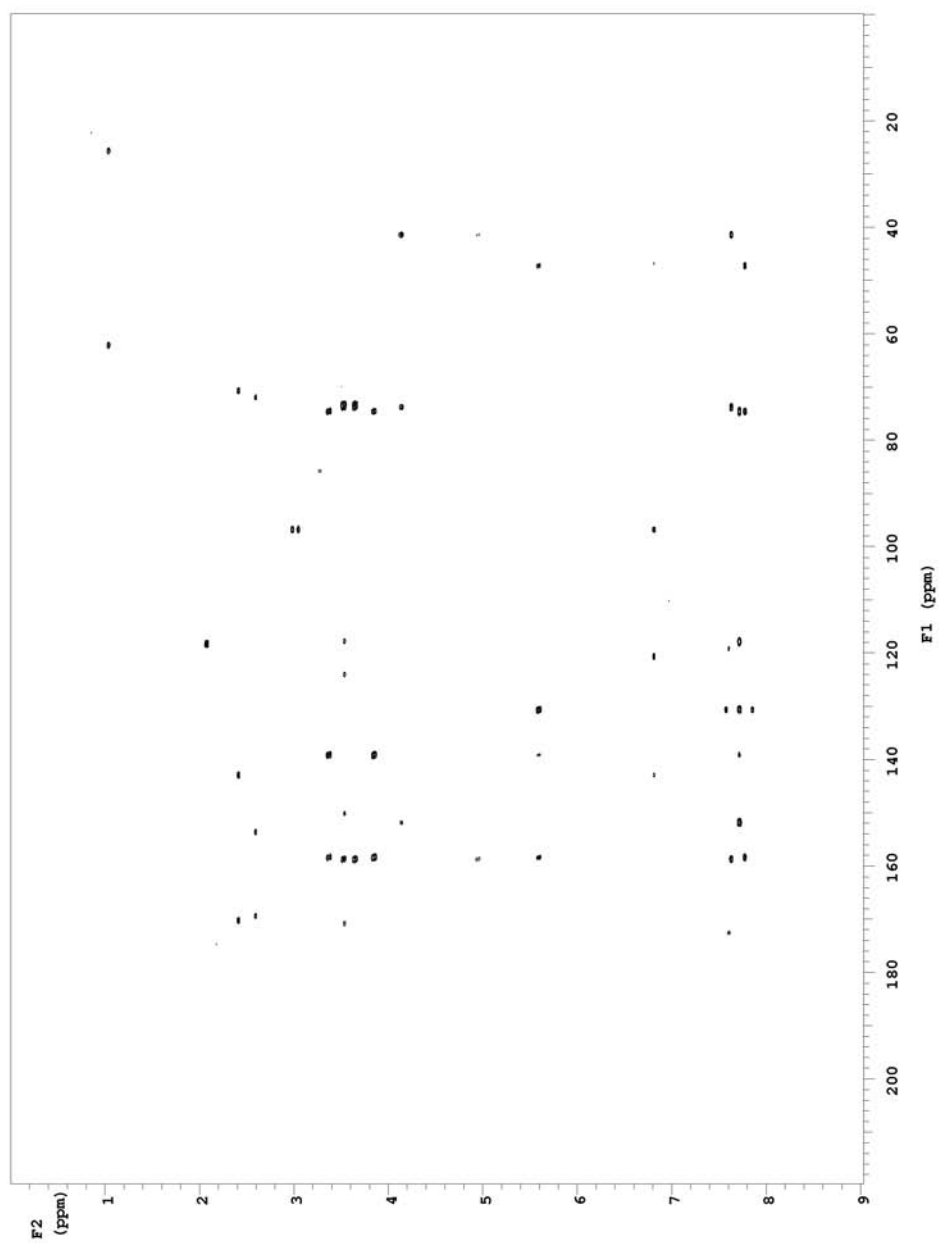


^{13}C spectrum of LL-PAA216 (**54**) (150 MHz, CD_3OD)



COSY spectrum of LL-PAA216 (**54**) (600 MHz, CD₃OD)

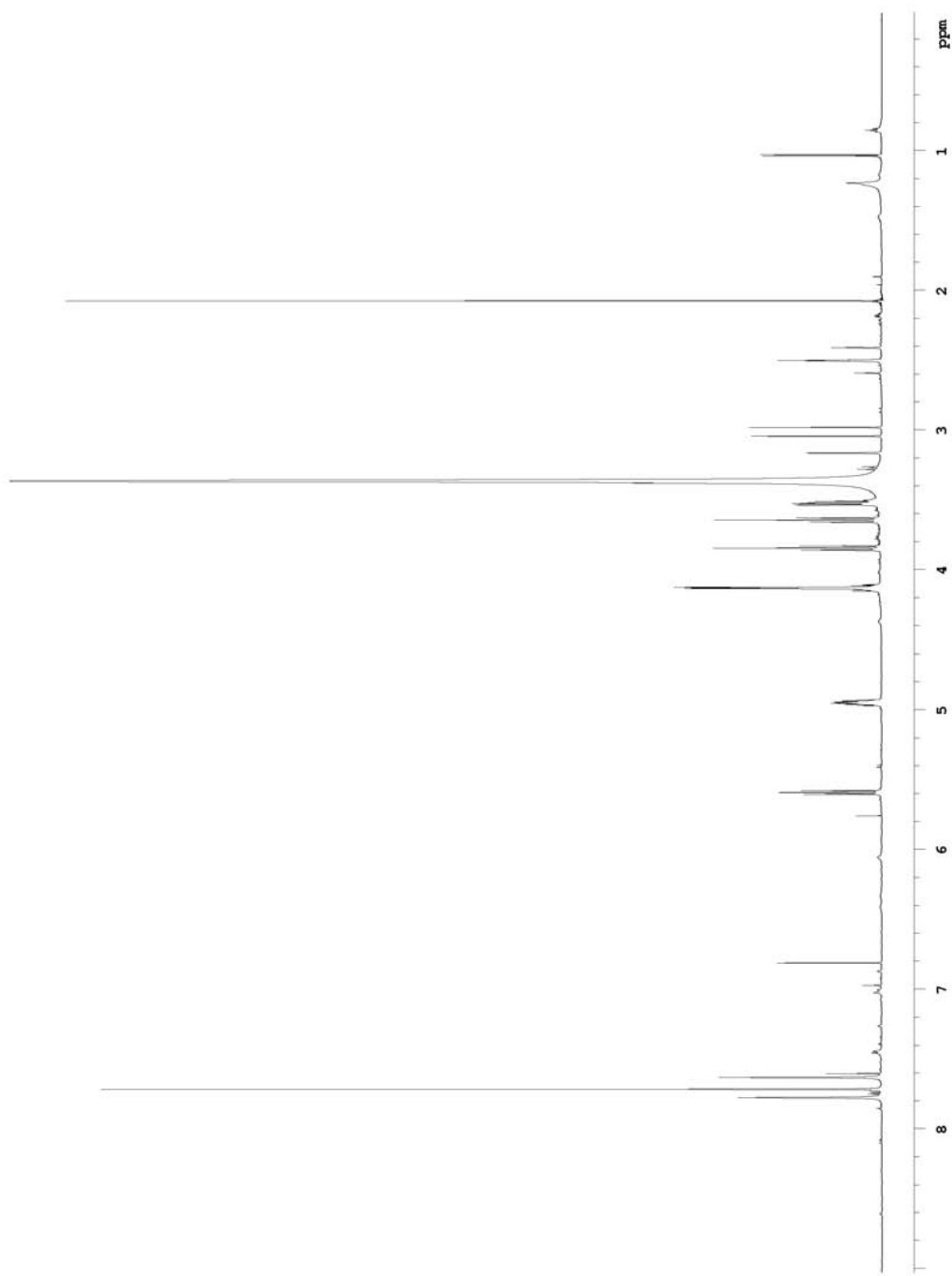
Coupled HSQC spectrum of LL-PAA216 (**54**) (600 MHz, CD₃OD)



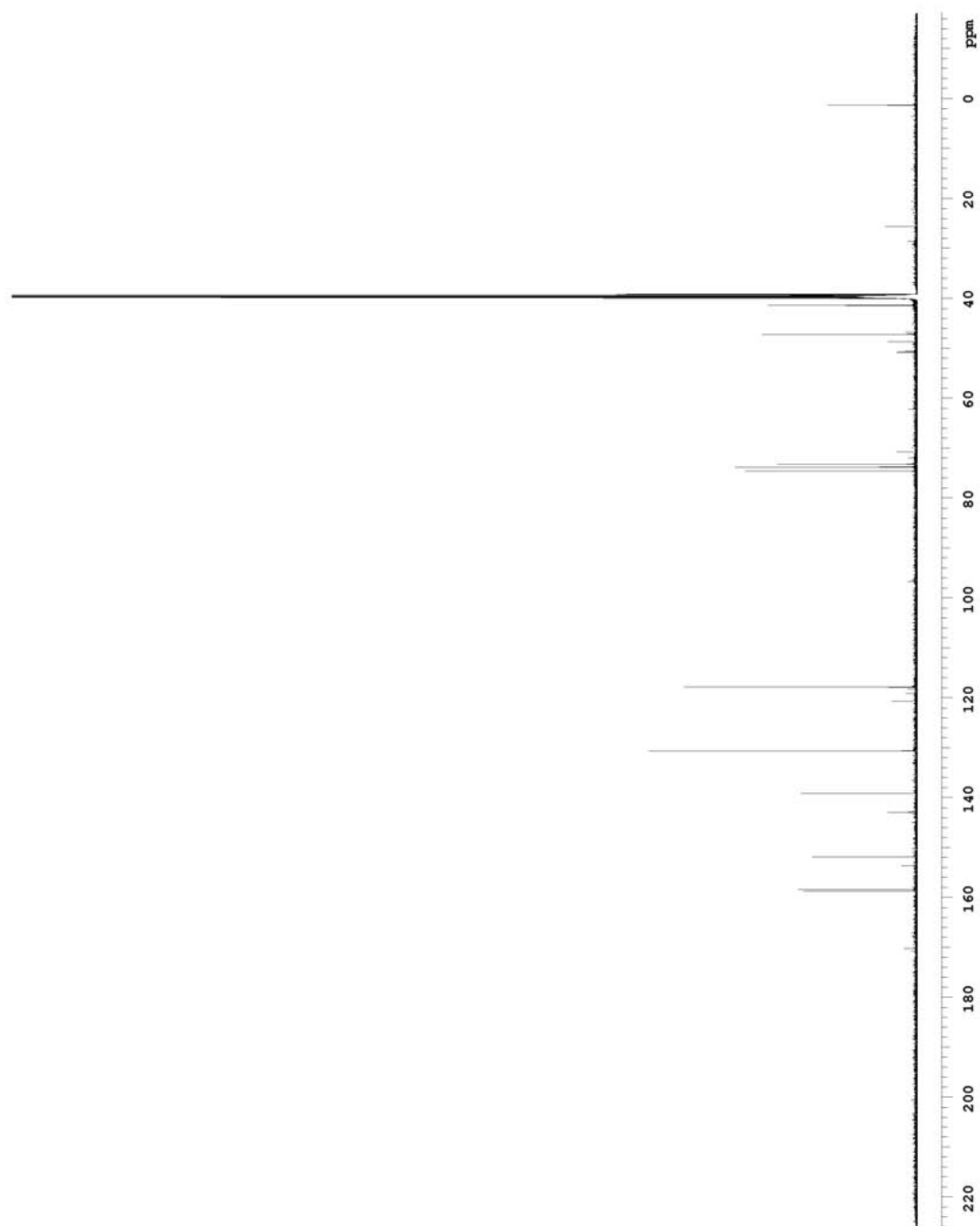
HMBC spectrum of LL-PAA216 (**54**) (600 MHz, CD_3OD)

Appendix H

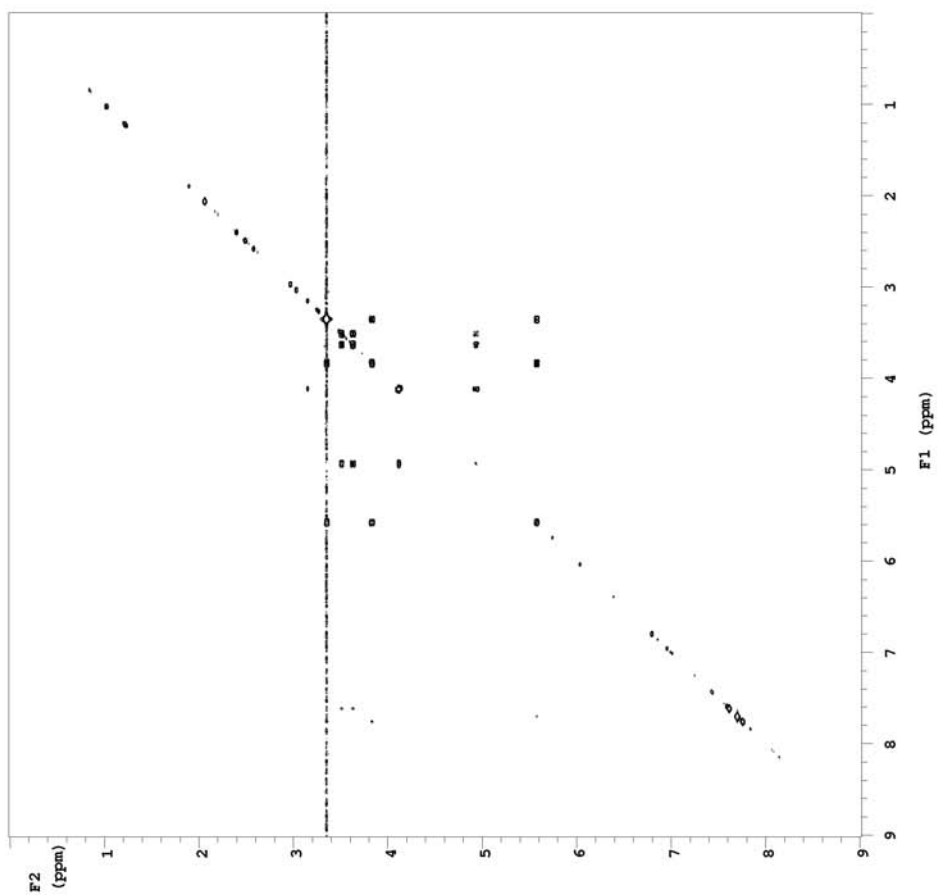
LL-PAA216 Spectra



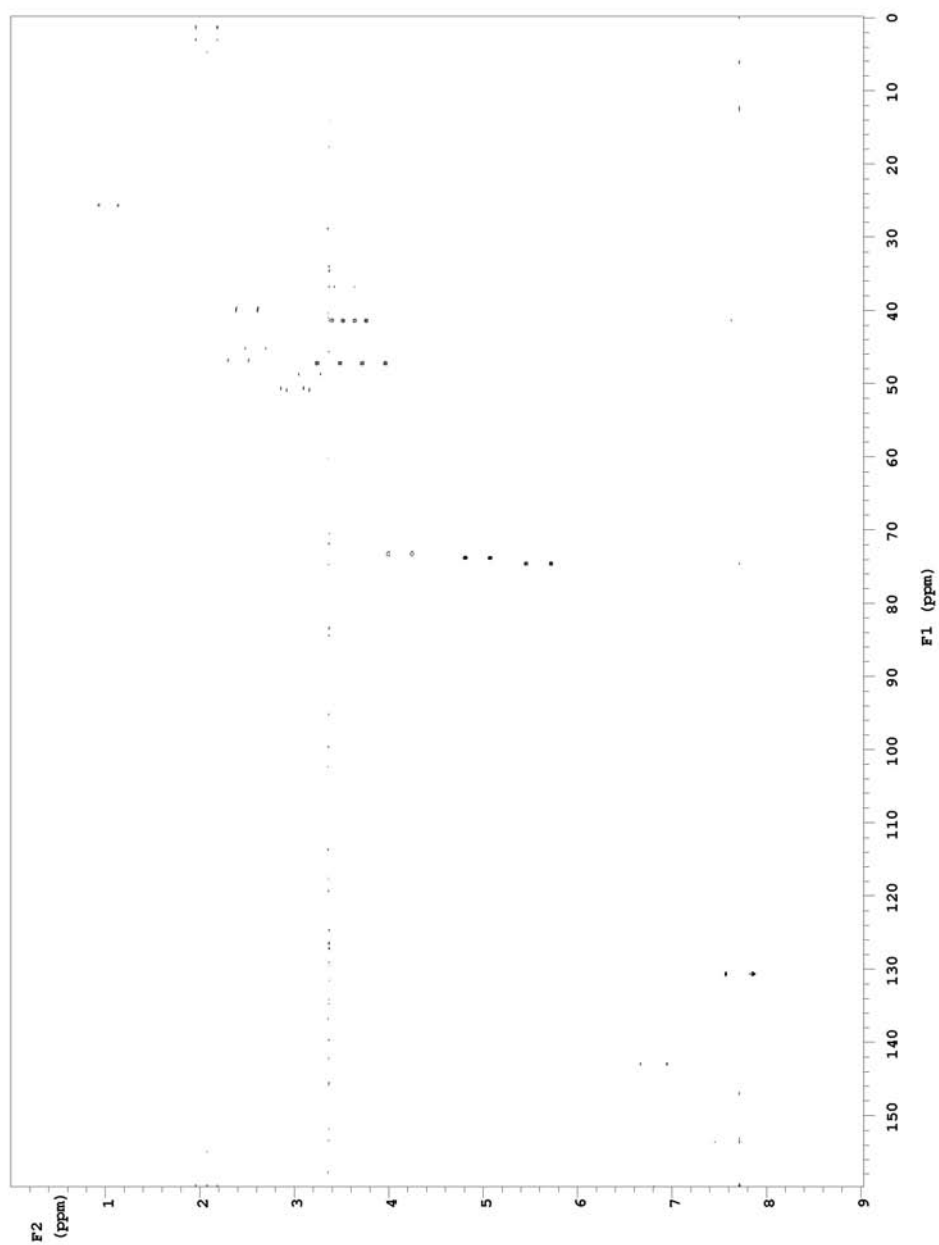
^1H NMR spectrum of LL-PAA216 (**54**) (600 MHz, d_6 -DMSO)



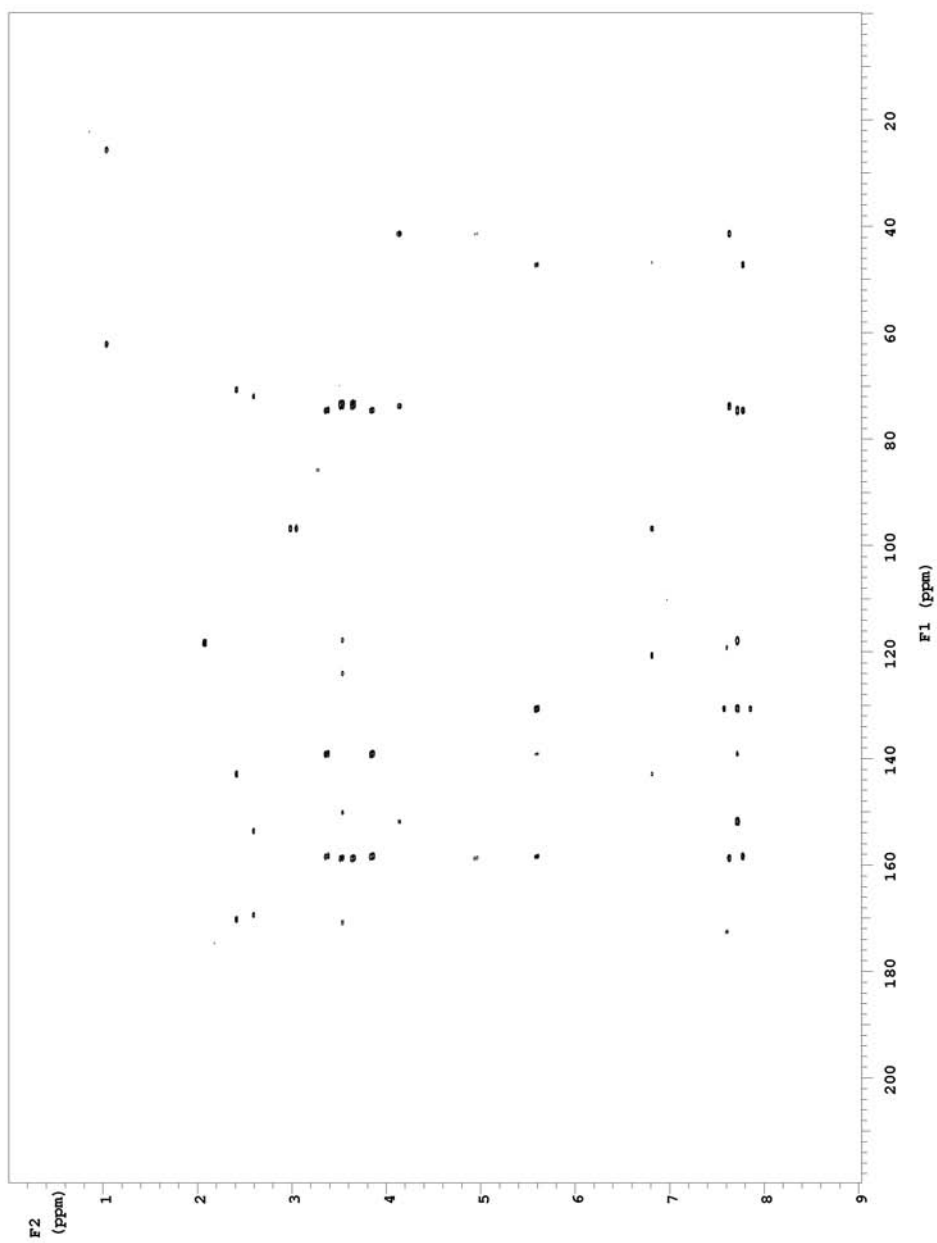
^{13}C spectrum of LL-PAA216 (**54**) (150 MHz, $\text{d}_6\text{-DMSO}$)



COSY spectrum of LL-PAA216 (**54**) (600 MHz, d₆-DMSO)



Coupled HSQC spectrum of LL-PAA216 (**54**) (600 MHz, d_6 -DMSO)



HMBC spectrum of LL-PAA216 (**54**) (600 MHz, d_6 -DMSO)

References

1. Cragg, G. M.; Boyd, M. R.; Khanna, R.; Kneller, R.; Mays, T. D.; Mazan, K. D.; Newman, D. J.; Sausville, E. A. *Pure Appl. Chem.* **1999**, *71*, 1619–1633.
2. Newman, D. J.; Cragg, G. M.; Snader, K. M. *Nat. Prod. Rep.* **2000**, *17*, 215–234.
3. *Drug discovery handbook*; Gad, S. C., Ed.; John Wiley & Sons: New Jersey, 2005.
4. *Drug discovery from nature*; Grabley, S., Thiericke, R., Eds.; Springer-Verlag: Berlin, 1999.
5. Baker, D. D.; Chu, M.; Oza, U.; Rajgarhia, V. *Nat. Prod. Rep.* **2007**, *24*, 1225–1244.
6. Davies, J. *Can. J. Infect. Dis. Med. Microbiol.* **2006**, *17*, 287–290.
7. Cragg, G. M.; Newman, D. J. *Expert Opin. Investig. Drugs* **2000**, *9*, 2783–2797.
8. Haefner, B. *Drug Discov. Today* **2003**, *8*, 536–544.
9. Donia, M.; Hamann, M. T. *Lancet Infectious Diseases* **2003**, *3*, 338–348.
10. Capon, R. J. *Eur. J. Org. Chem.* **2001**, *4*, 633–645.
11. Wallace, R. W. *Mol. Med. Today* **1997**, *3*, 291–295.
12. Jaspars, M. *Chemistry & Industry* **1999**, *2*, 51–55.
13. Cragg, G. M.; Newman, D. J.; Snader, K. M. *J. Nat. Prod.* **1997**, *60*, 52–60.
14. Bergmann, W.; Feeney, R. J. *J. Am. Chem. Soc.* **1950**, *72*, 2809–2810.
15. Bergmann, W.; Feeney, R. J. *J. Org. Chem.* **1951**, *16*, 981–987.
16. Bergmann, W.; Burke, D. C. *J. Org. Chem.* **1955**, *20*, 1501–1507.
17. Bodey, G. P.; Freireich, E. J.; Monto, R. W.; Hewlett, J. S. *Cancer Chemother. Rep.* **1969**, *53*, 59–66.
18. Faulkner, D. J. *Nat. Prod. Rep.* **2000**, *17*, 1–6.
19. Bergquist, P. R. *Sponges*; Hutchinson & Co.: London, 1978.
20. Dawkins, R. *The Ancestor's Tale: A Pilgrimage to the Dawn of Life*, 1st ed.; Houghton Mifflin: New York, 2004.
21. *Systema Porifera : a guide to the classification of sponges*; Hooper, J. N. A., van Soest, R. W. M., Willenz, P., Eds.; Kluwer Academic/Plenum Publishers: New York, 2002.
22. Enticknap, J. J.; Kelly, M.; Peraud, O.; Hill, R. T. *Appl. Environ. Microbiol.* **2006**, *72*, 3724–3732.
23. Vacelet, J.; Donadey, C. *J. Exp. Mar. Biol. Ecol.* **1977**, *30*, 301–314.
24. Faulkner, D. J.; Unson, M. D.; Bewley, C. A. *Pure Appl. Chem.* **1994**, *66*, 1983–1990.

25. Bewley, C. A.; Faulkner, D. J. *Angew. Chem. Int. Ed* **1998**, *37*, 2163–2178.
26. Keyzers, R. A.; Northcote, P. T.; Davies-Coleman, M. T. *Nat. Prod. Rep.* **2006**, *23*, 321–334.
27. Sperry, S.; Valeriote, F. A.; Corbett, T. H.; Crews, P. *J. Nat. Prod.* **1998**, *61*, 241–247.
28. Manes, L. V.; Bakus, G. J.; Crews, P. *Tetrahedron Lett.* **1984**, *25*, 931–934.
29. Kelly-Borges, M.; Vacelet, J. *Mem. Queensl. Mus.* **1995**, *38*, 477–503.
30. Crews, P.; Bescansa, P.; Bakus, G. J. *Experientia* **1985**, *41*, 690–1.
31. Crews, P.; Bescansa, P. *J. Nat. Prod.* **1986**, *49*, 1041–52.
32. Jaisamut, S.; Thengyai, S.; Yuenyongsawad, S.; Karalai, C.; Plubrukarn, A.; Suwanborirux, K. *Pure Appl. Chem.* **2009**, *81*, 1019–1026.
33. Quiñoà, E.; Crews, P. *Tetrahedron Lett.* **1987**, *28*, 3229–3232.
34. Sashidhara, K. V.; White, K. N.; Crews, P. *J. Nat. Prod.* **2009**, *72*, 588–603.
35. Kim, D. Y.; Lee, I. S.; Jung, J. H.; Yang, S. I. *Arch. Pharm. Res.* **1999**, *22*, 25–29.
36. Nicholas, G. M.; Eckman, L. L.; Ray, S.; Hughes, R. O.; Pfefferkorn, J. A.; Barluenga, S.; Nicolaou, K. C.; Bewley, C. A. *Bioorg. Med. Chem. Lett.* **2002**, *12*, 2487–2490.
37. Nicolaou, K. C.; Hughes, R.; Pfefferkorn, J. A.; Barluenga, S.; Roecker, A. J. *Chem. Eur. J.* **2001**, *7*, 4280–4295.
38. Nicolaou, K. C.; Hughes, R.; Pfefferkorn, J. A.; Barluenga, S. *Chem. Eur. J.* **2001**, *7*, 4296–4310.
39. Piña, I. C.; Gautschi, J. T.; Wang, G. Y. S.; Sanders, M. L.; Schmitz, F. J.; France, D.; Cornell-Kennon, S.; Sambucetti, L. C.; Remiszewski, S. W.; Perez, L. B.; Bair, K. W.; Crews, P. *J. Org. Chem.* **2003**, *68*, 3866–3873.
40. Shim, J. S.; Lee, H. S.; Shin, J.; Kwon, H. J. *Cancer Lett.* **2004**, *203*, 163–169.
41. Jiang, Y. H.; Ahn, E. Y.; Ryu, S. H.; Kim, D. K.; Park, J. S.; Yoon, H. J.; You, S.; Lee, B. J.; Lee, D. S.; Jung, J. H. *BMC Cancer* **2004**, *4*, 1471–2407.
42. Kim, D.; Lee, I. S.; Jung, J. H.; Lee, C. O.; Choi, S. U. *Anticancer. Res.* **1999**, *19*, 4085–4090.
43. Shin, J.; Lee, H. S.; Seo, Y.; Rho, J. R.; Cho, K. W.; Paul, V. J. *Tetrahedron* **2000**, *56*, 9071–9077.
44. Tabudravu, J. N.; Eijssink, V. G. H.; Gooday, G. W.; Jaspars, M.; Komander, D.; Legg, M.; Synstad, B.; van Aalten, D. M. F. *Bioorg. Med. Chem.* **2002**, *10*, 1123–1128.
45. Meragelman, K. M.; McKee, T. C.; Boyd, M. R. *J. Nat. Prod.* **2001**, *64*, 389–392.
46. Field, J. J.; Singh, A. J.; Kanakkanthara, A.; Halafihi, T.; Northcote, P. T.; Miller, J. H. *J. Med. Chem* **2009**, *52*, 7328–7332.

47. Tanaka, J.; Higa, T. *Tetrahedron Lett.* **1996**, *37*, 5535–5538.
48. Morris, G.; Fournier, N. *Clin. Cancer Res.* **2008**, *14*, 7167–7172.
49. Jordan, M. A.; Wilson, L. W. *Nat. Rev.* **2004**, *4*, 253–265.
50. Miller, J. H.; Singh, A. J.; Northcote, P. T. *Mar. Drugs* **2010**, *8*, 1059–1079.
51. Lipinski, C. A.; Lombardo, F.; Dominy, B. W.; Feeney, P. J. *Adv. Drug Deliv. Rev.* **1997**, *23*, 3–25.
52. West, L. M. *The isolation of Secondary Metabolites from New Zealand Marine Sponges*, PhD, Victoria University of Wellington, 2001.
53. Singh, A. J. *Secondary Metabolites from the New Zealand Marine Sponge Mycale hentscheli*, MSc, Victoria University of Wellington, 2007.
54. Ryan, J. M. *Novel Secondary Metabolites from New Zealand Marine Sponges*, PhD, Victoria University of Wellington, 2007.
55. Wojnar, J. M. *Isolation of New Secondary Metabolites from New Zealand Marine Invertebrates*, PhD, Victoria University of Wellington, 2008.
56. Dowle, K. O. *New Nitrogenous Spongian Diterpenes from the New Zealand Marine Sponge Darwinella oxeata*, MSc, Victoria University of Wellington, 2008.
57. Popplewell, W. L. *Isolation and Structure Elucidation of New Secondary Metabolites from New Zealand Marine Red Algae*, PhD, Victoria University of Wellington, 2008.
58. Capon, R. J.; Macleod, J. K. *Aust. J. Chem.* **1987**, *40*, 341–346.
59. Minale, L.; Cimino, G.; DeStefano, S.; Sodano, G. *Fortschr. Chem. Org. Naturst.* **1976**, *33*, 1–72.
60. Yagi, H.; Matsunaga, S.; Fusetani, N. *Tetrahedron* **1993**, *49*, 3749–3754.
61. Roll, M. D.; Chang, W. J. C.; Scheuer, P. J.; Gray, G. A.; Shoolery, J. N.; Matsumoto, G. K.; Van, D. G. D.; Clardy, J. *J. Am. Chem. Soc.* **1985**, *107*, 2916–2920.
62. Ichiba, T.; Scheuer, P. J. *J. Org. Chem.* **1993**, *58*, 4149–4150.
63. Copp, B. R.; Ireland, C. M. *J. Nat. Prod.* **1992**, *55*, 822–823.
64. Gopichand, Y.; Schmitz, F. J. *Tetrahedron Lett.* **1979**, *41*, 3921–3924.
65. Kernan, M. R.; Cambie, R. C.; Bergquist, P. R. *J. Nat. Prod.* **1990**, *53*, 615–622.
66. Pordesimo, O. E.; Schmitz, F. J. *J. Org. Chem.* **1990**, *55*, 4704–4709.
67. Kazluskas, R. L. R. O.; Murphy, P. T.; Wells, R. J. *Tetrahedron Lett.* **1980**, *21*, 2277–2280.
68. Carney, J. R.; Scheuer, P. J. *J. Nat. Prod.* **1993**, *56*, 153–157.
69. *MarinLit: Marine Literature Database*, 2010.
70. Rogers, E. W.; Molinski, T. F. *J. Nat. Prod.* **2007**, *70*, 1191.

71. Motti, C. A.; Freckelton, M. L.; Tapiolas, D. M.; Willis, R. H. *J. Nat. Prod.* **2009**, *72*, 290.
72. Xynas, R.; Capon, R. J. *Aust. J. Chem.* **1989**, *42*, 1427–1433.
73. Cimino, G.; Rosa, S. D.; Stefano, S. D.; Self, R.; Sodano, G. *Tetrahedron Lett.* **1983**, *24*, 3029–3032.
74. Fattorusso, E.; Minale, L.; Sodano, G. *J. Chem. Soc., Perkin Trans. 1* **1972**, 16–18.
75. Borders, D. B.; Morton, G. O.; Wetzel, E. R. *Tetrahedron Lett.* **1974**, *31*, 2709–2712.
76. Takada, N.; Watanabe, R.; Suenaga, K.; Yamada, K.; Ueda, K.; Kita, M.; Uemura, D. *Tetrahedron Lett.* **2001**, *42*, 5265–5267.
77. Hayakawa, I.; Teruya, T.; Kigoshi, H. *Tetrahedron Lett.* **2006**, *47*, 155–158.
78. Kita, M.; Tsunematsu, Y.; Hayakawa, I.; Kigoshi, H. *Tetrahedron Lett.* **2008**, *49*, 5383–5384.
79. Carney, J. R.; Scheuer, P. J.; Kellyborges, M. *Tetrahedron* **1993**, *49*, 8483–8486.
80. Radisky, D. C.; Radisky, E. S.; Barrows, L. R.; Copp, B. R.; Kramer, R. A.; Ireland, C. M. *J. Am. Chem. Soc.* **1993**, *115*, 1632 – 1638.
81. Schmidt, E. W.; Harper, M. K.; Faulkner, D. J. *J. Nat. Prod.* **1995**, *58*, 1861 – 1867.
82. Cheng, J.; Ohizumi, Y.; Walchli, M. R.; Nakamura, H.; Hirata, Y.; Sasaki, T.; Kobayashi, J. *J. Org. Chem.* **1988**, *53*, 4621–4624.
83. Kobayashi, J.; Cheng, J.; Yamamura, S.; Ishibashi, M. *Tetrahedron Lett.* **1991**, *32*, 1227–1228.
84. Antunes, E.; Copp, B. R.; Davies-Coleman, M. T.; Samaai, T. *Nat. Prod. Rep.* **2005**, *22*, 62–72.
85. Urban, S.; Hickford, S. J. H.; Blunt, J. W.; Munro, M. H. G. *Curr. Org. Chem.* **2000**, *4*, 765–807.
86. Leahy, D. *Victoria University of Wellington, New Zealand. Personal communication*, 2009.
87. Crews, P.; Naylor, S. *Prog. Chem. Org. Nat. Prod.* **1985**, *48*, 203–269.
88. Hanson, J. R. *Nat. Prod. Rep.* **1986**, *3*, 123–132.
89. Kazlauskas, R.; Murphy, P. T.; Quinn, R. J.; Wells, R. J. *Tetrahedron Lett.* **1977**, 61–64.
90. Roll, D. M.; Ireland, C. M.; Lu, H. S. M.; Clardy, J. *J. Org. Chem.* **1988**, *53*, 3276–3278.
91. Jiménez, C.; Quiñoà, E.; Adamczeski, M.; Hunter, L. M.; Crews, P. *J. Org. Chem.* **1991**, *56*, 3403–3410.
92. Jiménez, C.; Quiñoà, E.; Crew, P. *Tetrahedron Lett.* **1991**, *32*, 1843–1846.

93. Segraves, N. L.; Lopez, S.; Johnson, T. A.; Said, S. A.; Fu, X.; Schmitz, F. J.; Pietraszkiewicz, H.; Valeriote, F. A.; Crews, P. *Tetrahedron Lett.* **2003**, *44*, 3471–3475.
94. Segraves, N. L.; Robinson, S. J.; Garcia, D.; Said, S. A.; Fu, X.; Schmitz, F. J.; Pietraszkiewicz, H.; Valeriote, F. A.; Crews, P. *J. Nat. Prod.* **2004**, *67*, 783–792.
95. Schmidt, E. W.; Faulkner, D. J. *Tetrahedron Lett.* **1996**, *37*, 3951–3954.
96. Sullivan, B.; Faulkner, D. *Tetrahedron Lett.* **1982**, *23*, 907–910.
97. Bishara, A.; Rudi, A.; Akin, M.; Neumann, D.; Ben-Califa, N.; Kashman, Y. *Org. Lett.* **2008**, *10*, 4307–4309.
98. Bishara, A.; Rudi, A.; Akin, M.; Neumann, D.; Ben-Califa, N.; Kashman, Y. *Org. Lett.* **2008**, *10*, 153–156.
99. Bishara, A.; Rudi, A.; Goldberg, I.; Akin, M.; Neumann, D.; Ben-Califa, N.; Kashman, Y. *Org. Lett.* **2009**, *11*, 3538–3541.
100. Bishara, A.; Rudi, A.; Akin, M.; Neumann, D.; Ben-Califa, N.; Kashman, Y. *Tetrahedron* **2010**, 1–7.
101. Bishara, A.; Rudi, A.; Goldberg, I.; Akin, M.; Kashman, Y. *Tetrahedron Lett.* **2009**, *50*, 3820–3822.
102. Bishara, A.; Rudi, A.; Akin, M.; Neumann, D.; Ben-Califa, N.; Kashman, Y. *Tetrahedron Lett.* **2008**, *49*, 4355–4358.
103. Klein, D.; Braekman, J. C.; Daloze, D.; Hoffmann, L.; Demoulin, V. *Tetrahedron Lett.* **1996**, *37*, 7519–7520.
104. Klein, D.; Braekman, J. C.; Daloze, D.; Hoffman, L.; Castillo, G.; Demoulin, V. *J. Nat. Prod.* **1999**, *62*, 934–936.
105. Stratmann, K.; Burgoyne, D. L.; Moore, R. E.; Patterson, G. M. L.; Smith, C. D. *J. Org. Chem.* **1994**, *59*, 7219–7226.
106. Ratnayake, R.; Fremlin, L. J.; Lacey, E.; Gill, J. H.; Capon, R. J. *J. Nat. Prod.* **2008**, *71*, 403–408.
107. Seo, C.; Yim, J. H.; Lee, H. K.; Park, S. M.; Sohn, J. H.; Oh, H. *Tetrahedron Lett.* **2008**, *49*, 29–31.
108. Albizati, K. F.; Holman, T.; Faulkner, D. J.; Glaser, K. B.; Jacobs, R. S. *Experientia* **1987**, *43*, 949–950.
109. Yunker, M. B.; Scheuer, P. J. *J. Am. Chem. Soc.* **1978**, *100*, 307–309.
110. Tsuda, M.; Shigemori, H.; Ishibashi, M.; Sasaki, T.; Kobayashi, J. J. *J. Org. Chem.* **1992**, *57*, 3503–3507.
111. Höller, U.; König, G. M.; Wright, A. D. *J. Nat. Prod.* **1997**, *60*, 832–835.
112. Tran, N. H.; Hooper, J. N. A.; Capon, R. J. *Aust. J. Chem.* **1995**, *48*, 1757–1760.
113. Elkhayat, E.; Edrada, R. A.; Ebel, R.; Wray, V.; van Soest, R.; Wiryowidagdo, S.; Mohamed, M. H.; Müller, W. E. G.; Proksch, P. *J. Nat. Prod.* **2004**, *67*, 1809–1817.

114. Kirsch, G.; Kong, G. M.; Wright, A. D.; Kaminsky, R. *J. Nat. Prod.* **2000**, *63*, 825–829.
115. Ruzicka, Z. L. *Experientia* **1953**, *9*, 357–367.
116. Ebada, S. S.; Lin, W.; Proksch, P. *Mar. Drugs* **2010**, *8*, 313–346.
117. de Silva, E. D.; Scheuer, P. J. *Tetrahedron Lett.* **1980**, *21*, 1611–1614.
118. Butler, M. S.; Capon, R. J. *Aust. J. Chem.* **1992**, *45*, 1705–1743.
119. de Silva, E.; Scheuer, P. *Tetrahedron Lett.* **1981**, *22*, 3147–3150.
120. Bourguet-Kondracki, M. L.; Debitus, C.; Guyot, M. *J. Chem. Res. (S)* **1996**, 192–193.
121. Kobayashi, M.; Okamoto, T.; Hayashi, K.; Yokoyama, N.; Sasaki, T.; Kitagawa, I. *Chem. Pharm. Bull.* **1994**, *42*, 265–270.
122. Tasdemir, D.; Concepcion, G. P.; Mangalindan, G. C.; Harper, M. K.; Hajdu, E.; Ireland, C. M. *Tetrahedron* **2000**, *56*, 9025–9030.
123. de Rosa, S.; de Stefano, S.; Zavodnik, N. *J. Org. Chem.* **1988**, *53*, 5020–5023.
124. Cambie, R. C.; Craw, P. A.; Bergquist, P. R.; Karuso, P. *J. Nat. Prod.* **1988**, *51*, 331–334.
125. Cao, S.; Foster, C.; Lazo, J. S.; Kingston, D. G. *Bioorg. Med. Chem.* **2005**, *13*, 5094–5098.
126. Montagnac, A.; Pais, M.; Debitus, C. *J. Nat. Prod.* **1994**, *57*, 186–190.
127. de Rosa, S.; Crispino, A.; de Giulio, A.; Iodice, C.; Pronzato, R.; Zavodnik, N. *J. Nat. Prod.* **1995**, *58*, 1776–1780.
128. de Rosa, S.; Crispino, A.; de Giulio, A.; Iodice, C.; Tommonaro, G. *J. Nat. Prod.* **1997**, *60*, 844–846.
129. de Rosa, S.; Carbonelli, S. *Tetrahedron* **2006**, *62*, 2845–2849.
130. Tsuda, M.; Endo, T.; Mikami, Y.; Fromont, J.; Kobayashi, J. *J. Nat. Prod.* **2002**, *65*, 1507–1508.
131. Kernan, M. R.; Faulkner, D. J.; Jacobs, R. S. *J. Org. Chem.* **1987**, *52*, 3081–3083.
132. Kernan, M. R.; Faulkner, D. J.; Parkanyi, L.; Clardy, J.; de Carvalho, M. S.; Jacobs, R. S. *Experientia* **1989**, *45*, 388–390.
133. König, G. M.; Wright, A. D.; Sticher, O. *J. Nat. Prod.* **1992**, *55*, 174–178.
134. Potts, B. C. M.; Capon, R. J.; Faulkner, D. J. *J. Org. Chem.* **1992**, *57*, 2965–2967.
135. Reddy, M. V. R.; Harper, M. K.; Faulkner, D. J. *J. Nat. Prod.* **1997**, *60*, 41–43.
136. Namikoshi, M.; Suzuki, S.; Meguro, S.; Nagai, H.; Koike, Y.; Kitazawa, A.; Kobayashi, H.; Oda, T.; Yamada, J. *Fish. Sci.* **2004**, *70*, 152–158.
137. Ettinger-Epstein, P.; Motti, C. A.; de Nys, R.; Wright, A. D.; Battershill, C. N.; Tapiolas, D. M. *J. Nat. Prod.* **2007**, *70*, 648–651.

138. Zhou, G. X.; Molinski, T. F. *J. Asian Nat. Prod. Res.* **2006**, *8*, 15–20.
139. Kobayashi, J.; Zeng, C. M.; Ishibashi, M.; Sasaki, T. *J. Nat. Prod.* **1993**, *56*, 436–439.
140. Gauvin-Bialecki, A.; Akinin, M.; Smadja, J. *Molecules* **2008**, *13*, 3184–3191.
141. Ueoka, R.; Nakao, Y.; Fujii, S.; van Soest, R. W. M.; Matsunaga, S. *J. Nat. Prod.* **2008**, *71*, 1089–1091.
142. de Freitas, J. C.; Blankemeier, L. A.; Jacobs, R. S. *Experientia* **1984**, *40*, 864–865.
143. Glaser, K. B.; Jacobs, R. S. *Biochem. Pharmacol.* **1986**, *35*, 449–453.
144. Deems, R. A.; Lombardo, D.; Morgan, B. P.; Mihelich, E. D.; Dennis, E. A. *Biochim. Biophys. Acta* **1987**, *917*, 258–268.
145. Reynolds, L. J.; Morgan, B. P.; Hite, G. A.; Mihelich, E. D.; Dennis, E. A. *J. Am. Chem. Soc.* **1988**, *110*, 5172–5177.
146. Potts, B. C. M.; Faulkner, D. J.; Jacobs, R. S. *J. Nat. Prod.* **1992**, *55*, 1701–1717.
147. Reynolds, L. J.; Mihelich, E. D.; Dennis, E. A. *J. Biol. Chem.* **1991**, *266*, 16512–16517.
148. Potts, B. C. M.; Faulkner, D. J.; de Carvalho, M.; Jacobs, R. S. *J. Am. Chem. Soc.* **1992**, *114*, 5093–5100.
149. de Rosa, M.; Giordano, S.; Scettri, A.; Sodano, G.; Soriente, A.; Pastor, P. G.; Alcaraz, M. J.; Pay, M. *J. Med. Chem.* **1998**, *41*, 3232–3238.
150. Mann, J. *Nature* **1992**, *358*, 540.
151. Glaser, K. B.; de Carvalho, M. S.; Jacobs, R. S.; Kernan, M. R.; Faulkner, D. J. *Mol. Pharmacol.* **1989**, *36*, 782–788.
152. Kernan, M. R.; Barrabee, E. B.; Faulkner, D. J. *Comp. Biochem. Physiol.* **1988**, *89B*, 275–278.
153. Faulkner, D. J. *Synthesis* **1971**, 175–189.
154. Liu, Y.; Mansoor, T. A.; Hong, J.; Lee, C. O.; Sim, C. J.; Im, K. S.; Kim, N. D.; Jung, J. H. *J. Nat. Prod.* **2003**, *66*, 1451–1456.
155. Fattorusso, E.; Lanxotti, V.; Magno, S.; Mayol, L.; di Rosa, M.; Ialenti, A. *Bioorg. Med. Chem. Lett.* **1991**, *1*, 639–644.
156. de Rosa, S.; de Giulio, A.; Crispino, A.; Iodice, C.; Tommonaro, G. *Nat. Prod. Lett.* **1997**, *10*, 267–274.
157. Gottlieb, H. E.; Kotlyar, V.; Nudelman, A. *J. Org. Chem.* **1997**, *62*, 7512–7515.